

Land Cover Change and Climate on the North American Great Plains

by

Shira Ellen Gerstein

A thesis  
presented to the University of Waterloo  
in fulfilment of the  
thesis requirement for the degree of  
Master of Science  
in  
Geography

Waterloo, Ontario, Canada, 2014

© Shira Ellen Gerstein 2014

## **Author's Declaration**

I hereby declare that I am the sole author of this thesis. This is a true copy of the thesis, including any required final revisions, as accepted by my examiners.

I understand that my thesis may be made electronically available to the public.

## Abstract

Changing land cover from prairie grasslands to intensive, primarily cereal agriculture, over the North American Great Plains since the mid-19<sup>th</sup> century, has had a hydrological and climatological impact on that ecosystem (Pielke, Sr., et al., 2011). Agriculture has introduced timed harvest seasons, irrigation, and C3 photosynthesizing crops with poorer water efficiency than the grasses it replaced. All of these changes have been linked to exacerbated drought conditions and warmer temperatures; however, few studies have quantified this relationship at the continental scale. In order to evaluate the change imposed by this shift in land use and land cover, the observation based 20<sup>th</sup> Century Reanalysis Project (20CR) was used to quantify the climatological differences in temperature and humidity between areas of natural prairie and agriculture over the 20<sup>th</sup> century. An additional analysis used the Observation Minus Reanalysis (OMR) technique to isolate the surface climate signal found in the 20CR. We find indications that changing land cover had an impact on climate. However, using observation based data returned no evidence of a statistically significant change due to the small land use and land cover change (LULCC) signal within the larger climate noise. Therefore, an idealised modelling experiment was undertaken using the Geophysical Fluid Dynamics Laboratory (GFDL) AM2-LM2 atmosphere-land model to remove these other influences. This experiment compared the results of two model simulations: one where the entirety of the prairie was preserved as grassland (GRASS), and another where the entire prairies had been converted into an agricultural area (AGRIC). Relative to GRASS, the AGRIC simulation has reduced surface albedo and root zone depth, and increased roughness length over the prairies, which collectively cause a significant summer drying. This occurs when the shallower rooting zone limited potential evapotranspiration (PET) forcing the additional energy created by turbulent mixing and a lower

surface albedo to warm the air, surpassing PET and reaching drier conditions faster. While not conclusive, the results presented in this thesis represent a step towards filling the gaps in understanding land-atmosphere interactions and connecting LULCC to climate.

## **Acknowledgements**

First, I would like to acknowledge Dr. Christopher Fletcher, who acted as my academic advisor during the process of conceptualizing, realizing, and executing this thesis. Working with Dr. Fletcher has allowed me to explore new areas of climate science and to combine my interest in prairie weather with current modelling techniques.

I would also like to thank Dr. Derek Robinson, Dr. Christopher Derksen, and Dr. Richard Petrone, for volunteering as members of my thesis committee and for their guidance during course work and conversations.

Thank you to Adam Saunders, Chad Thackery, Mina Rohanizadigan, Maliha Majeed, Janine Baijnath, Heather MacKinnon, and Susie Castela, for their help, support, and ideas over the past two years.

Finally, I would like to acknowledge my parents, for setting the bar too high.

# Table of Contents

<b>Author’s Declaration .....</b>	<b>ii</b>
<b>Abstract.....</b>	<b>iii</b>
<b>Acknowledgements .....</b>	<b>v</b>
<b>Table of Contents .....</b>	<b>vi</b>
<b>List of Figures.....</b>	<b>viii</b>
<b>Chapter 1 Introduction .....</b>	<b>1</b>
1.1 Background .....	1
1.1.1 The Prairies as a Natural Ecosystem.....	1
1.1.2 Palaeoclimatological Evolution of the Prairies.....	5
1.1.3 History of Agricultural Development .....	6
1.2 Literature Review .....	8
1.2.1 Biological Differences .....	8
1.2.2 Hydrological and Climatological Changes .....	11
1.2.3 Remote Influences on Prairie Climate .....	14
1.3 Motivation .....	16
1.4 Objective .....	18
1.5 Structure .....	18
<b>Chapter 2 Data and Methods.....</b>	<b>19</b>
2.1 Data Descriptions .....	19
2.1.1 Global Potential Vegetation Dataset.....	20
2.1.2 20 <sup>th</sup> Century Reanalysis Project.....	22
2.1.3 Observation Data .....	23
2.2 Model Description.....	24
2.2.1 Coupled Atmosphere and Land Model v.2.1 .....	24
2.2.2 Hydrologic Cycle within LM v.2.1 .....	26
2.3 Study and Model Experiment Designs.....	30
2.3.1 Reanalysis Study.....	30
2.3.2 Observation Minus Reanalysis Variation .....	33
2.3.3 Model Experiment .....	34
<b>Chapter 3 Reanalysis and Observation Studies.....</b>	<b>38</b>

3.1	Reanalysis Method Results .....	38
3.2	Observation Minus Reanalysis Results .....	47
3.2.1	Temporal Inhomogeneity .....	48
3.3	Summary and Impetus for Model Experiment .....	52
<b>Chapter 4 Model Experiment .....</b>		<b>54</b>
4.1	Whole Prairie Results .....	54
4.1.1	Net Radiation and the Energy Balance .....	57
4.1.2	Water Balance .....	61
4.2	Subdividing the Prairies .....	66
4.2.1	Northern Prairie .....	69
4.2.2	Southern Prairie .....	72
4.3	Limitations and Summary .....	75
<b>Chapter 5 Future Research Possibilities and Conclusions.....</b>		<b>78</b>
5.1	Research Summary.....	78
5.2	Future Directions.....	80
<b>References.....</b>		<b>84</b>

## List of Figures

Figures		Page
1.1	Geographic extent of the North American prairies; with overlay showing the temperature and precipitation gradients.	3
1.2	Figure 1.2: Extent of the High Plains Aquifer outlined with areas of irrigated agriculture highlighted in blue based on available satellite data from 1992. The aquifer overlaps area from 8 states: Wyoming (WY), South Dakota (SD), North Dakota (ND), Colorado (CO), Kansas (KS), Oklahoma (OK), Texas (TX), and New Mexico (NM).	5
1.3	Historical drought record for the Western United States, including the prairies, beginning in 800 B.C.E.	12
2.1	Pathways of water within the LM2 component of AM2-LM2.	27
2.2	Average percentage agricultural cell coverage ( $C_f$ ) of the Global Potential Vegetation Dataset (GVPD) for the first and last 20 years of the 20th century. A $C_f$ value of 1 represents a completely agricultural cell; a $C_f$ value of 0 represents a cell which is has no agricultural coverage.	31
2.3	Outline of $C_f$ subset areas used to delineate natural (CTRL) and cropped (PERT) areas. The $\leq 25\%$ (CTRL) and $\geq 75\%$ (PERT) areas represent the percentile limits for cells to be categorized as one category or another. The white area shows those cells which fit into neither category.	32
2.4	Factorial experiment design. The arrows represent the two directions in which change was evaluated; between the two land cover types and across time.	33
3.1	Annual change in $C_f$ from 1900-1999.	38
3.2	Left: Temperature in $^{\circ}\text{K}$ for each land cover area for both time periods, including the difference between each area at the beginning and end of the 20 <sup>th</sup> century as well as the difference in each area over time. Right: The plotted mean value with statistical significance represented as two standard deviations from the areal mean.	39
3.3	Atmospheric water vapour content in $\text{Kg}/\text{m}^2$ represented as described in Figure 3.2.	40
3.4	Convective available potential energy in $\text{J}/\text{Kg}$ represented as described in Figure 3.2.	41

3.5	Mean annual temperature in °K for CTRL and PERT land cover areas. The paler lines above and below CTRL and PERT represent the maximum and minimum values from within the 20CR ensemble.	42
3.6	Mean annual atmospheric water vapour content in Kg/m <sup>2</sup> represented as described in Figure 3.5.	43
3.7	Mean annual convective available potential energy in J/Kg represented as described in Figure 3.5.	43
3.8	20 <sup>th</sup> century seasonal mean temperatures in °K. Plots are limited to 20°N-90°N in the Western hemisphere.	45
3.9	20 <sup>th</sup> century seasonal mean atmospheric water vapour content in Kg/m <sup>2</sup> represented as described in Figure 3.8.	46
3.10	20 <sup>th</sup> century seasonal mean convective available potential energy in J/Kg represented as described in Figure 3.8.	46
3.11	Calculated OMR temperature anomalies in °K represented as described in Figure 3.2, including both (A) CRUTEM4 and (B) University of Delaware versions of OMR.	48
3.12	Inter-annual variability in the OMR results for temperature anomalies in °K represented as described in Figure 3.2, including both (A) CRUTEM4 and (B) University of Delaware versions of OMR.	51
3.13	Difference in temperature anomaly in °K between the first and second halves of the 20 <sup>th</sup> century over North America. The top two panels represent the OMR using the CRUTEM4 (C) observations and the bottom two panels represent the OMR using the University of Delaware (D) observations represented as described in Figure 3.2.	52
4.1	(A) Monthly mean albedo for the whole prairie (blue), the northern prairie (red), and south prairie (blue) in the control case. (B) Monthly response in mean caused by replacing the grassland with the agricultural scenario (AGRIC-GRASS). The whole, north, and south area divisions will be discussed in section 4.2 and 4.3. Statistical significance ( $p \leq 0.05$ ) is indicated by a dot in a colour corresponding to the related plot line.	55
4.2	Mean monthly temperature in °K represented as described in Figure 4.1a/b. Dots representing statistical significance are on the line in this case.	56
4.3	Map of response temperature results (°K). Plots are limited to 20oN-90oN in the Western hemisphere. Areas of stippling within the maps represent cells where	56

	the response was considered statistically significant ( $p \leq 0.05$ ).	
4.4	(A) GRASS net radiation and (B) response net radiation in $W/m^2$ represented as described in Figure 4.2.	58
4.5	Map of response outgoing shortwave radiation results in $W/m^2$ represented as described in Figure 4.3.	58
4.6	Map of response upwelling longwave radiation results in $W/m^2$ represented as described in Figure 4.3.	59
4.7	(A) GRASS energy balance and (B) response energy balance in $W/m^2$ represented as described in Figure 4.2.	60
4.8	(A) GRASS atmospheric water balance and (B) response atmospheric water balance in mm/month. (C) GRASS land water balance and (D) response land water balance for the entire prairies. Statistical significance is represented as described in Figure 4.2. In A and B, Delta (P-E) is the net moisture left on the ground (effective precipitation). In C and D, Total (R+G) is the total water available on the ground. Root zone and groundwater contribute to this total.	63
4.9	Map of response groundwater storage in $Kg/m^2$ represented as described in Figure 4.3.	68
4.10	Map of GRASS snow mass in $Kg/m^2$ represented as described in Figure 4.3	68
4.11	Map of response snow mass in $Kg/m^2$ represented as described in Figure 4.3.	69
4.12	Northern Prairie: (A) GRASS net radiation and (B) response net radiation in $W/m^2$ . (C) GRASS energy balance and (D) response energy balance in $W/m^2$ . Statistical significance is represented as described in Figure 4.2.	71
4.13	Northern Prairie: Atmospheric and land water balance as described in Figure 4.8.	72
4.14	Southern Prairie: Net radiation and energy balance as described in Figure 4.8.	74
4.15	Southern Prairie: Atmospheric and land water balance as described in Figure 4.8.	75

## **Chapter 1: Introduction**

### **1.1 Background**

Oftentimes, the relationship between climate and agriculture is referenced by the influence that climate has on growing conditions and crop yields. However, it has been shown that the widespread shift in land cover, towards a more heavily cultivated planet, has also contributed to shifting climate (Pielke, Sr., et al., 2006). Current estimates suggest that 35-39% of all non-glaciated land, an area of approximately 4.9 billion hectares, has been converted from the natural land cover into agricultural fields and cultivated areas (Foley, et al., 2011; Pielke, Sr., et al., 2011). When evaluated from a global standpoint, the seemingly minor landscape alterations have been shown to have serious climatological and hydrological implications (Pielke, Sr., et al., 1998). Even at smaller spatial scales, many studies have demonstrated that land cover change has a significant impact on climate (Pielke, Sr., et al., 2006). The influence of anthropogenic change on climate is part of an area of research called Land Use and Land Cover Change (LULCC). The remainder of Chapter 1 will present an overview of the current available literature on LULCC and discuss the changes that have already occurred. The literature review will be specific to the North American Great Plains as this ecosystem will be the focus of this thesis. In Canada, the ecosystem is referred to as the Canadian Prairies, whereas in the United States, they are formally called the Great Plains. Both titles describe the same environment. For the purposes of this thesis, the term prairie(s) or North American Great Plains will be used to describe the entire area.

#### **1.1.1 The Prairies as a Natural Ecosystem**

Before Europeans came to settle in central North America during the mid 19<sup>th</sup> century, the prairies were a major ecosystem that stretched from, north to south, the centre of Alberta and

Saskatchewan to northern Mexico and from, west to east, the foothills of the Rocky Mountains to Illinois (Figure 1.1). This area covers approximately 15% of the entire continent; roughly 300 million hectares of land (Anderson, 2006; Pielke, Sr., et al., 2007). The prairies contain three primary hydroclimatologic zones as defined by the updated Koppen-Geiger climate classification scheme. In the northeast, the climate is described as cold, without a dry season, and with a variable hot and warm climate. The southeastern prairies are defined as a temperate region, without a true dry season but with hot summer temperatures. The entire western prairies, along the Rocky Mountains, is more climatically uniform as an arid, steppe environment with a cold climate where mean annual temperature is below 18 °C (Peel, Finlayson, & McMahon, 2007). This scheme uses observational data to categorize the planet's climate zones based on three categories: primary climate, precipitation, and temperature. The distinction between each class within each category is based on quantitative boundaries (Rubel & Kettek, 2010; Peel, Finlayson, & McMahon, 2007). Generally, this presents the prairies as having a northwest-southeast temperature gradient (cooler in the northwest) and an east-west precipitation gradient (wetter in the east) (Lauenroth, Burke, & Gutmann, 1999).

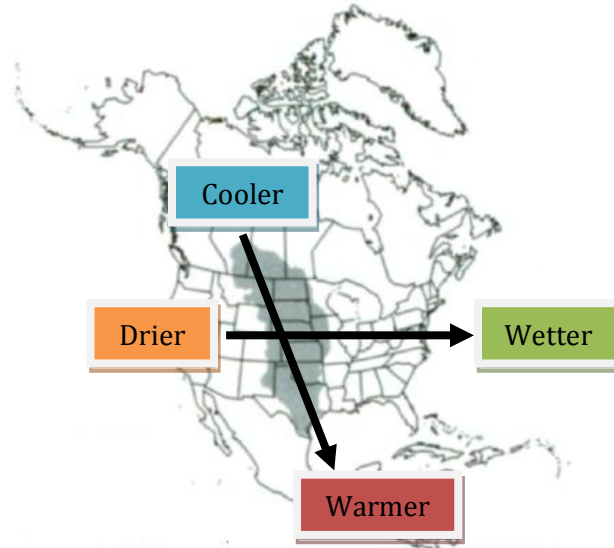


Figure 1.1: Geographic extent of the North American prairies; with overlay showing the temperature and precipitation gradients.

---

*Note.* Adapted from: Sieg, C. H., & Flather, C. H. (1999). Recent biodiversity patterns in the Great Plains: Implications for restoration and management. *Great Plains Research*, 9, 277-313.

Within these regions are found the three main plant communities of the prairies. All three are built up of a variety of grass species and, in some places, smaller herbaceous shrubs (Weaver, 1954). Each community is broadly defined by the height of the plant varieties found within, a variable determined exclusively by water supply. This includes water from precipitation, snowmelt, and runoff (Weaver, 1954). The three plant communities are: the tallgrass (true prairie) grasses, found in the easternmost prairies, short grass varieties found in the far western prairies, and the mixed-grass prairie which grows in the central region (Anderson, 2006). The grasses are all supported by deep and/or dense root systems which allow plants to access stored soil water resources (Weaver, 1954). Tallgrass prairie species are found where the greatest annual precipitation occurs (625-1200 mm/year), and can grow to between 1.8 and 2.4 m in height. In the dry west (300-400 mm/year), short grasses do not exceed 0.3-0.5 m in height. Mixed grasses prairies (400-500 mm/year) grow to between 0.8 and 1.2 m height (Anderson, 2006). The location of different subspecies within each larger community is determined by their

temperature tolerance. Those plants with a higher heat tolerance migrated south and while more cold tolerant varieties are found in the northern region (Kebart & Anderson, 1987). Permanent groundwater reservoirs are present in the prairies, but they are found at too great a depth for the plant roots to access. The largest such reservoir is called the High Plains Aquifer and covers an area of over 45 million hectares across 8 states in the central prairie region (Figure 1.2) (Gutentag, et al., 1984). The aquifer has a mean saturated thickness of 60 m depth and a mean water table depth of 30 m (Strassberg, Scanlon, & Chambers, 2009). It is therefore almost completely isolated from the rooting zone of prairie grasses which has a depth range between 0.5 and 7 m, where 7 m is an extreme anomaly (Anderson, 2006). The separation between the root zone and groundwater reservoirs means that groundwater recharge largely occurs after a precipitation event during the dormant season. The roots take up most of the water quickly during the growing season (Anderson, 2006). Parts of the prairies do experience annual snowfall, however only in certain areas. Expected annual snowfall is determined by external factors (e.g. El Nino Southern Oscillation (ENSO)) which will be further discussed in section 1.2.3 (Kunkel, et al., 2009). In general, the northern prairie experiences the bulk of snowfall, but the entire prairies receive less snow than areas along the same latitude in North America (Brown, Brasnett, & Robinson, 2010). Snowmelt feeds water to permanent surface rivers and prairie potholes, which are only found in the northern prairies, primarily in Canada (Fang, 2010). The High Plains region also contains wetlands, known as playas, which are important for groundwater recharge but receive water inputs from precipitation and overland sheet flow only (O'Connell, et al., 2012). These small wetlands only cover approximately 6% of the southern portion of the aquifer (area within Texas and New Mexico), yet account for slightly less than 50% of groundwater recharge (Wood & Sanford, 1995).

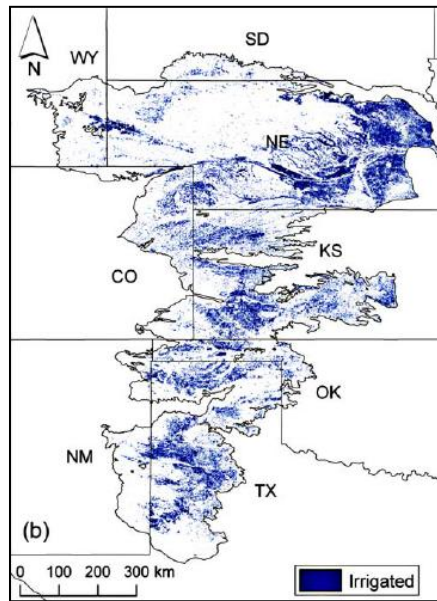


Figure 1.2: Extent of the High Plains Aquifer outlined with areas of irrigated agriculture highlighted in blue based on available satellite data from 1992. The aquifer overlaps area from 8 states: Wyoming (WY), South Dakota (SD), North Dakota (ND), Colorado (CO), Kansas (KS), Oklahoma (OK), Texas (TX), and New Mexico (NM).

---

*Note.* Adapted from Strassberg, G., Scanlon, B. R., & Chambers, D. (2009). Evaluation of groundwater storage monitoring with the GRACE satellite: Case study of the High Plains aquifer, central United States. *Water Resources Research*, 45, 1-10.

### 1.1.2 Palaeoclimatological Evolution of the Prairies

The origins of this ecosystem are found approximately 7.5 million years ago during the Miocene-Pliocene transition (Axelrod, 1985; Eronen, et al., 2012). At this point, the palaeoclimatological record shows a worldwide trend towards greater aridity and declining CO<sub>2</sub> concentrations as the planet cooled and the Antarctic Ice Sheet expanded. Grasslands began to flourish around the world as forests retreated (Anderson, 2006; Ehleringer, Cerling, & Helliker, 1997). Additionally, the Miocene was a period of increasing seasonality. Anderson (2006), has referred to this as a monsoon climate over North America. It is hypothesized that all of these factors led to the dominance of grassland species. The desiccated biomass during the dry season provided fuel for substantial fires, which kept trees or larger vegetation from retaking grasslands (Keeley & Rundel, 2005). Fires would have also been started by lightning strikes at the

beginning of the dry season (Anderson, 2006). Herbivory by grazing mammals also contributed to a lesser extent by keeping vegetation short and holding back encroaching forests (Axelrod, 1985). All of these changes are found within the plant and animal fossil record (Anderson, 2006; Keeley & Rundel, 2005). By the Pliocene, temperatures had begun to cool and by the transition to the Pleistocene epoch, approximately 1.8 million years ago, the Northern Hemisphere was under a period of glaciation (Lyle, et al., 2008). During this period, the number of grazing species increased (Anderson, 2006). From the end of the last glaciations until the present day, precipitation decreased and the prairies took the form that it is found in now, a large, dry, grassland area surrounded by forests (Axelrod, 1985).

### **1.1.3 History of Agricultural Development**

Any substantial human impact in North America is the product of less than 300 years of development, largely by European settlers. In that time, the vast majority of the grasslands have been taken over for cropland and pastures (Ramankutty & Foley, 1999). Pre-European Aboriginal settlements were present, however their extremely small scale excludes them from this discussion. During the middle of the 19<sup>th</sup> century, both the Canadian and American governments began to focus on pushing their influence further west into the centre of the continent. Two acts were created, the Canadian Dominion Lands Act of 1872 and the American Homestead Act of 1862. These promised pioneers large farming properties, among other things, as long as they could settle the land (Sieg & Flather, 1999). These acts were brought about at the same time that both national rail networks were undergoing similar massive western expansions. This even further opened the west to farming, allowing goods to be transported much quicker (Schafer & Holland, 2009). For the next century, prairie agriculture boomed and land was quickly converted, replacing huge portions of the natural grassland. The conversion was so

expansive that, depending on the province or state, between 82 and 99% of all tallgrass prairie, 30-99% of all mixed grass prairie, and between 20 and 86% of all shortgrass prairie had been replaced by the mid-1990s (Samson & Knopf, 1994). The mass conversion continued, and by 2003, approximately 70% of the entire prairies, across all three plant groups, had been converted for agricultural purposes. (Samson, Knopf, & Ostlie, 2004). What replaced the grasses were largely cereal crops such as corn, maize, wheat, soybean, and barley (Leff, Ramankutty, & Foley, 2004).

Unfortunately, the prairie climate and limited available water made it impossible to sustain these types of crops without intervention. The first farmers relied almost completely on aboveground sources of water, precipitation, and snowmelt (Rosenberg, et al., 1999). However, these practices soon proved unsustainable. The crops have greater water needs and relying on natural sources of water made farmers extremely susceptible to droughts, which are a regular occurrence on the prairies. By putting the prairies under greater than normal water stress, the drought, which occurred during the 1930s was exacerbated, leading to the Dust Bowl period that devastated the entire agricultural industry (Cook, et al., 2007). The interactions between agriculture and drought will be further discussed in section 1.2.2. Recognizing a need for a change in practices, North American farmers became more reliant on irrigation, which draws water from deep groundwater reservoirs to supplement the greater water needs of the introduced crop species. One particular area, the High Plains region in the centre of the American prairies, is the largest irrigated area in the entire United States (Scanlon, et al., 2007). In 2000, irrigation accounted for approximately 97% of the roughly 24 km<sup>3</sup> of water taken up from the High Plains Aquifer (Strassberg, Scanlon, & Chambers, 2009). The heavy irrigation is an unsustainable practice. Rodell & Famiglietti (2002) found that by 1980, approximately 205 km<sup>3</sup> of water had

been removed by farmers. The height of the water table was found to have dropped significantly; in some places more than 30 m due to irrigation demands. In Canada, this did not occur as drastically. There is much more available surface water due to the damming of major rivers and the spring snowmelt. As of 1991, groundwater only accounted for 4% of all water usage in Canada (Gan, 2000). From surface water sources, there has been a loss of 50-75% of all prairie wetlands in Canada (Fang, et al., 2010) and rivers have been severely modified to conform to agricultural needs throughout the prairies. Tile drainage and channel widening and straightening have increased the rate of flow and have made surface water resources more polluted and have increased sediment loads in streams. Additionally, the heavy dependence on groundwater has meant that some surface water sources are being cut off from groundwater discharge as the water table sinks, and remain dry during the summer (Dodds, et al., 2004; McGee, Boon, & van Meerveld, 2012).

## **1.2 Literature Review**

The following section will describe the changes that have been brought about as a result of the agricultural conversion of the prairie grasslands. The differences between the natural prairie, as described in section 1.1, and the agricultural environment that replaced it are the result of the physiological differences in the plant species found within each land cover type. These changes influenced the hydrological and climatological cycles, effectively reshaping the ecosystem over a period of approximately 100 years.

### **1.2.1 Biological Differences**

The most important change that occurs as a direct result of LULCC is the type of vegetation. As natural grasslands, the prairies were dominated largely by grasses that were part of the C4 photosynthesizing plant variety. What distinguishes C4 from the more primitive C3

plant variety are the temperature conditions and the photosynthetic efficiency of light use. C4 plants are better adapted to arid and/or semiarid conditions and as a result are able to photosynthesize at greater rates under hotter conditions (Still, et al., 2003; Pearcy, et al., 1981). Growing season daytime temperatures should be above 30°C, assuming adequate water availability for C4 plants to dominate the prairies (Anderson, 2006). Because C3 species are generally able to survive a wider range of temperatures, they are generally more common around the world (Teeri & Stowe, 1976). Conversely, the most common prairie crops are predominantly C3 plants (Still, et al., 2003). Corn is the exception. Having been originally cultivated in tropical Mesoamerica, as opposed to Europe and Asia, it is a C4 plant and is therefore naturally more adapted to the prairies (Wilkes, 2004). Within the context of this thesis, the most important difference between the two varieties (C3 and C4) is their water efficiency (Still, et al., 2003). The C4 varieties are better adapted to retaining and conserving water within the plant, allowing them to survive the hotter temperatures. The C3 grasses have greater water requirements to prosper and they use water less efficiently, losing more to the atmosphere (Anderson, 2006; Teeri & Stowe, 1976).

The poorer water efficiency is combined with a significantly different root structure, which further limits crops access to naturally available water sources. Left to grow to full sensecense, these crops would develop a very similar root profile to the natural grasses. Both categories of plants develop a maximum rooting depth of slightly deeper than 2 m ( $2.1\pm 0.2$  m for crops and  $2.6\pm 0.2$  m for temperate grasslands measured in the central prairies) (Canadell, et al., 1996). The 7 m depth discussed in Anderson (2006) in section 1.1.1, is an extreme outlier in a sample which yielded a mean depth of 2.36 m with a standard error of 0.24 m. Schenk & Jackson (2002a) found that root depth (of natural vegetation) is controlled largely by mean annual

precipitation. As a result, vegetation in drier areas, like the prairies, has the shallowest rooting depths. However, the lateral spread of roots tends to be greater in such environments. Such a development allows plants to take advantage of near surface soil moisture over a larger area. Moreover, there is less competition and crowding, giving each plant more space to expand laterally (Schenk & Jackson, 2002a). The relationship between precipitation and root depth is so strong that the percentage of roots at depth can be tracked logarithmically against an aridity gradient moving from wet to dry (Schenk & Jackson, 2002b). This applies to both C3 and C4 varieties of grasses and demonstrates the importance of water infiltration into the soil. Specific changes to the hydrology on the prairies, and subsequently precipitation and infiltration will be discussed in the next section.

When discussing root depth and lateral spread in cropped fields, harvest practices play an important role in controlling root development. The structured growing season, where the fields are left bare until the crops are planted (Pielke, Sr., et al., 2007) and the harvesting of crops inhibit full root development. A controlled experiment carried out in Missouri found that: 90% of winter wheat, 84% of soybean, and 91% of corn root biomass was found within the top 0-20 cm of the soil after harvest (Buyanovsky & Wagner, 1986). The differences in root physiology and water efficiency (C3 crops) have meant that crops in the prairies are extremely restricted in access to water sources. These distinctions help to explain why the pre-irrigation drought seasons were so severe when compared against prairie droughts from the same time. By providing irrigation, farmers were able to overcome the limitation of C3 water use efficiency with previously inaccessible groundwater. Overall, this increased the total amount of available surface water, Subsequently, the potential evapotranspiration rate (PET) is increased, increasing the potential flux of water from the biosphere to the atmosphere. Calculating the change to the actual

evapotranspiration rate (AET), the flux of water within the maximum potential rate is difficult given the large scale of the study areas as well as the variety of different grass species within the prairies.

From aboveground there are a few biological differences between the prairies grasses and the replacing crop species. Prairie crops tend to be taller than the grasses, increasing their roughness length, and therefore modifying the aerodynamic resistance which carries an influence on the flux of water to the atmosphere. Furthermore, the crops have a greater leaf area index (LAI) than the grasses which will also increase the PET. All of these changes are made more drastic if the fields are irrigated (Pielke, Sr., et al., 2007).

### **1.2.2 Hydrological and Climatological Changes**

The combination of the new vegetation and the impact that it has had on water fluxes between the soil, plants, and atmosphere has a compounding impact on the larger hydrological and climatological patterns. Through the use of several environmental proxies, it has become possible to plot the past 1200 year hydrological history of the western prairies (Figure 1.3) (Cook, et al., 2004). What these records have revealed is that droughts are an expected, cyclical event on the prairies. However, it has also revealed that events known as ‘megadroughts’ also occur. This historical proxy record helps to contextualize 20<sup>th</sup> and 21<sup>st</sup> century droughts. These are periods of extended and extreme drought, more severe than any recorded in modern times. The most intense ‘megadrought’ example occurred in the mid-10<sup>th</sup> century and lasted for 23 years. The closest modern facsimile to this was the drought of 2002, which displayed a similar pattern of high aridity in the west. This drought however, only lasted for one year. The earlier droughts (pre-20<sup>th</sup> century) were found to have occurred during a time when aridity and solar irradiance were both higher than they are today (Cook, et al., 2007).

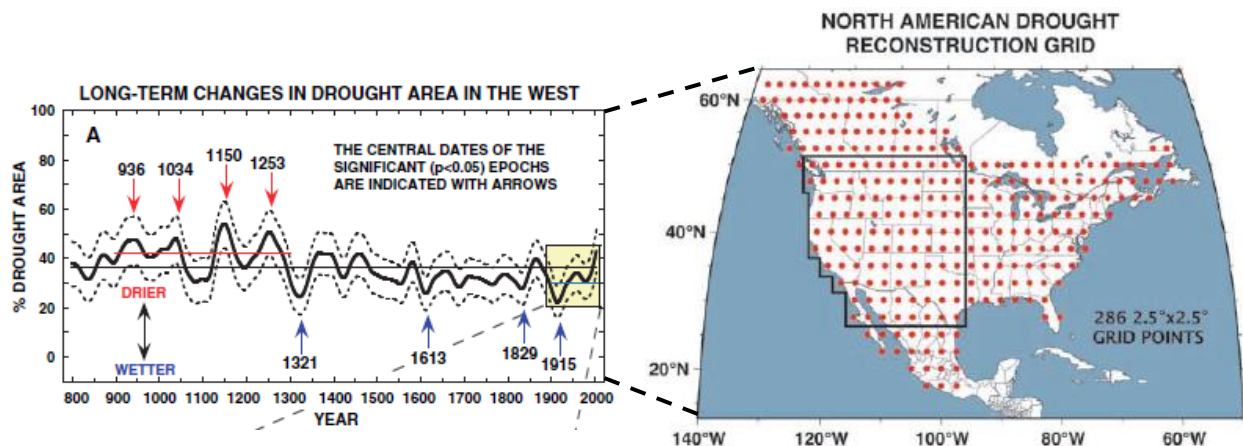


Figure 1.3: Historical drought record for the Western United States, including the prairies, beginning in 800 B.C.E.

*Note.* Adapted from Cook, E. R., Woodhouse, C. A., Eakin, C. M., Meko, D. M., Stahle, D. W. (2004). Long-term aridity changes in the Western United States. *Science*, 306, 1015-1018.

The Dust Bowl was the worst drought in North America since 1700. The year 1934, the driest year of that drought, was the driest single year since 1580. One change that separates this period from the previous 500 years, is the introduction of agriculture. This event is even more surprising in the drought record because the decades leading into the 1930s, were above average years in the Palmer Drought Severity Index (PDSI) (Fye, Stahle, & Cook, 2003). The PDSI is a very commonly used drought index, which is used to track meteorological and hydrological droughts (when precipitation is reduced and when that reduction has an impact on surface and/or subsurface water sources) (Heim, Jr., 2002). It does this by estimating a given year's supply and demand for water using antecedent precipitation and temperature (Mishra & Singh, 2010). Drought is also influenced by sea surface temperatures (SST), specifically the variations in the Pacific Decadal Oscillation (PDO) and ENSO, which influence soil moisture, particularly in the American prairies (Mo & Schemm, 2007) (section 1.2.3). However, the influence of agriculture should be emphasized, particularly in the prairies where Dirmeyer, et al. (2013) found that climate in the prairies has a significant influence on atmospheric conditions.

From a climatological perspective, the largest change between the original grassland and agriculture not related to biological functions is plant albedo. In general, crops and grasses (all varieties) have a very similar range of albedo (Oke, 1987). Agricultural fields however have periods where bare soil is exposed both before the growing season and after the harvest periods. In the natural grasslands, growth begins as soon as the snow melts and continues until it returns. This gives the grasslands a higher albedo during the snow free period (Pielke, Sr., et al., 2007). Few studies have conducted more in-depth intra-annual analysis of albedo variability between the two land cover types. Song (1999) however conducted a field scale experiment that found that under natural grassland conditions, prairie albedo decreases in a linear pattern between spring and early winter, meaning they get darker as they mature in a highly predictable way. A maize and a winter wheat field in Kansas were also observed. After the crops began to develop a canopy, covering the bare soil, it was found that maize albedo increased as the field reached senescence. Winter wheat followed a more similar pattern to the grassland, decreasing steadily until harvest. However, the decrease occurred at a much slower rate. Both crop types did have an average lower albedo than the grasslands case (Song, 1999). These results cannot be directly extrapolated onto the whole prairies. For example, Wang & Davidson (2007) found that summertime albedo for grasslands in Saskatchewan had very little inter-monthly variability. Nevertheless, in general, it can be stated that the shift in land cover results in a slight decrease in albedo overall. In the southern prairies, this difference is further emphasized because the growing season is long enough to allow for multiple crop rotations, creating multiple periods of bare soil throughout the year (Zhang, 2012).

The implication of this modification to albedo is found in the calculation of net radiation. There is an increase in energy available at the surface which has an influence on convective

activity within the planetary boundary layer (Mahmood, Leaper, & Quintanar, 2011). By modifying the PBL, introducing agriculture also influences cumulus convective precipitation (Pielke, Sr., 2001). The land cover change has made temperatures warmer at the surface. When combined with the biological changes (LAI, roughness length, and PET) that facilitate changes to the water flux, agriculture on the prairies has been shown to increase convective activity (Pielke, Sr., 2001; Mahmood, Leaper, & Quintanar, 2011). Given the same potential storm conditions, Pielke, Sr., (2001) found that a mixed natural and cropped area produced thunderstorms while the completely natural control area only produced cumulus clouds with no activity (Pielke, Sr., 2001).

### **1.2.3 Remote Influences on Prairie Climate**

Land cover has an impact on prairie climate patterns (Pielke, Sr., et al., 2011). However, the prairies are a massive ecosystem that crosses approximately 35 degrees of latitude. As such, there are many other forces that control aspects of the overarching climatology. There is a body of research that has investigated how external climate patterns, such as teleconnections, have influenced the prairies. These patterns are both continental and synoptic (i.e. global) in scale. All of the vegetative and climatic changes described in sections 1.2.1 and 1.2.2 have been shaped by three large air masses: the Polar, Gulf, and Mountain Pacific masses. The influence of the masses is seen in the temperature and precipitation gradients across the continent (Anderson, 2006). The Gulf Mass moves northwesterly into the eastern prairies, bringing humidity and causing a higher volume of precipitation and convective storms. This effect fades as the Gulf Mass runs into the Pacific Mass, moving east over the Rocky Mountains, which produces the drier and warmer climate in the western prairies. The temperature gradient is controlled by the Polar Mass which brings cool air and snowfall from the Arctic, into the Canadian region. The mixing area in the

centre of the continent produces the mixed grass species (Anderson, 2006; Kebart & Anderson, 1987). On an even larger scale, is the climate forcing exerted by SST, which has been frequently linked to climate variability and moisture advection on and into the western continental United States (Cook, et al., 2004; Hu & Huang, 2009). The reverse relationship, how LULCC may be impacting these large teleconnection patterns, has not been explored in the literature. (Pielke, Sr., et al., 2011). Different phases of the ENSO cycle have been linked, by multiple sources, to variability in precipitation, a connection which is modified by the seasons. The connection is further modified by other lower-frequency signals, such as the PDO which occurs generally in correlation with ENSO (Hu & Huang, 2009; McCabe, et al., 2008). Both can have an individual impact, however, when both ENSO and PDO are in the same phase with El Nino and a warm PDO (La Nina and a cool PDO), there is an anomalous increase in soil moisture (decrease). This is not as strong when each teleconnection is in the opposite phase (Hu & Huang, 2009). In the northern prairies, ENSO also carries implications for extreme snowfall events. During an El Nino event, when the northern prairies are experiencing anomalously high temperatures, the probability of extreme events is depressed. However, the influence of teleconnections cannot be taken in isolation, particularly during the 20<sup>th</sup> century (Kunkel, et al., 2009). Climate change has played a role in increasing temperatures and modifying soil moisture as well.

So far, only natural remote influences have been discussed. These two processes have been acting on the prairies for a very long time. Anthropogenic climate change however, also has a remote influence on prairie climate. The Intergovernmental Panel on Climate Change (IPCC) (2007) Fourth Assessment Report demonstrated that global mean temperatures have been increasing, and are expected to continue increasing into the future due to rising concentrations of greenhouse gases in the atmosphere. On the prairies, the increase in carbon dioxide (CO<sub>2</sub>) is

expected to increase temperatures. Moisture availability is expected to decrease in the south as arid conditions expand, but increase in the north, creating a more humid environment (Polley, et al., 2013). The CO<sub>2</sub> concentration has increased 37% since 1750 to 379 ppm globally (IPCC, 2007). While it is driving changes to climate, it is increasing biomass in semi-arid grasslands, despite soil moisture limitations (Morgan, et al., 2011). Where there is snow, snowpack volume is expected to decrease and melt times are expected to begin earlier. Precipitation is expected to generally decrease with a greater proportion of rain falling as part of extreme convective events (Polley, et al., 2013).

is expected to counter rising temperatures over semi-arid grasslands. CO<sub>2</sub> increases have been shown to increase aboveground biomass, but suppress transpiration, and subsequently improve water use efficiency, reducing water loss through transpiration. However, this was found to benefit C4 grass varieties over C3 species (Morgan, et al., 2011). This means that the remaining natural grasslands may actually benefit in the short term from climate change. Agriculture will likely suffer more under hotter temperatures, placing more emphasis on irrigation in future. Additionally, any increase in water use efficiency would be erased, irrespective of plant functional type, due to a period of sustained drought which would quickly consume the excess soil moisture (Morgan, et al., 2011). The future of prairie agriculture in North America is therefore at risk of sustained droughts under more water stressed conditions due to irrigation, while supporting ill-adapted crop species.

### **1.3 Motivation**

Based on the content of the literature review, it can be stated that the literature has reached a consensus that the shifting of land use and land cover (either natural or anthropogenic) can have an impact on climate (Pielke, Sr., 2005). There are a large number of studies which

have examined this phenomenon, primarily from one of two perspectives. The first is a global perspective, wherein a model is used to evaluate changes in net radiation and surface albedo over areas which have historically undergone some form of land cover alteration. The results of these studies are generally averaged over the entire planet as in Matthews, et al. (2003). The second perspective is a much more regional or local approach. These studies typically look at microclimatological and/or ecohydrological changes within a given area. They either compare contemporary sites under different vegetation regimes or are longitudinal studies that track changes in a location as it undergoes a change in land cover, as in Adegoke, Pielke, Sr., & Carleton (2005). Studies from both of these perspectives use a mixture of modelling tools and observational data to complete their analysis. The first methodology is extremely broad in scope and the results cannot provide any insight into the impact of change on a specific ecosystem. The second overcomes this limitation; however, such small scale studies rarely evaluate ecosystems in their entirety. This thesis bridges the two spatial scales and seeks to explain how agricultural development in the North American prairies has specifically influenced the short term and long term climatology of the entire prairie ecosystem. The prairies in particular were selected for this study site because the transition from the natural prairie grasses to extensive croplands occurred so quickly. Since 1700, no other part of the world has undergone such an extensive transition to cultivated lands (Ramankutty & Foley, 1999). The historical nearness of this event has therefore made it possible to find records of the pre-existing climate. These factors, and the geographic size and relative vegetative uniformity of the prairies, make the ecosystem a good testing site for evaluating the climatic impacts of agriculture on a large scale.

## **1.4 Objective**

It is hypothesized, based on the presented literature, that the shift in land cover over the North American prairies has had a recognizable impact on the climatology over the same region. The objective of this research is to explain how agricultural development may create these changes and to illustrate the importance of including land use and land cover change in future discussions of anthropogenic climate change. Both in-situ observational and modelled data will be used to test this hypothesis.

## **1.5 Structure**

This document contains five chapters. The first chapter outlines the body of research which has been conducted so far on the interaction between agricultural development and climate, with a particular focus on outcomes in the North American Prairies. This chapter places these changes within their proper historical context and explains both internal and external forces which control prairie climate. Additionally, this chapter describes the motivation and objectives of this particular study. Chapter 2 describes each of the data, methodologies, and models used to test the hypothesis of this thesis. Chapter 3 outlines the first study conducted in this thesis. This study uses available historical land cover and climate data to compare changes in climate across the 20<sup>th</sup> century. Chapter 4 outlines the second study, which was done in a modelled environment. This methodology used a comparison of one year's modelled climate under two distinct land cover types (agriculture and grassland) over North America in order to evaluate the instantaneous differences in the radiation balance and the water cycle caused directly by the change in land cover. The final chapter, Chapter 5, summarizes the results of the two studies and proposes possible future research directions.

## **Chapter 2: Data and Methods**

### **2.1 Data Descriptions**

This chapter will present the data and methodologies that were used in generating the results that will be presented in Chapters 3 and 4. These chapters present two different methods to answer the question of how the introduction of agriculture has changed prairie climate.

Chapter 3 uses observation based historical datasets to present the long term changes that have actually been observed on the prairies. In Chapter 4, a coupled atmospheric and land model is used to simulate the differences in climate between the two land cover types (natural prairie grasslands and agriculture) over the period of one full year. Comparing the differences over one year ensures that the entire growing season is presented in the results and any residual effects that the change in land cover may have on winter (snow volume) can also be demonstrated.

In the first method, the observation analysis used the 20<sup>th</sup> century portion of the Global Potential Vegetation Dataset from Ramankutty & Foley (1999) to identify areas within the prairies that are both heavily cultivated, to represent the human induced perturbation (PERT), and remain largely natural, to act as a control area (CTRL). This process will be further elaborated on in the following sections (2.3.1). These areas were then used to mask out the climate data at the beginning and end of the 20<sup>th</sup> century. The climate data within the CTRL and PERT areas were then averaged over the two prairie regions at both the beginning and end of the 20<sup>th</sup> century for the purposes of comparison. Three different climate datasets were used in this first experiment. They were the 20<sup>th</sup> Century Reanalysis Project, which is a global dataset of tropospheric climate variability that uses only surface pressure reports to generate reanalysis climate data between 1871 and 2001 (Compo, et al., 2011). The second two are temperature datasets, which are created based on actual in-situ observations. The first is the CRUTEM4 temperature anomaly data from the Climate Research Unit (CRU) at the University of East

Anglia (Jones, et al., 2012). The second is from the University of Delaware and is described in Matsuura & Willmott (2009). Each dataset will be further described in sections 2.1.1 - 2.1.3.

In the second method used in this thesis, the modelling experiment used the Geophysical Fluid Dynamics Laboratory (GFDL) coupled global atmosphere and land model (AM2-LM2). The model was run for a control scenario (GRASS) wherein the prairies were covered exclusively by a predefined grassland land cover type. A second perturbation scenario (AGRIC) was run where the grasslands were replaced by a globally generic agriculture land cover type. This change was limited to only those cells classified as grassland within North America. Other grassland areas around the world remained grasslands in the perturbation simulation. The two land cover types were distinguished from each other by the depth scale of the root distribution, the root biomass areal density, the roughness length, and the potential range of albedo under snow-free condition. All of these changes took place within the land model component. The atmosphere model was left unperturbed under the AGRIC scenario. The GRASS scenario results were then subtracted from the AGRIC scenario results (AGRIC-GRASS). The resulting plots demonstrated the changes to the environment caused by only changing the land cover type. Chapter 4 presents the monthly mean hydroclimatological conditions for the GRASS scenario and the response. Both experiments were conducted in a LINUX operating system using the C-shell command programming language. The analysis was completed using CDO (Climate Data Operators) and plots and maps were generated using NCL (NCAR Command Language) developed by the National Centre for Atmospheric Research and Microsoft Excel.

### **2.1.1 Global Potential Vegetation Dataset**

The Global Potential Vegetation Dataset (GPVD) is comprised of two components (Ramankutty & Foley, 1999). The first is a global static map of natural vegetation cover. This

map is intended as a tool to contextualize agricultural development. It shows which ecosystems are under agricultural pressure. Natural vegetation was characterized differently over areas dominated by human activity from those regions where human land use influences dominate. In the first case, vegetation type was determined for each cell based on a classification scheme with 15 separate vegetation type classes. Only upland vegetation types (non-wetland areas) were included (Ramankutty & Foley, 1999). This scheme is a reclassification of the DISCover land cover classification from the Olson Global Ecosystem framework (Ramankutty & Foley, 1999). DISCover is a satellite based dataset that uses a finer resolution than the 5 min resolution that the GPVD was built on. The second case, where human land use dominates within a cell, the natural vegetation was determined by the potential vegetation dataset described in Haxeltine & Prentice (1996). Potential vegetation refers to the natural vegetation type that would exist within a cell before human activity. Human land use was considered dominant within a cell if it passes either of the following conditions: when crop cover (calculated in the second component) in 1992 accounted for >50% of the cell, or the dominant vegetation type (of all 15 DISCover classes) accounted for <20% of the entire cell area (Ramankutty & Foley, 1999).

The second component of the GPVD is a series of global annual maps between 1700 and 1992, which was created based on a global cropland extent map produced for 1992 by Ramankutty & Foley (1998). A second version of this dataset displays changes in pasture lands over the same time period. Pasture connotes land used for livestock. That map compiled the cropland classes from the DISCover classification scheme against available cropland inventory data for 1992 on a 5 minute longitude and latitude resolution grid. Each cell is assigned a crop coverage value which, for the purposes of this thesis, will be referred to as  $C_f$  (crop fraction). The  $C_f$  value represents the fractional area of the cell that is covered by croplands. Using 1992 as

initial conditions, a land cover change model was used to backcast the historical  $C_f$  values for each cell. The maps are set on a 0.5 degree resolution latitude by longitude grid. An updated version of the original dataset was used, which includes the years 1993-2007. An inventory was collected of historical croplands directly from the Food and Agriculture Organization (FAO) of the United Nations at the national level. Information for large nations, including Canada and the United States were supplemented by subnational records for the purpose of imposing constraints on the land cover change model (Ramankutty & Foley, 1998; Ramankutty & Foley, 1999).

### **2.1.2 20<sup>th</sup> Century Reanalysis Project**

Climate reanalysis is a method used to interpolate synoptic scale weather by using the weighted mean of available meteorological observations and a first guess, 56 member ensemble, result from a numerical weather prediction (NWP) model (Compo, et al., 2011). First guess refers to the model output, which backcasts weather under observed boundary conditions. The 20<sup>th</sup> Century Reanalysis Project (20CR) specifically, uses the 2008 National Centres for Environmental Prediction (NCEP) Global Forecast System as its NWP and treats interpolated monthly sea-surface temperatures and sea-ice concentration as boundary conditions. The only meteorological observations included in this reanalysis product are surface pressure and sea-level pressure reports. Historically, these three observations have been consistently taken since the end of the 19<sup>th</sup> century. Data was assimilated using the multivariate Ensemble Kalman Filter data assimilations system (Compo, et al., 2011). The ensemble refers to the number of times that the NWP was run. The 56 runs were averaged to produce the final climate data product. The final product of the 20CR contains global tropospheric climate variability data generated between 1871 and 2008 at a 2 degree spatial resolution with data available at 6-hourly intervals (Compo, et al., 2011).

There are inherent errors in this type of climate data. Over time, data assimilation techniques, observation networks, and NWP models all change. This introduces sources of error, which will be discussed in more detail in Chapter 3. This makes it difficult to create consistent reanalysis products, particularly ones which have a long historical reach. This is somewhat overcome in 20CR by the retroactive standardization of each source of error however, as Ferguson & Villarini (2012), demonstrates, there are still errors in the final product. This study tested the 20CR for inter-annual homogeneity in the central United States. The study found a change in all variables between 1940 and 1950 which was not substantiated by the Climate Research Unit (CRU) version 3.1 records for the same period. Due to the newness of the 20CR product (published in 2011), relatively few such studies have been carried out on this particular product. Ferguson & Villarini (2012) is also the only critique that directly addresses the study area of this thesis.

### **2.1.3 Observation Data**

Two separate in-situ climate observation datasets were used in the observation analysis. The CRUTEM4 is a 5 degree latitude by longitude resolution dataset of air temperature (over land) and sea surface temperatures (over the oceans) monthly anomalies based on a climatology taken between 1961 and 1999. The CRUTEM4 dataset was created using monthly temperature station data from 4842 separate stations around the world. The climate anomaly method was used to reduce the bias that can be introduced by varying densities of observation stations. The dataset includes information from January of 1850 until the present (Jones, et al., 2012). The second dataset is the Terrestrial Air Temperature: 1900-2008 Gridded Monthly Time Series. This dataset was created at the University of Delaware. It uses three spatial interpolation methods to create a 0.5 degree latitude by longitude resolution grid of monthly average air temperature. Grid

cells without available monthly air temperature data were determined based on neighbouring cells. This means that even at the beginning of the 20<sup>th</sup> century, this series provides a full planet resolution, despite the issues associated with station network densities being low during that period (Matsuura & Wilmott, 2009). The two separate datasets were used because each dataset was created using a different methodology and because the University of Delaware dataset presents an interpolated global map for the entire century.

## **2.2 Model Description**

### **2.2.1 Coupled Atmosphere and Land Model v.2.1**

All of the results presented in Chapter 4 of this thesis are the product of the GFDL (Geophysical Fluid Dynamics Laboratory) coupled atmosphere and land model (AM2-LM2) (Anderson, et al., 2004). The land model used is a modified version of the Land Dynamics model (LaD), first published in Milly & Shmakin (2002a). The global model is divided into individual cells and the hydrologic and radiation cycles are calculated separately for each cell. LM2 primarily moves water between three major reservoirs (root zone, groundwater and the snowpack) based on a series of strictly defined linear pathways (Milly & Shmakin, 2002a). There are 18 distinct soil layers which store energy as sensible heat. Latent heat is stored within the snowpack layer and glaciers but not in the surface soil. The original LaD model did not account for soil latent heat, so temperature changes in the root zone reservoir are ignored and soil water is not allowed to freeze (Milly & Shmakin, 2002a; Anderson, et al., 2004). After being integrated into the AM2 model, every soil grid cell is assigned 300 kg/m<sup>3</sup> of ‘freezable water’ which is never integrated into the larger hydrologic cycle. The movement of water through the full hydrologic cycle for unglaciated cells will be described in full in the next section (2.2.2).

To simulate the differences to the energy and water cycling found under different land cover and soil types, the LaD model prescribed a set of defining variables for each land cover and soil type. Land cover type was defined by: snow free surface albedo, roughness length, non-water-stressed bulk stomatal resistance, rooting depth of vegetation, and snow masking depth. Snow masking depth takes into account that a different critical mass of snow is required to cover vegetation of different heights before the albedo of an area can increase (Milly & Shmakin, 2002a). Soil type is determined by the prescribed variables: available water content, ground heat capacity, and thermal diffusivity (Milly & Shmakin, 2002a).

The net radiation is calculated by:

$$R_n = R_s(1 - A) + R_l - \sigma T_0^4 \quad (2.1),$$

where  $R_s$  is the incoming solar radiation,  $R_l$  is the atmospheric radiation,  $\sigma$  represents the Stephen-Boltzmann constant, and  $T_0^4$  is the surface temperature. The emissivity of the planet is taken as a global constant. Albedo is calculated as the weighted mean of snow free ( $A_n$ ) and deep-snow albedo ( $A_s$ ):

$$A = (1 - \beta)A_n + \beta A_s \quad (2.2),$$

$$\text{where: } \beta = W_s / (W_s + W_s^*) \quad (2.3).$$

In the second equation,  $W_s^*$  is the snow masking depth and  $W_s$  is the water balance of the snowpack. The deep snow albedo is a function of temperature and ranges between 0.45 and 0.6 over nonglaciaded cells (Milly & Shmakin, 2002a).x

On its own, the AM2 atmospheric model uses a gridpoint dynamical core in association with the staggered Arakawa B grid with a resolution of  $2^\circ$  latitude x  $2.5^\circ$  longitude. The atmosphere is divided into 24 distinct vertical layers with the top of the model set at 40 km. The first nine layers are within the bottom 1.5 km of the atmosphere, ensuring a fine resolution within

the boundary layer (Anderson, et al., 2004). Radiation is set on a diurnal cycle and calculated on a 3 hour basis. The model also contains a fully prognostic cloud scheme which contributes to the calculated aerosol concentrations and vertical diffusion of temperature throughout the vertical axis. Additionally, the cloud scheme helps in the determination of convection patterns and in distinguishing deep and shallow convective patterns. The model differs over time based on a gravity wave scheme (winds) and advective patterns. The calculation of precipitation in the AM2 has the biggest influence on LM2 and the results presented below. This is a part of the convection parameterization. For deep convection areas, 0.975 is the fraction of water which is condensed in cumulus clouds and eventually becomes precipitation. Deep convection dissipates at 500 hPa. Under shallow convection, that fraction is 0.5 and it dissipates below 800 hPa (Anderson, et al., 2004). The remaining water then becomes a source of condensate for cloud formation. Convective precipitation can be re-evaporated, however since evaporation from water bodies is not included in the LM2, it will not be changed directly by an altered land cover.

### **2.2.2 Hydrologic Cycle within LM v.2.1**

Water cycling within the GFDL model is based upon a very simplistic set of pathways. Each cell within the model is treated as an individual entity and there is no transfer of water between cells at any stage of the water cycle (Milly & Shmakin, 2002a). The only time that water can be moved to a different location is when it is stored in the atmosphere (Anderson, et al., 2004). The entire series of pathways is shown in Figure 2.1. Once water has been transpired out of a cell in the land model, the atmosphere model (AM2) contains a mechanism for lateral movement of water stored in the atmosphere (Anderson, et al., 2004). In the land model, water enters the cell as precipitation (both as rain and as snow), where it is immediately sent to the root zone (Milly & Shmakin, 2002a).

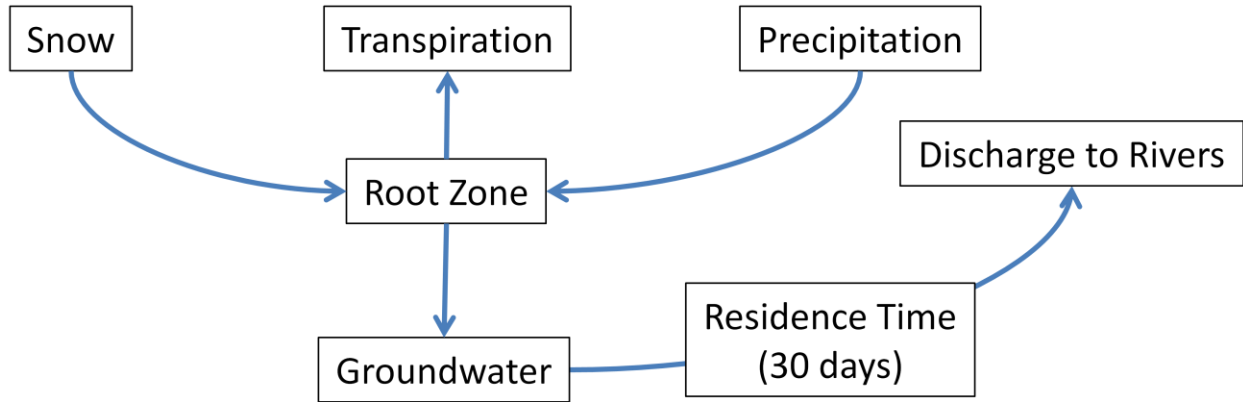


Figure 2.1: Pathways of water within the LM2 component of AM2-LM2.

The total water balance equation does not include a separate surface and root zone water component. Instead, they are combined as a root zone term.

$$W = W_S + W_R + W_G + W_I \quad (2.4),$$

where  $W_S$  is the water storage in the snow pack on the ground,  $W_R$  is the root zone storage,  $W_G$  is storage as groundwater, and  $W_I$  is the water stored within glaciers (Milly & Shmakin, 2002a).

Root zone water does not contribute to evaporation directly (Milly & Shmakin, 2002b). Instead, the land model completely excludes evaporation from soil or intercepted stores and all water that moves to the atmosphere does so through a ‘big leaf’ transpiration model (Milly & Shmakin, 2002a). The model still refers to this term as evaporation. Evaporation is controlled by the non-water-stressed bulk stomatal resistance, a prescribed variable in the original LaD model, aerodynamic resistance, as well as a field capacity term determined by the land cover type (Milly & Shmakin, 2002b). When the LaD model was restructured into the LM2, there was a discrepancy between the expected and actual rate of evaporation based on the amount of precipitation being created, and the radiation balance, in the AM2 (Anderson, et al., 2004). In order to close this gap, the prescribed stomatal resistance was reduced by a factor of 5, thereby increasing the rate of transpiration (Anderson, et al., 2004). This effectively replaced the

evaporation rate. Therefore, once precipitation reached the root zone, the movement of water is controlled by a series of strict pathways and residence times. Root zone water is the balance between precipitation, snowmelt, evaporation, and discharge to the groundwater reservoir (Milly & Shmakin, 2002a), expressed as:

$$\frac{dW_R}{dt} = P_R + M_S - E_R - D \quad (2.5),$$

where  $P_R$  is incoming precipitation and snow that moves directly into the root zone,  $M_S$  is the rate of snowpack melt,  $E_R$  is the rate of evaporation, and  $D$  is the rate of drainage from the root zone (Milly & Shmakin, 2002a). Precipitation is not calculated by the LM2 model. It is calculated in the AM2 component of the model and is controlled by atmospheric processes including cloud cover and convective energy (Anderson, et al., 2004). The evaporation component in this case excludes evaporation from open water bodies. It is a parameterized variable which is a function of the ratio of the density of air ( $\rho$ ) to the combined force of aerodynamic resistance  $r_a$  and stomatal resistance  $r_s$  (prescribed) (Milly, 1992). In other words, the balance between the atmosphere's ability to absorb moisture and the resistance factors working against transpiration (Milly & Shmakin, 2002a):

$$E_R = \frac{\rho_a}{r_a + r_s} [q_s(T_o) - q_a] \min \left[ \left( \frac{W_R}{0.75W_R^*} \right), 1 \right] \quad (2.6),$$

where  $\rho_a$  represents the density of air,  $q_s(T_o)$  is the mixing ratio of water vapour assuming completely saturated conditions, and  $q_a$  represents the mixing ratio at a given height. The second half of the statement is a mixing ratio for water vapour given a surface temperature assuming a minimum of water availability (Milly & Shmakin, 2002a). Field capacity is expressed as  $W_R^*$  as it is the maximum possible value of root zone water storage ( $W_R$ ). It is calculated as the product of the available water capacity (AWC) which is pre-determined based on the soil type, and the root depth ( $Z_R$ ), which is a function of the vegetation type (Milly & Shmakin, 2002a):

$$dW_R^* = AWC * Z_R \quad (2.7).$$

Within this study therefore, the shift in land cover type will have an impact on the storage of root zone water. Because the root zone is shallower in the agricultural type, making the field capacity smaller, the residence time of water in that particular reservoir will be reduced. If the field capacity is being exceeded faster than  $E_R$  can remove soil water, the excess is drained to the groundwater reservoir. However, until this condition is met ( $W_R = W_R^*$ ), discharge does not occur and the water remains in the root zone (Milly & Shmakin, 2002a). This prevents the root zone reservoir from drying completely.

Once water has been moved to the groundwater reservoir, it is kept there for a prescribed residence time ( $\tau$ ) before being converted to outflow and sent out of the reservoir. Milly & Wetherald (2002), explain the process by which the residence time is derived. This paper quantifies the factors that influence the variability of discharge from river basins on a monthly time scale. The calculated residence time is then applied to every cell within each of the river basins (Milly & Shmakin, 2002a). The rate of discharge is then modified to account for water reservoirs (i.e., groundwater and surface water). Unfortunately, this model is strongly based on observational data inputs for calculating variability in precipitation and discharge anomalies (Milly & Wetherald, 2002). This limits the area (i.e. cells) where residence time can be calculated to the few river basins with sufficient data, which are described in Milly & Dunne (2002). In total, this dataset only provides a distinct residence time for 175 large river basins around the world (Milly & Dunne, 2002). In all other instances, a generalized residence time of 30 days was used (Milly & Shmakin, 2002a). The 30 day residence time was utilized in approximately 95.5% of all cells in the global map. Once the groundwater has exceeded its residence time, it is converted into runoff and sent back to the surface (Anderson, et al., 2004).

Runoff is treated as basin discharge and is calculated in the model on a basin scale (Milly & Shmakin, 2002b).

## **2.3 Study and Model Experiment Designs**

### **2.3.1 Reanalysis Study**

The first study used the GPVD and 20CR to track changes in climate and land cover across the 20<sup>th</sup> century. The purpose of this study was to compare temperature at 850 hPa in Kelvin, atmospheric water vapour content (WVC) in  $\text{kg/m}^2$ , and convective available potential energy (CAPE) in J/kg over PERT areas against the CTRL areas which have remained as grasslands. These three climate variables were selected for comparison because the literature has shown that these variables change as a direct result of the shift in land cover. The first two variables have been shown within the literature to have been modified due to the biological differences between the natural grasses and crops and the introduction of irrigation which has increased the amount of water available to evapotranspiration (Pielke, Sr., et al., 2007). Changes to CAPE are more secondary. It has been directly linked to the available atmospheric moisture and temperature (Oke, 1987). As such, increases in these variables through LULCC have more recently been linked to increases in CAPE and, subsequently, convective storms (Pielke, Sr., et al., 2007; Raddatz & Hanesiak, 2008).

To measure changes over time, these variables were compared at the beginning and end of the century. To do this, first, the prairie area was isolated from the global GPVD annual maps by masking out all cells which, in the static ground cover type map, were not classified as either grasslands/steppe or savannah. Then, all landmasses outside of  $119^{\circ}\text{W} - 92^{\circ}\text{W}$ ;  $30^{\circ}\text{N} - 77^{\circ}\text{N}$  and all areas with an elevation greater than 1300 m above sea level were also masked out. This left only those cells within North America which could be considered, assuming the complete

absence of human activity, prairie (Figure 2.3). The elevation restriction was imposed to remove the adjacent Rocky Mountain ecosystem, which has its own unique climate (Peel, Finlayson, & McMahon, 2007). The final modification to the GPVD dataset was to average the  $C_f$  values (percentage of cell covered by agriculture) of the annual maps over the first twenty years (1900-1919) and last twenty years (1980-1999) (Figure 2.3). The 1900-1919 map was then divided into two subsets: one where  $C_f \geq 75\%$  and one where  $C_f \leq 25\%$ . The first category defines the PERT areas and the second defines the CTRL cells.

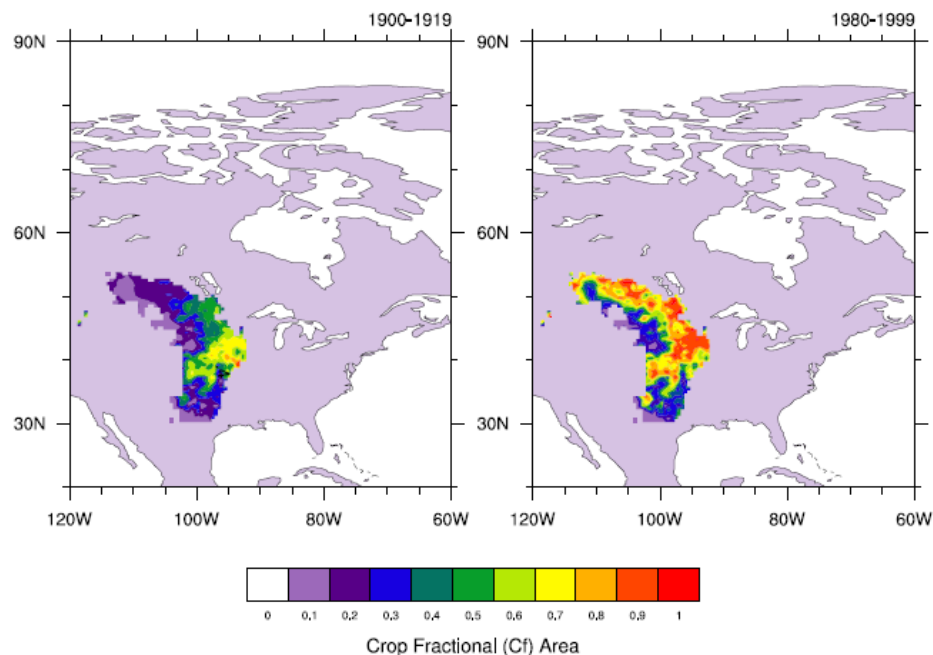


Figure 2.2: Average percentage agricultural cell coverage ( $C_f$ ) of the Global Potential Vegetation Dataset (GPVD) for the first and last 20 years of the 20th century. A  $C_f$  value of 1 represents a completely agricultural cell; a  $C_f$  value of 0 represents a cell which has no agricultural coverage.

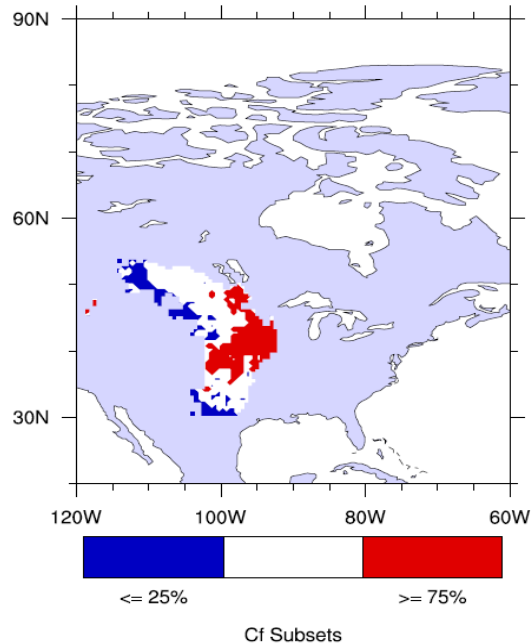


Figure 2.3: Outline of  $C_f$  subset areas used to delineate natural (CTRL) and cropped (PERT) areas. The  $\leq 25\%$  (CTRL) and  $\geq 75\%$  (PERT) areas represent the percentile limits for cells to be categorized as one category or another. The white area shows those cells which fit into neither category.

The cells designated as either CTRL or PERT for 1900-1919 maintained that definition for the 1980-1999 map. This ensured that when comparing the three climate variables between perturbed and natural cells across time, there was no change in the spatial extent of cropland. The only change would be in the  $C_f$  value over time. The final step was to average the climate data from the 20CR over the four different maps (perturbed and control from 1900-1919 and from 1980-1999). The results were then entered into a factorial experiment (Figure 2.4) and change was calculated for both subsets over time (the results from the beginning of the century were subtracted from the results from the end) and the difference between the two subsets was calculated at both points in time. Plots that show the mean annual variability of all three climate variables were also created for all three of the climate variables in order to more fully describe the long term trends across time. Statistical significance was calculated by taking the mean temperature, WVC, and CAPE conditions over both the CTRL and PERT areas at both time

periods across the 20CR ensemble. Then, the results, which will be discussed in the next chapter, were considered statistically significant if the change (over time or between land cover types) was greater than two standard deviations of the calculated field area mean.

20 yr	CTRL	PERT	Effect of LULCC
1900-1919	↓	↓	→
1980-1999	↓	↓	→
Effect of Climate Change	↓	↓	

Figure 2.4: Factorial experiment design. The arrows represent the two directions in which change was evaluated; between the two land cover types and across time.

### 2.3.2 Observation Minus Reanalysis Variation

Observation Minus Reanalysis (OMR) is a tool which was subsequently used to refine the results produced using the 20CR and GVPD. OMR was first described in Kalnay & Cai (2003) as a method to remove the troposphere level climate influence from observation data. A tropospheric reanalysis dataset (i.e. 20CR) is subtracted from the observation data. The resulting dataset contains information between the in-situ network locations and is more accurate to conditions within the planetary boundary layer (PBL) (Kalnay, et al., 2006). The OMR variation was used because the results generated using the 20CR alone will not strongly reflect any changes to climate created by the change in land cover. Available literature has shown that the changes which occur as a result of LULCC are found primarily within the PBL. There may be secondary impacts on higher atmospheric processes, however these are less significant (Findell, et al., 2009). It was found that when the OMR method was applied, it became possible to observe the effects of agricultural development and to identify urban heat islands (Kalnay & Cai, 2003). Additionally, the reanalysis data can help overcome biases introduced into surface observation datasets by changing observation collection methods and in-situ station placements. Since 2003, this method has been applied to several different projects, primarily in China and the United States (Kalnay, et al., 2006; Fall, et al., 2010). Using this method, only temperature was

examined. This was done primarily because temperature data from the beginning of the century is more commonly available than other forms of climate data (Compo, et al., 2011). Secondly, any changes to surface temperature act as a good initial indicator of LULCC in the prairies (Dirmeyer, 2013).

The two temperature observation datasets (i.e. CRUTEM4 and University of Delaware) were used in the OMR variation separately. In order to make the two datasets comparable, the University of Delaware data was converted into an anomaly dataset using the same climatology (1961-1999) that was used in Jones, et al. (2012) for the CRUTEM4 data.

In this experiment, statistical significance was calculated exactly the same way as in the reanalysis experiment. Significance was taken as a change greater than two standard deviations of the mean temperature anomaly value for each 20 year period.

### **2.3.3 Model Experiment**

The OMR variation of the reanalysis study is able to better isolate the influence of LULCC on climate from the climate variability of the 20<sup>th</sup> century. However, the results still cannot be used to conclusively quantify only climate impact of agriculture. Therefore, this study is an extension of that line of investigation, which will rely on a modeled environment using the AM2-LM2 climate model from the GFDL. The purpose of this study is to evaluate the change in climate when the entire prairie region is converted into an agricultural zone. This method will remove the influence of climate change and climate variability. It will also remove the historical spatial biases which are inherent in the observation data and which limited the reanalysis and OMR studies. The reanalysis study was focused primarily on a few key climatic variables. However, using a model environment, it becomes possible to evaluate changes to the hydrologic cycle as a whole, as well as the changes to PBL climate through changes in net radiation. There

are two main ways that agriculture has impacted the water balance. The first is the introduction of new vegetation types, which impact the transfer of water between the ground and the boundary layer. The second is the use of irrigation techniques to supplement water shortages with groundwater drawn to the surface. By using this model environment to generate a uniform change across the entire study area, this study will demonstrate only the influences of the first change. The second change is beyond the scope of the present study and remains an opportunity for future research.

The first step of this study was to run a control scenario. This scenario assumed a completely natural environment where the entire area of the prairies was defined by the grasslands land cover type (GRASS). The model was run for a 12 month period beginning in December and ending in November of the following year. The scenario was simulated 97 times, each under different initial conditions. This created a large enough ensemble from which to draw a statistically significant set of mean conditions. The results of this ensemble were used to generate a picture of the expected energy balance and water cycle across one full year. The first month was discarded from the analysis due to the potential influence of a ‘spin up’ period. The initial conditions of each ensemble member may have artificially influenced the climate conditions before the model reached a stable state for the rest of the year (Annamalai, Okajima, & Watanambe, 2007; Fletcher & Kushner, 2010).

The second step of this study was to use the GRASS scenario results as a baseline dataset from which the significance of converting grasslands to agriculture could be evaluated. In the perturbation scenario (AGRIC), any cell within North America classified as grassland in the land cover map, was re-designated as an agricultural cell. Within the LM2, agriculture is one of the ten land cover types. However, it is not included in the original land cover map which designated

each cell as one of the other nine ‘natural’ land cover types (Milly & Shmakin, 2002a). No other modification was carried out in the AGRIC scenario. The agriculture type does not represent any particular crop type explicitly. In comparison with the grasslands definition, agriculture differs in half of the ten prescribed variables. The depth of roots is slightly shallower in the agriculture definition (0.25 m) than the grasslands (0.26 m). The root biomass areal density is however much less dense in the agriculture definition with only  $0.15 \text{ kg/m}^2$  compared to  $1.4 \text{ kg/m}^2$  in the grasslands. The third difference is in the roughness length of the vegetation types which is 0.4 m in the agricultural definition and 0.07 m in the grasslands definition. The snow free (summer-time) albedo is strictly defined for both land cover types and is slightly greater for the grassland cover type (0.18) than the agricultural type (0.16) (Milly & Shmakin, 2002a).

In general, all of these changes indicate that the grassland land cover type has a slightly deeper rooting system with a larger and denser root network, however the above ground portion of the grasses are substantially shorter. The albedo difference indicates a lighter plant colour, lending itself to a greater reflectivity. All of these differences agree with the observed differences between prairie grasses and prairie crops found in the literature (Steyaert & Knox, 2008). Moreover, based on the given parameters, the agricultural type closely represents wheat, an appropriate crop type for the North American prairies (Dorman & Sellers, 1989).

Once the AGRIC ensemble had been created, the ensemble mean of the GRASS scenario was subtracted from the ensemble mean of the AGRIC scenario. The residual results were then plotted alongside the control results. Statistical significance of the change between the two land cover types was evaluated using a Student’s T-test; a p value threshold of  $\leq 0.05$  was implemented. The results were displayed in two different formats. A set of control and response plots were created that represent the monthly mean values of each relevant variable. The second

format was as a set of maps that show seasonal changes in the residual data. For the plots, if any month demonstrated a statistically significant change, it was identified on the residual plots by a larger marker placed either below or on top of the monthly average values. Using the same Student's T-test statistical test, an overlay was created wherein any cells that display a significant change were covered by a stippled pattern.

## Chapter 3: Reanalysis and Observation Studies

This chapter discusses the results produced by both the basic reanalysis experiment and the Observation Minus Reanalysis variation. Both of these studies rely on observational data, collected and created at different scales and with different methodologies. The purpose of using this type of data was to evaluate if the relationship between LULCC and climate could be observed at the whole ecosystem scale within the available climate record.

### 3.1 Reanalysis Method Results

The change in land cover represented by Figure 2.2 is the product of a steady increase in agriculture over the 20<sup>th</sup> century (Figure 3.1). The difference in  $C_f$  between the CTRL and PERT remained very stable over the entire period. The mean of  $\Delta C_f \approx 53\%$  between a range from 45-56%. This clear difference in the GVPD allows the two different land cover types to be compared directly since neither area displays a disproportionate increase in  $C_f$ . While the CTRL area does increase to a maximum  $C_f$  of 20.4% by 1990, challenging the definition of CTRL cells as “natural prairie”, the increase in the PERT  $C_f$  mean that the comparison can still be made across areas of a similar spread of agricultural coverage.

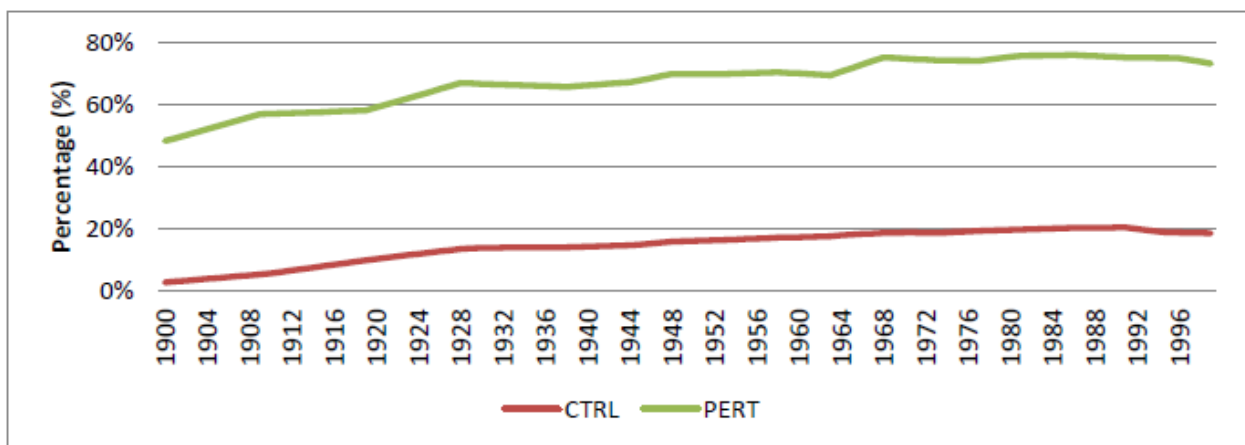


Figure 3.1: Annual change in  $C_f$  from 1900-1999.

As discussed in the previous chapter, the temperature, atmospheric water vapour content (WVC), and the convective available potential energy (CAPE) were the three climate variables analysed using the reanalysis method. CAPE is a measure of the available energy to a rising air parcel. This variable is influenced by available latent heat in the boundary layer. As the vertical flux of moisture increased, measured by a shrinking Bowen ratio (amount of sensible heat relative to latent heat ( $\beta = Q_H/Q_{LE}$ )), CAPE increases. Larger CAPE values have been connected in the literature to convective cloud development and subsequently, convective storms (Raddatz, 2005). This section will discuss first the difference in the two twenty year periods (1900-1919 and 1980-1999) and will then present the average annual results in order to discuss any trends or anomalous periods that are not explained by the first analysis.

It was found that at the beginning of the century, temperatures, measured in degrees Kelvin, were 2.5°K cooler over PERT areas compared to the CTRL (Figure 3.2). At the end, both CTRL and PERT had cooled, although not significantly (CTRL = 0.35°K; PERT = 0.65°K). The PERT had cooled slightly more than the CTRL, increasing the difference to 2.8° cooler temperatures in PERT for 1980-1999.

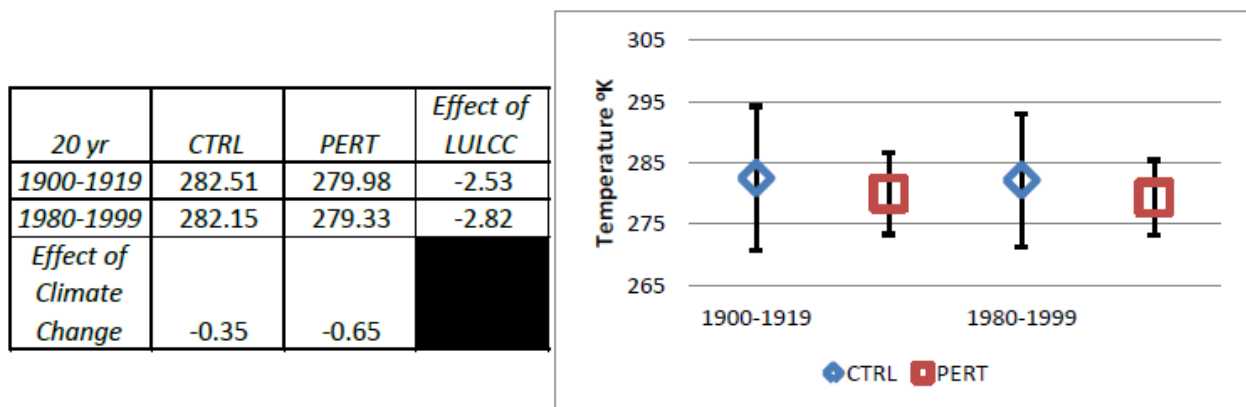


Figure 3.2: Left: Temperature in °K for each land cover area for both time periods, including the difference between each area at the beginning and end of the 20<sup>th</sup> century as well as the difference in each area over time. Right: The plotted mean value with statistical significance represented as two standard deviations from the areal mean.

The atmospheric water vapour content, measured in  $\text{Kg/m}^2$ , was shown to be greater in the PERT than the CTRL in the 1900-1919 time period by  $3.35\text{Kg/m}^2$  (Figure 3.3). Over time, both CTRL and PERT increase, however the change in CTRL ( $0.58\text{ Kg/m}^2$ ) is approximately four times larger than in the PERT ( $0.12\text{ Kg/m}^2$ ). By the end of the century, the difference between PERT and CTRL has decreased to  $2.88\text{ Kg/m}^2$ . The change between the CTRL and PERT areas over time and the changes between the two land cover types at both time periods was not found to be statistically significant. Neither was the change in WVC from the beginning to the end of the century found to be significant.

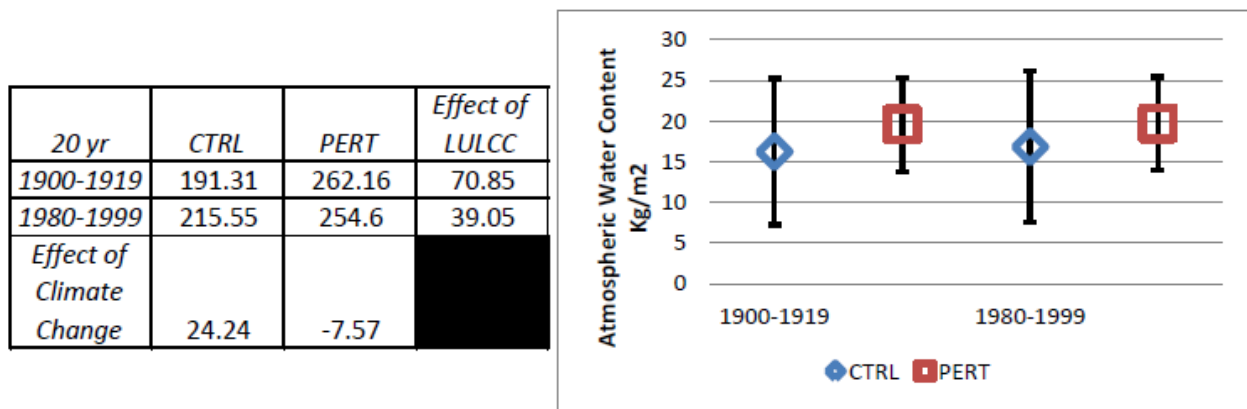


Figure 3.3: Atmospheric water vapour content in  $\text{Kg/m}^2$  represented as described in Figure 3.2.

Finally, the total convective available potential energy was also found to be greater over the PERT areas at the beginning of the century by  $70.85\text{ J/Kg}$  (Figure 3.4). The CAPE over the CTRL area increased from  $191.31$  to  $215.55\text{ J/Kg}$  ( $\Delta +24.24\text{ J/Kg}$ ) by the 1980-1999 time period. In this time, the PERT CAPE actually decreased by  $7.57\text{ J/Kg}$  reducing the difference between both areas by 55%. However, the change in PERT over time was found to not be statistically significant within the two twenty year periods.

20 yr	CTRL	PERT	Effect of LULCC
1900-1919	16.22	19.57	3.35
1980-1999	16.8	19.69	2.88
Effect of Climate Change	0.58	0.12	

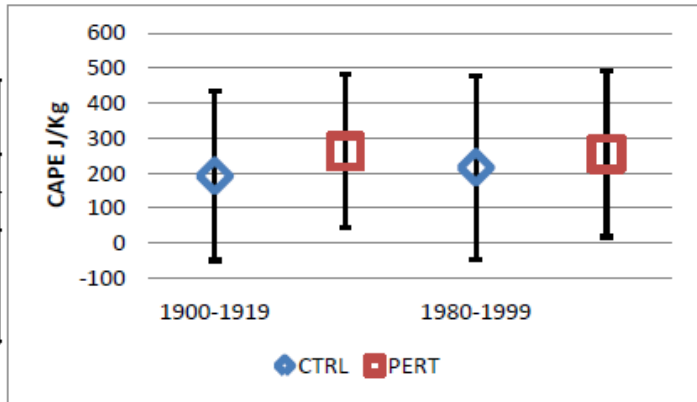


Figure 3.4: Convective available potential energy in J/Kg represented as described in Figure 3.2.

The results of this study indicate that as temperatures have cooled over the entire prairie region, total WVC has slightly increased, and CAPE has become more uniform over the 20<sup>th</sup> century. However, none of these changes were found to be significant. Nevertheless, the results partially reflect the expected outcomes of LULCC found in the literature. The decreasing temperature however, is occurring despite the lower albedo of crop species and cultivated fields and the early century desertification, which was occurring under agriculture. Later irrigation may have overcome this process by the 1980-1999 period; and irrigation appears to be represented in the WVC increase as the literature has demonstrated that irrigation does increase PET. The change in CAPE only occurred in the CTRL area. The increased rate of convection may have been caused by the increasing WVC without an increase in temperature because CAPE has been shown to be more sensitive to variability in humidity instead of temperature (Riemann-Campe, Fraedrich, & Lunkeit, 2009). This does not explain why no change occurred over the PERT area, which experienced the same increase in  $C_f$ .

The calculated two standard deviations of the mean over each land cover area are so large that presenting the first and last 20 year periods for each variable does not sufficiently describe the long term 20<sup>th</sup> century trends. Therefore, these three variables are also presented as mean annual plots wherein the inter-annual variability is clearly presented. These plots make it

apparent that the differences in the land cover characteristics between the CTRL and PERT cases cannot completely explain the trends being presented in the 20CR. The maximum and minimum ensemble member annual values were also included in the annual plots to show the degree of internal variability with the 20CR ensemble for each climate variable. Temperature (Figure 3.5) shows that there was a mid-century (1930s and 1940s) increase in temperature over both land cover areas. Temperature then decreases until the 1980s when it begins to increase slowly again. These times match the two major periods during the 20<sup>th</sup> century where drought was significant (Cook, et al., 2007). With temperature, the CTRL and PERT areas experience extremely similar inter-annual variation which indicates that both areas are likely being influenced by the same forces. There is very little variation within the ensemble for temperature.

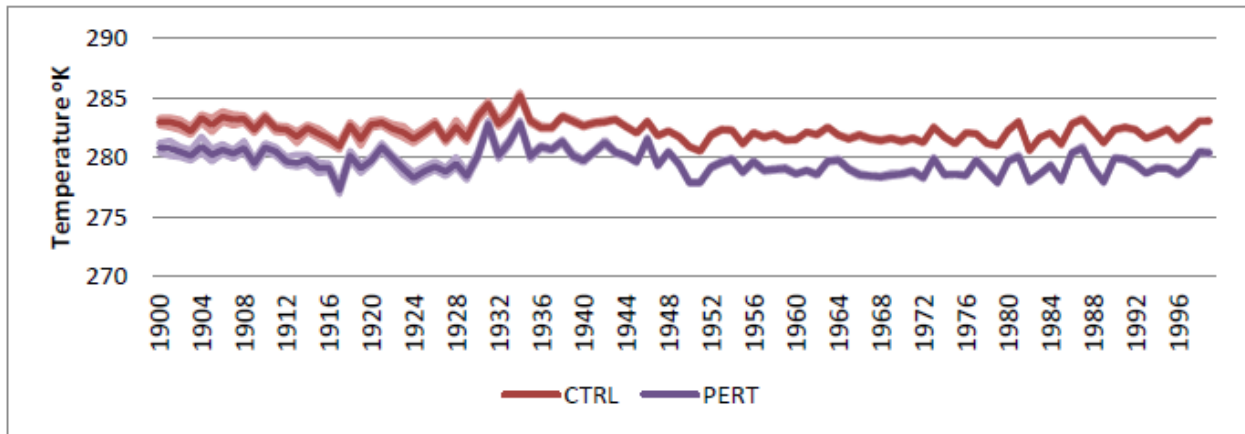


Figure 3.5: Mean annual temperature in °K for CTRL and PERT land cover areas. The paler lines above and below CTRL and PERT represent the maximum and minimum values from within the 20CR ensemble.

Atmospheric water vapour content acts very differently. The WVC over both areas follows a similar trend; however the PERT areas show a much larger variance as well as greater volume for the entire century (Figure 3.6). This plot shows that the increase in WVC found in Figure 3.3 over time is likely not related to the introduction of irrigation. Between CTRL and PERT if introducing irrigation in the 1940s had a substantive role in WVC, there would be a

noticeable increase in the gap between both land cover areas. Like temperature, WVC has very variation between the 56 ensemble members. There is the most disagreement in the beginning of the century (until around 1940). The changes and variation to CAPE are more obvious between the CTRL and PERT (Figure 3.7); PERT has a greater variance. The PERT line in this figure explains why the decrease in PERT CAPE found in Figure 3.4 was not statistically significant. It appears to be more related to the smaller variance in the last twenty years from year to year than to a decrease. This becomes more prominent with the inclusion of the full ensemble range which shows an overlapping trend between CTRL and PERT for most of the century.

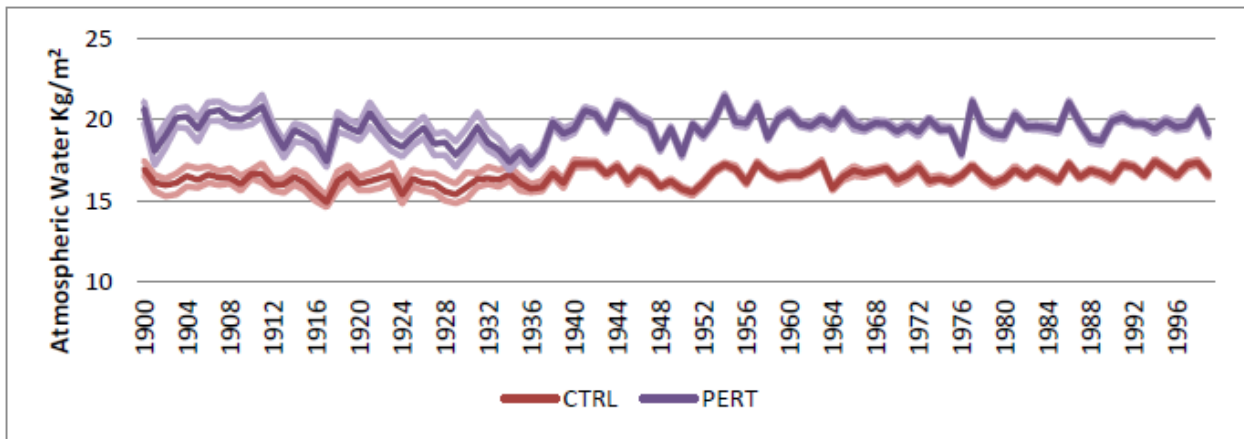


Figure 3.6: Mean annual atmospheric water vapour content in Kg/m<sup>2</sup> represented as described in Figure 3.5.

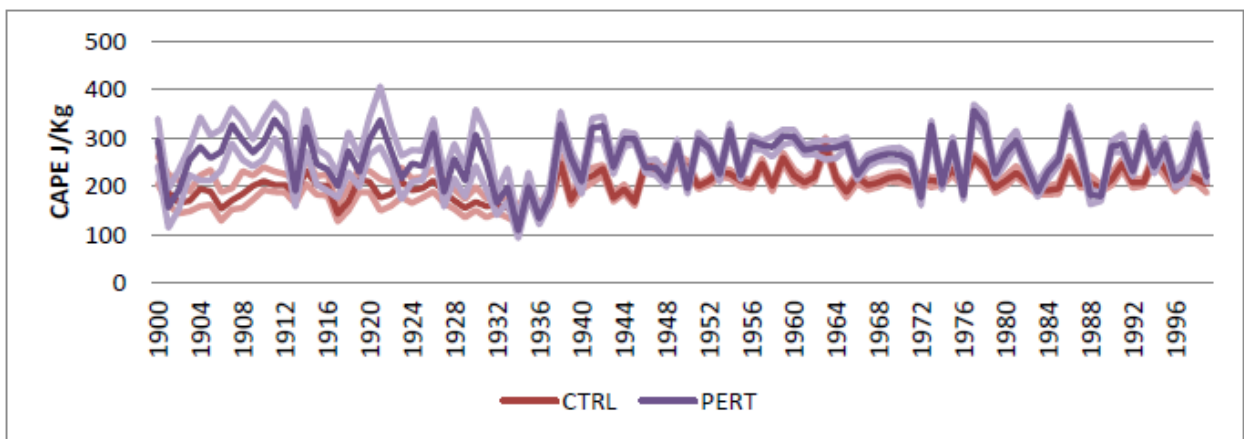


Figure 3.7: Mean annual convective available potential energy in J/Kg represented as described in Figure 3.5.

In comparing climate data over areas of concentrated natural prairie grasslands and agriculture, there are factors that make it difficult to conclusively correlate the observed changes from Figures 3.2 - 3.7 with the different land cover types. The disparity between the CTRL and PERT in both the WVC and CAPE annual plots may have been caused by the distance between the two study areas (Figure 2.3). The vast majority of the cells in the CTRL case are found in the western extent of the prairies while the PERT cells are found in the far eastern corner. Because they are each in a separate climatic region of the prairies, particularly because the regions are defined by available water and precipitation, it is likely that environmental factors outside of LULCC are causing much of the differences in the long term trends of both variables. If the change in land cover demonstrated in Figure 3.1 was the only variable influencing the changes in any of these three variables, the annual changes would be much more linear. One of the other potential, non-LULCC sources of the variance displayed in all three of these climate variables is natural variability. It is possible that the inter-annual variability would have occurred to some degree regardless of land cover.

Other limitations on the use of this methodology include the reanalysis dataset (20CR), which represents tropospheric climatological conditions, furthering the difficulty in relating changes observed by the study to changes which the literature has shown LULCC is imposing on boundary layer climate (Pielke, Sr., et al., 1998). For example, this particular reanalysis product has generated temperature conditions at 850 hPa (Compo, et al., 2011). This is an isobaric height that persists approximately 1-1.5 km above sea level. Any influence that land cover may have on climate will be found within the boundary layer, which is found within the first 1 km of the atmosphere (Oke, 1987). Moreover, as discussed in the literature review, the PDO and the ENSO both have large modifying impacts on the long term climate of central North America (Mo &

Schemm, 2007; Wittrock & Ripley, 1999). The following three map series (Figures 3.8 – 3.10) display the seasonal mean plots for all three climate variables. These plots were made by taking the seasonal mean over the entire 20<sup>th</sup> century and then taking the mean of all 56 ensemble members for each season. These plots show that it is much more likely that the results in Figures 3.2 - 3.7 are being influenced by changes in 20<sup>th</sup> century tropospheric circulation patterns.

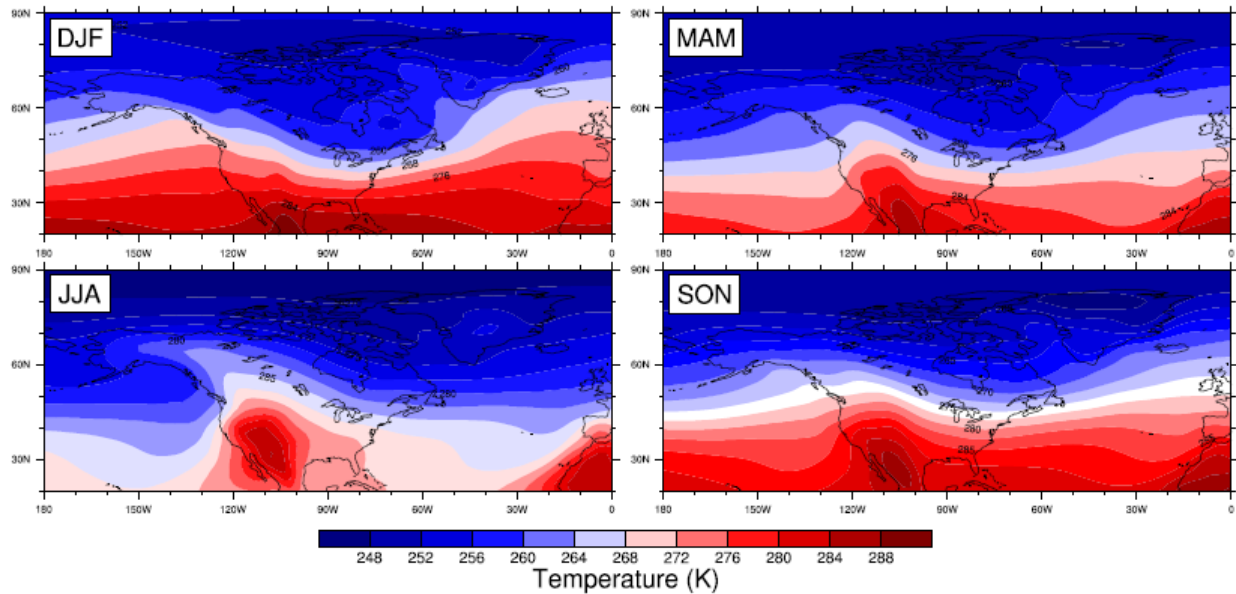


Figure 3.8: 20<sup>th</sup> century seasonal mean temperatures in °K. Plots are limited to 20°N-90°N in the Western hemisphere.

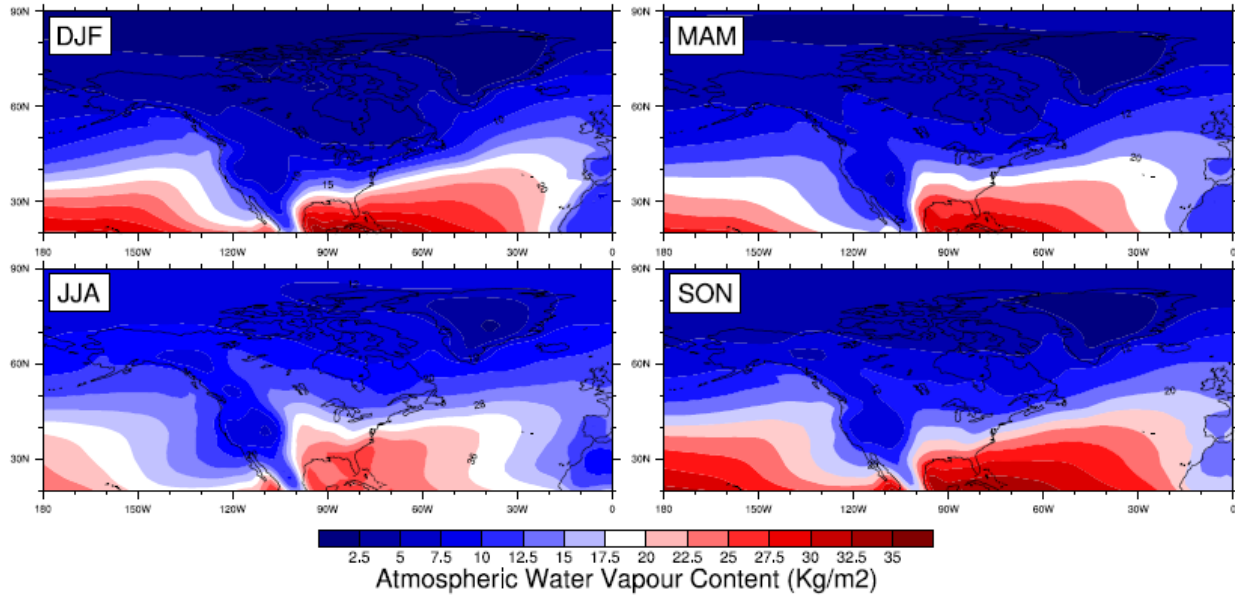


Figure 3.9: 20<sup>th</sup> century seasonal mean atmospheric water vapour content in Kg/m<sup>2</sup> represented as described in Figure 3.8.

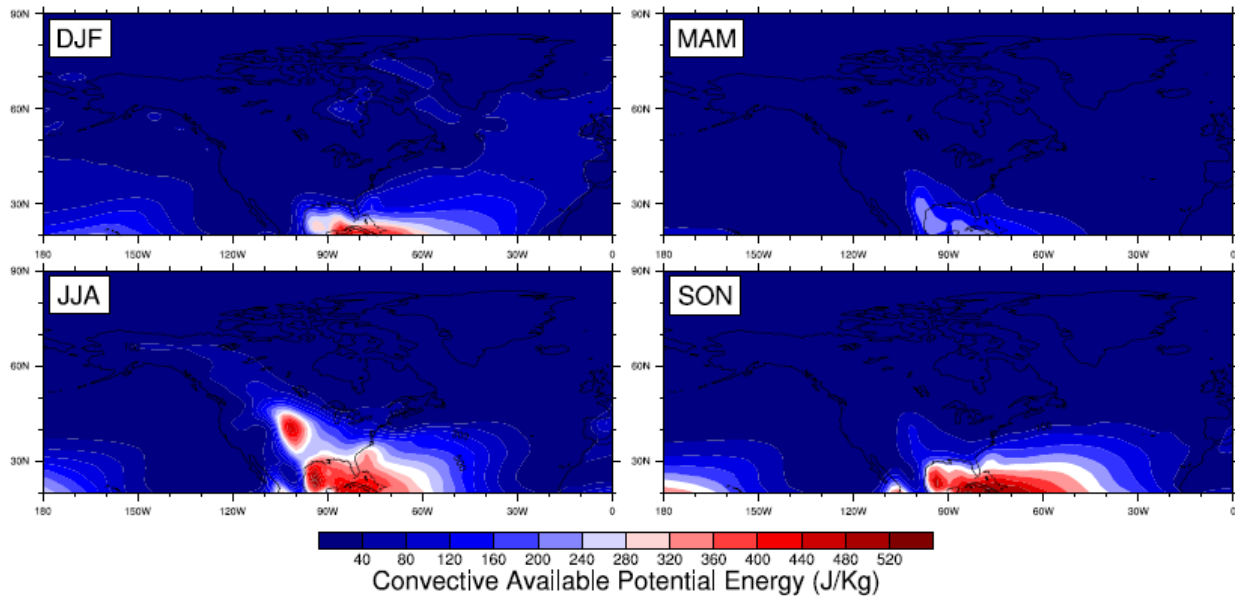


Figure 3.10: 20<sup>th</sup> century seasonal mean convective available potential energy in J/Kg represented as described in Figure 3.8.

Beyond the noted limitations in using only reanalysis data to evaluate the small change in climate caused by LULCC, there are sources of error that persist in reanalysis products that can influence their overall accuracy. On the spatial scale, there are issues associated with in-situ station network density (Sterl, 2004). The further a point within the reanalysis climate conditions

is away from an incorporated station, the greater the possibility of error within the model forecast. On a temporal scale, the density of in situ networks, particularly in North America, has changed over time. This alters the internal spatial error of the forecast, making it more difficult to compare reanalysis results across such a long period of time (Sterl, 2004). The 20<sup>th</sup> Century Reanalysis Project is an extremely new data product (2011) and as a result, there have been relatively few published evaluations of the data accuracy. Therefore the degree of spatial and temporal error is not well established. When taken into consideration all together, these limitations all indicate that the first methodology of this study cannot exclude natural variation from its results. In order to overcome these limitations, the second methodology, Observation Minus Reanalysis (OMR) was used to provide a way to extract the local surface level climate signal.

### **3.2 Observation Minus Reanalysis Results**

The twenty year comparison plots in Figure 3.11a show the 20<sup>th</sup> century changes in temperature found using the CRUTEM4 surface observation anomaly dataset. There is an increase in temperature of 1.2°K in the CTRL and of 1.3°K in the PERT. In both time periods, PERT was slightly cooler (1900-1919 = 0.18°K; 1980-1999 = 0.13°K), although this difference is not significant. However, unlike the 20CR temperature result, both the CTRL and PERT areas demonstrated a statistically significant change over time. The increasing temperature trend more accurately reflects the 20<sup>th</sup> century temperature trends shown in the literature. Climate change has raised the PBL temperature of North America (IPCC, 2007). Nevertheless, the cooling associated with the changes to albedo caused by the harvest cycles in agricultural fields (Song, 1999) is still observed. The second observation dataset (Terrestrial Air Temperature from the University of Delaware) presents very similar results after being transformed into anomaly data

(Figure 3.11b). It also presents a 20<sup>th</sup> century increase in surface temperatures with a cooler climate over the PERT areas. Temperature increased less in the CTRL and PERT areas for this dataset than in the CRUTEM4 case (CTRL = 0.9°K; PERT = 1.1°K). While the trends in this dataset do agree with the results produced by the CRUTEM4 data, none of the changes (either over time or between the two land cover types) is statistically significant.

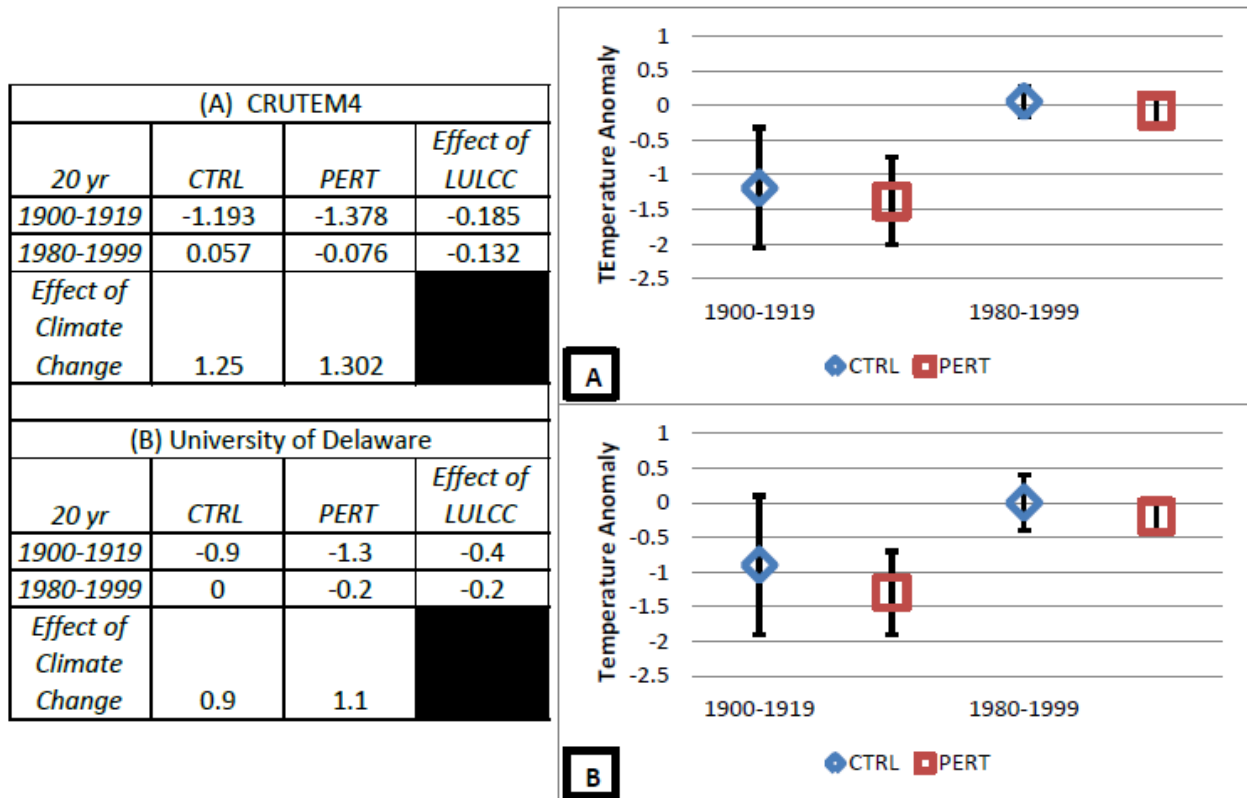


Figure 3.11a/b: Calculated OMR temperature anomalies in °K represented as described in Figure 3.2, including both (A) CRUTEM4 and (B) University of Delaware versions of OMR.

### 3.2.1 Temporal Inhomogeneity

While the OMR methodology is a good tool for making tropospheric reanalysis data relevant to the climate within the boundary layer, the results are still not completely able to describe the influence of the land cover on climate. The accuracy of the observation datasets used for the OMR is subject to the same sources of error introduced by changing in situ network densities and measurement standards (Jones, et al., 2012; Matsuura & Willmott, 2009) that

influence the accuracy of the 20CR and other reanalysis products (Sterl, 2004). In fact, these errors may actually be larger in the temperature observations. The surface pressure observations used to create the 20CR have a very consistent historic record dating to the beginning of the 19<sup>th</sup> century (Compo, et al., 2011). Implementing the OMR does minimize the influence that the observation dataset inhomogeneities may introduce, it cannot be said that they are completely removed. The 20CR data may also not have been the optimal reanalysis dataset to use with the OMR methodology. Kalnay, et al. (2006), states that the reanalysis dataset should not assimilate surface observations. This is because the purpose of OMR is to remove climate forcing processes above the boundary layer. The 20CR is based entirely on surface observations (section 2.1.2). However, this does not invalidate the results. When tested with a surface observation based reanalysis product, the final OMR product produced similar, but weaker results (Kalnay, et al., 2006). This does imply that the changes over time in the results presented above may actually be larger than presented.

Figure 3.12a/b presents the inter-annual variability of the OMR, using the anomaly versions of the two observation datasets, between 1900 and 1999. Before 1950, the temperature very obviously deviates from the 1961-1999 climatology. The variation appears to be greater in the PERT areas for both of the OMR anomaly datasets. After 1950, the anomalies are much smaller for both land cover cases. The difference between the first and last 50 years of the 20<sup>th</sup> century is further emphasized in Figure 3.13. In this figure, the top two panels represent the OMR using the CRUTEM4 anomaly and the bottom two panels represent the OMR using the University of Delaware anomaly for both time periods. These maps show that the negative anomaly is very strong, over the prairies particularly, in both datasets. While both anomalies

decrease after 1950 by a similar amount, the biases are larger in the University of Delaware OMR dataset.

Moreover, between the 1930s and early 1960s, there is a period of large bias in the anomaly data. During this time, the temperature anomaly becomes more negative before being reduced to within 1 degree of the 30 year climatology. This feature is not present in the 20CR temperature trend shown in Figure 3.5, indicating that there is a force within the boundary layer which is influencing this bias. It is difficult however, to attribute this bias or the overall 20<sup>th</sup> century temperature trend to LULCC alone. If the OMR had successfully isolated the influence of LULCC on temperature, there would be a clear distinction between the CTRL and PERT land cover areas. Instead, the extreme inter-annual variability presented in Figure 3.12a/b suggests that either there are other factors influencing the temperature over the two land cover areas making it difficult to isolate LULCC, or that LULCC is not having any measureable influence on the temperature of these areas in this study.

Even though these errors exist in the OMR methodology, making it more difficult to relate the changes in the OMR between the two land cover types across the 20<sup>th</sup> century (Figure 3.11a/b), the influence of LULCC still cannot be completely discarded. The difference in temperature from the 1900-1919 period to the 1980-1999 period more closely represent the observed surface warming for North America over the 20<sup>th</sup> century (IPCC, 2007) than the temperature results from the 20CR (Figure 3.5). Additionally, they show that there is still a difference between the two land cover types, despite the noise of climate change and large scale circulation patterns.

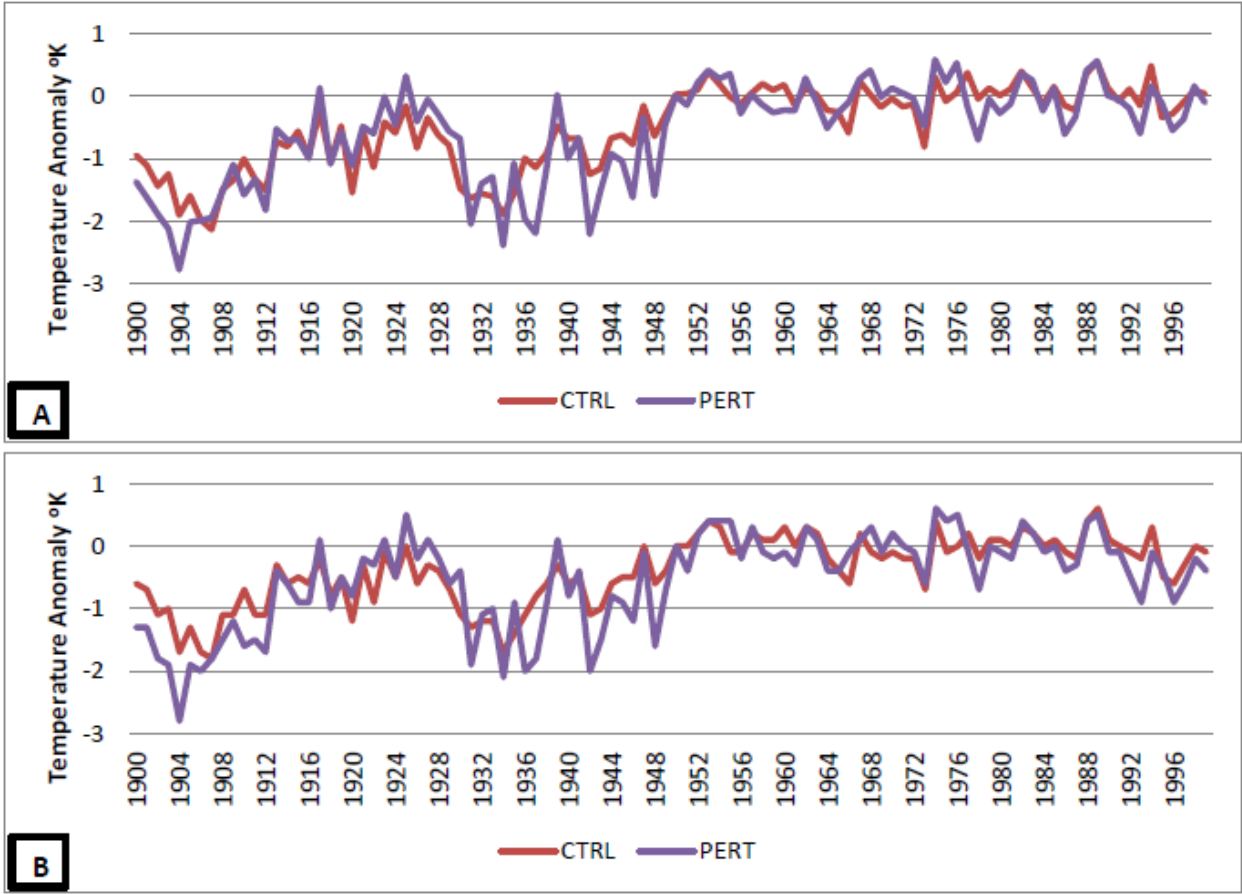


Figure 3.12a/b: Inter-annual variability in the OMR results for temperature anomalies in °K represented as described in Figure 3.2, including both (A) CRUTEM4 and (B) University of Delaware versions of OMR.

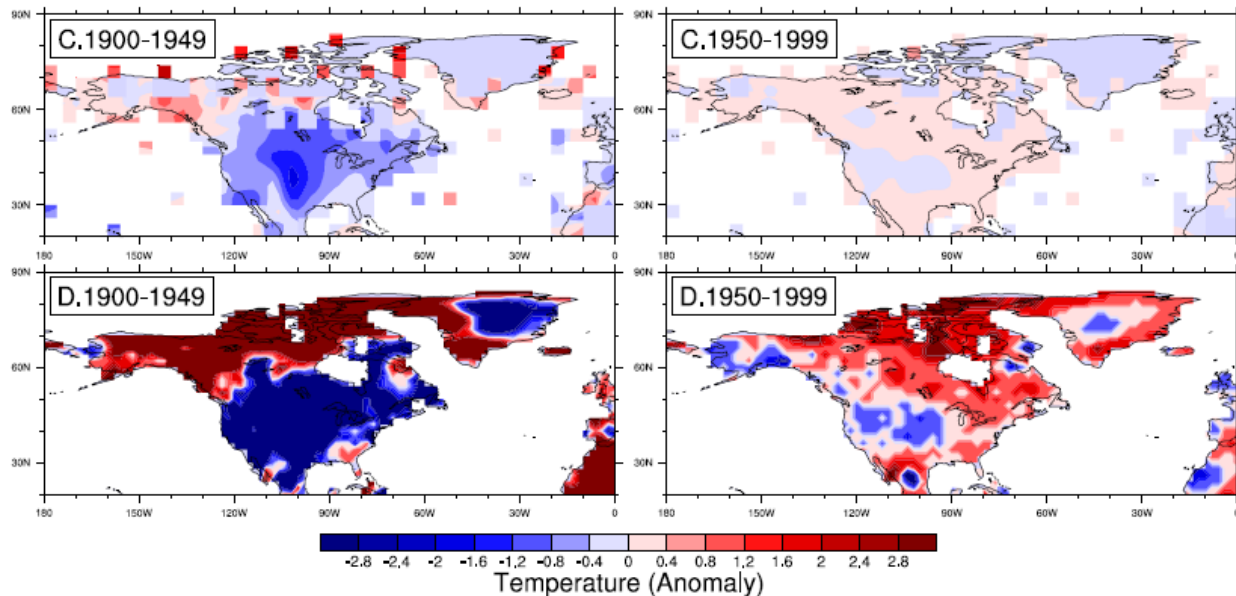


Figure 3.13: Difference in temperature anomaly in  $^{\circ}\text{K}$  between the first and second halves of the 20<sup>th</sup> century over North America. The top two panels represent the OMR using the CRUTEM4 (C) observations and the bottom two panels represent the OMR using the University of Delaware (D) observations represented as described in Figure 3.2.

### 3.3 Summary and Impetus for Model Experiment

In this chapter, the results of reanalysis and OMR studies are presented. The reanalysis study demonstrated generally that the mean temperature is cooling as a result of agricultural intensification. This is a century long process where the change in temperature appears to increase steadily as agricultural coverage increases. The trend is most apparent after the 1950s in the OMR mean annual results. It also showed that there was greater WVC over the PERT areas but that there was very little change (if any) over time. If the trend is due to LULCC, it is possible that the greater WVC is due to increased water availability as a result of irrigation. Finally, the results showed that changes to CAPE are not, either over time or between the two land cover types, easily distinguishable. CAPE is however greater over PERT areas.

The OMR study results show the influence of 20<sup>th</sup> century climate change on surface temperatures and demonstrate how difficult it is to isolate the climate signal produced by LULCC from the larger climate trends. The purpose of the reanalysis and OMR studies was to

use a simple method to test for a relationship between LULCC and changes in climate during the 20<sup>th</sup> century. While the results of these studies cannot be used to definitively state that changes in land cover are changing the climate of the North American prairies, they do indicate that there is some variation that LULCC can impose. By using only collected climate data, it is very difficult to fully isolate the impact of LULCC on a continental scale. One of the best ways to control for all of the potential outside variables is to simulate the change from prairie grasses to agriculture in a modelled environment. The following chapter therefore, will describe a separate experiment which will overcome the large number of limitations with using reanalysis and observation data as described in this chapter.

## Chapter 4: Model Experiment

This chapter will discuss the results produced by a modelling experiment that was conducted using the AM2-LM2 coupled model as described in section 2.3.3. The purpose of this study was to create two prairie simulations. The first simulation represented a situation where the entire region had been left as a massive grassland area (GRASS). The second simulation represented a completely agricultural prairie (AGRIC). The AGRIC case was then subtracted from the GRASS case to quantify the differences in climate over the prairies caused by the change in land cover.

### 4.1 Whole Prairie Results

In agreement with the results found in the reanalysis and observation study, the model study found that the shift in land cover type from the native prairie grasslands to a vast agricultural zone has had an impact on the region's climate. In general, the results have increased the certainty of this statement. The first changes which will be discussed are found in the prescribed variable 'snow free albedo'. During months with snow, the albedo range is the same for both agricultural and grassland cover types. However, during the snow free period, albedo is prescribed at 0.16 for agriculture and 0.18 for grasslands. The GRASS albedo is shown in Figure 4.1a, where the snow free period is shown to be between May and September. Over the entire year, the response plots show that under the AGRIC conditions, albedo is consistently lower than under GRASS conditions (Figure 4.1b). This change is only statistically significant during the April-October period. The difference in albedo between the two cases during these months is equal to the difference between the prescribed snow free albedo values ( $\alpha$  AGRIC (0.16) -  $\alpha$  GRASS (0.18) = -0.02). Therefore, the change in albedo during these months can be said to have been caused directly by the change in land cover type.

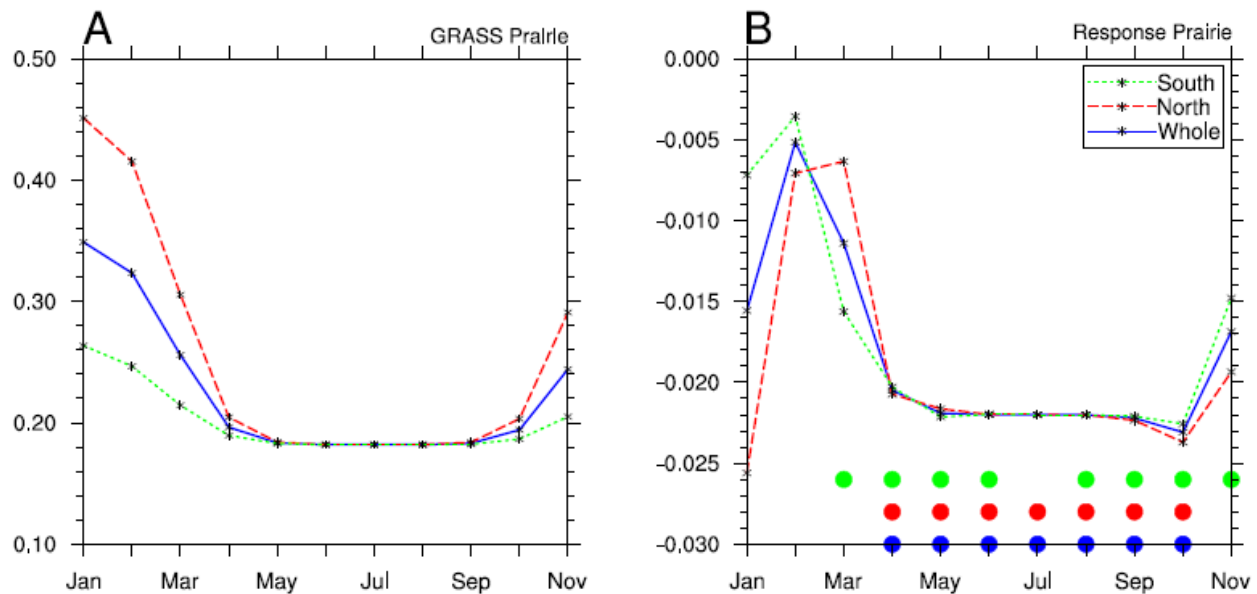


Figure 4.1a/b: (A) Monthly mean albedo for the whole prairie (blue), the northern prairie (red), and south prairie (blue) in the control case. (B) Monthly response in mean caused by replacing the grassland with the agricultural scenario (AGRIC-GRASS). The whole, north, and south area divisions will be discussed in section 4.2 and 4.3. Statistical significance ( $p \leq 0.05$ ) is indicated by a dot in a colour corresponding to the related plot line.

This direct change can therefore be treated as an initiation point for any subsequent changes in climate found in the response plots and maps for the prairie temperature and radiation balance. These changes will then have a cascading effect on the water balance. The movement of water is directly impacted by other prescribed variables, which further contribute to the differences found within the response results. The difference in surface albedo indicates a difference in the reflectivity (colour) of the ground cover. The decreased surface albedo over AGRIC indicates a greater absorption of incoming solar radiation by the vegetation cover. The increase is completely attributable to the vegetation change as the soil type in the model does not influence albedo. The temperature in the GRASS case (Figure 4.2a) shows that monthly mean temperature has a smooth progression across the year. The response plot of surface temperature (Figure 4.2b) reflects the increase in albedo. Temperature change is minimal and not statistically significant during the winter and spring seasons but the increase in temperature during the June – August

period is greater than then GRASS case. Additionally, the map in Figure 4.3 shows that the increase in temperature is highly localized over the prairies during summer. The increase in temperature has implications on both the radiation and water balance as at the peak month of July, temperature is increased by 2.5°C as a result of the perturbation.

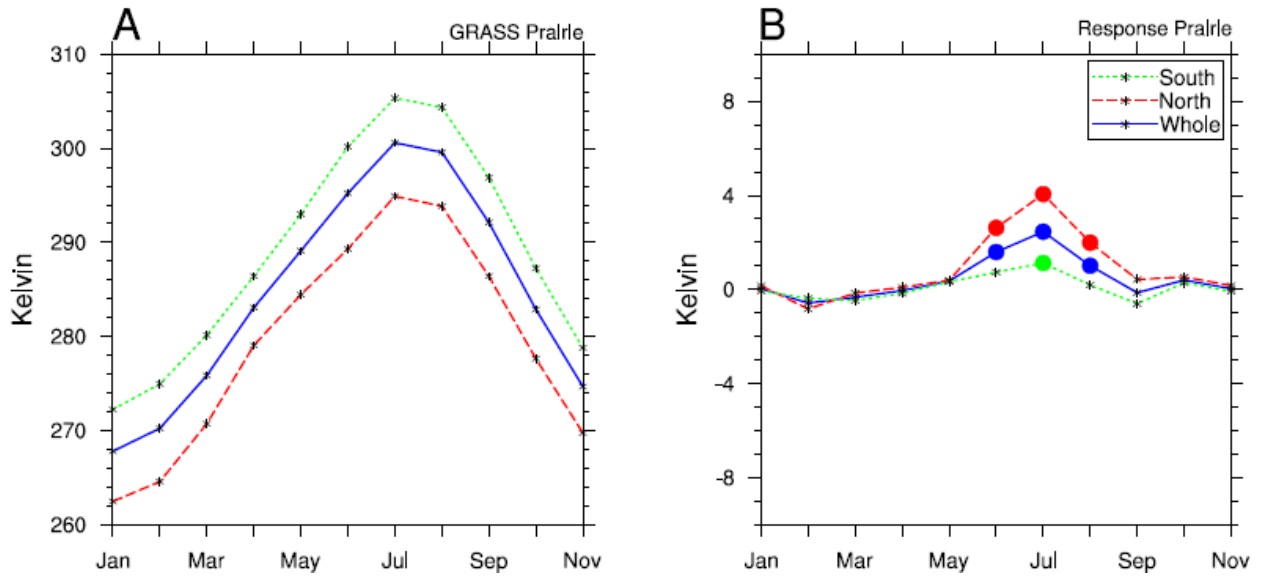


Figure 4.2a/b: Mean monthly temperature in °K represented as described in Figure 4.1a/b. Dots representing statistical significance are on the line in this case.

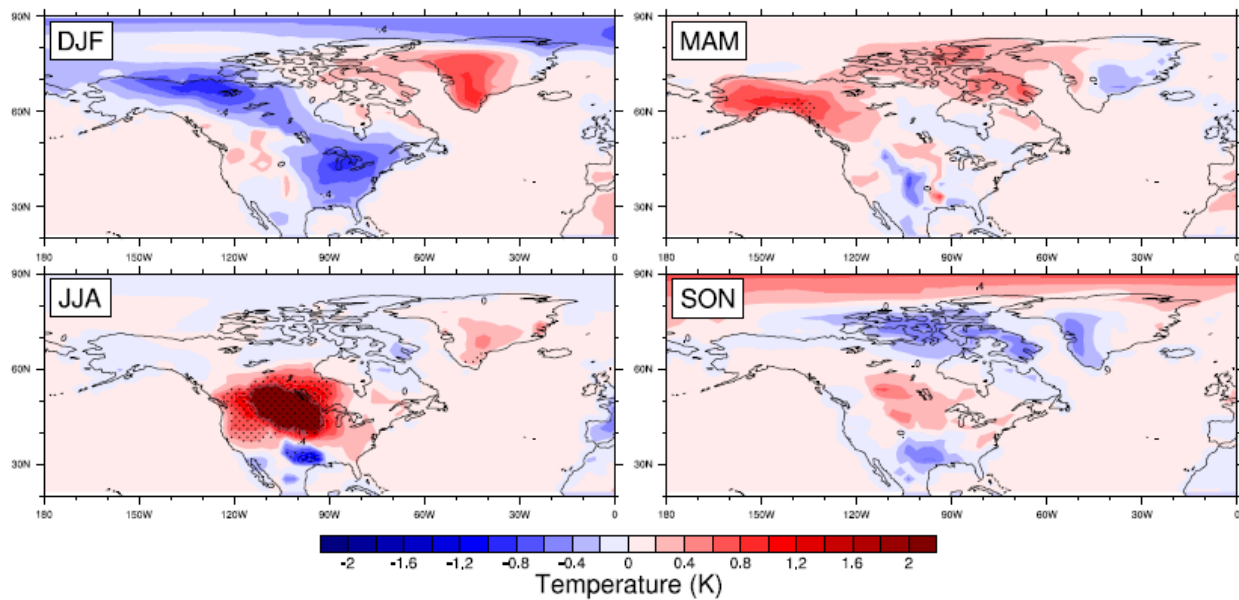


Figure 4.3: Map of response temperature results (°K). Plots are limited to 20°N-90°N in the Western hemisphere. Areas of stippling within the maps represent cells where the response was considered statistically significant ( $p \leq 0.05$ ).

#### **4.1.1 Net Radiation and the Energy Balance**

Once summertime albedo and temperature are changed by the shift from GRASS to AGRIC, it would be expected that there would be a cascading effect on both the net radiation and the energy balance. This is because of the Stephan-Boltzmann Law, which states that an increase in the temperature of a surface will increase its rate of energy radiation (Aguado & Burt, 2012). Under the GRASS scenario, net radiation reaches an annual maximum in June before decreasing into fall. Incoming short and long wave radiation, as well as upwelling longwave radiation peak in July (Figure 4.4a). In the AGRIC scenario, the warmer temperatures and lower albedo of the agricultural land cover do not have a significant impact on net radiation. Instead, the upwelling longwave radiation increases significantly between June and August and the reflected shortwave radiation is significantly reduced from April until the end of the year (Figure 4.4b). This shows that the total available energy within the system is not changed, but that the change in albedo is forcing more shortwave absorption at the surface in spring, driving up summer temperatures which are forcing an increase in the upwelling longwave radiation under AGRIC. These changes are immediately visible in the June-July-August (JJA) panels of Figures 4.5 and 4.6, where the entire prairie area is covered by the change in these two net radiation components. The change is also, particularly in Figure 4.5, strongly related to the change in land cover as the shape of the area of significant difference almost exclusively covers the study area.

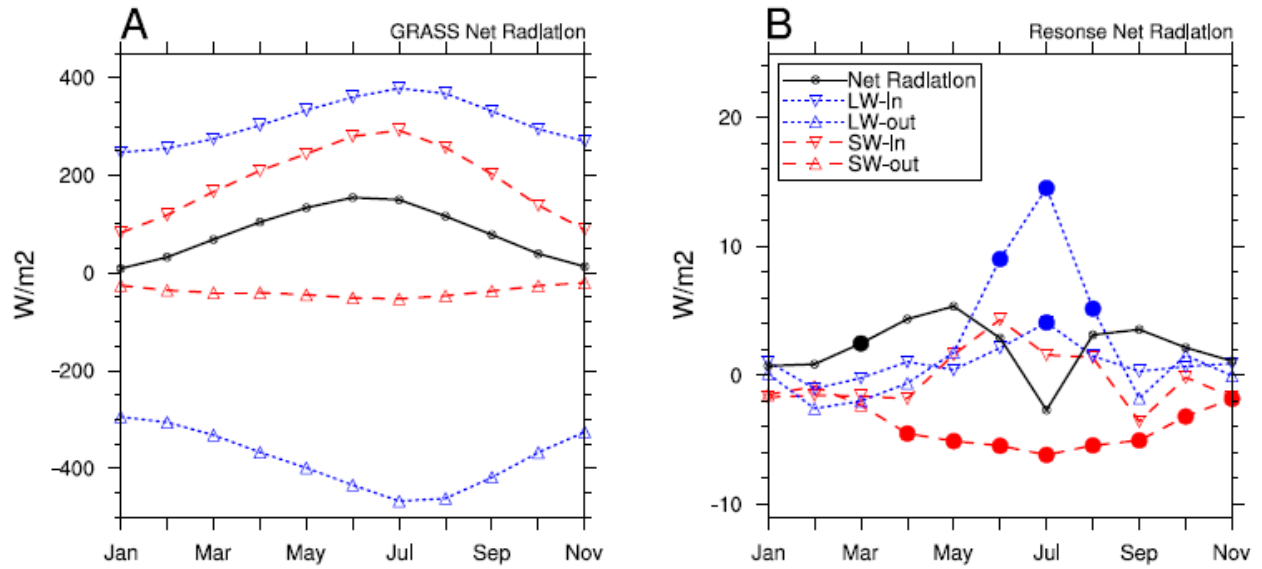


Figure 4.4a/b: (A) GRASS net radiation and (B) response net radiation in  $W/m^2$  represented as described in Figure 4.2.

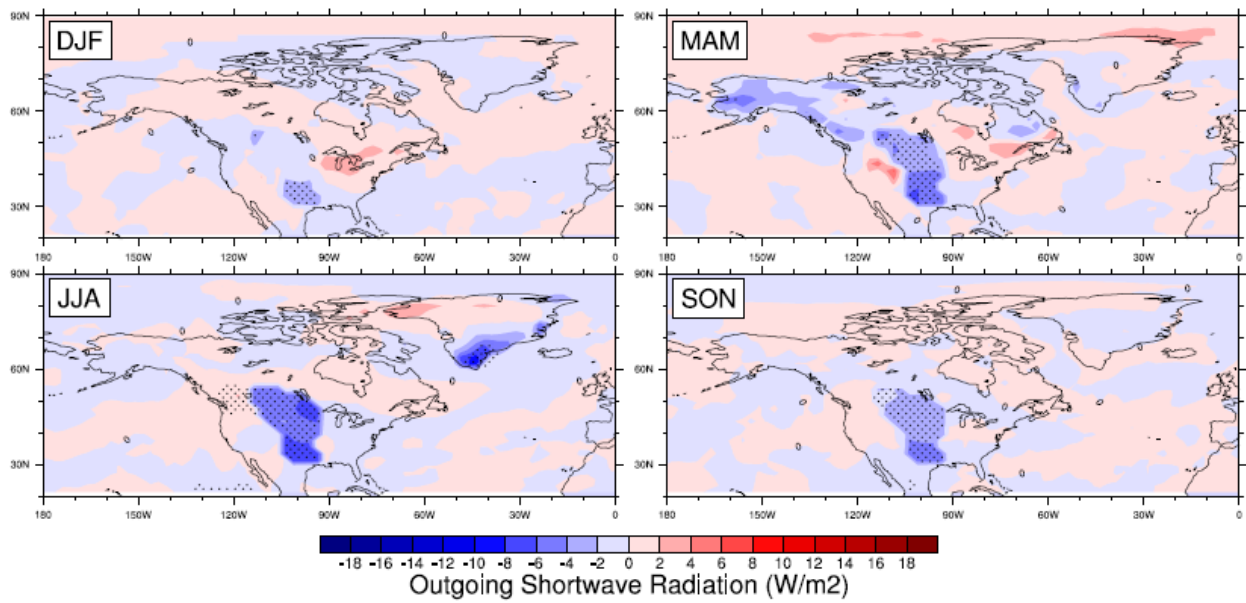


Figure 4.5: Map of response outgoing shortwave radiation results in  $W/m^2$  represented as described in Figure 4.3.

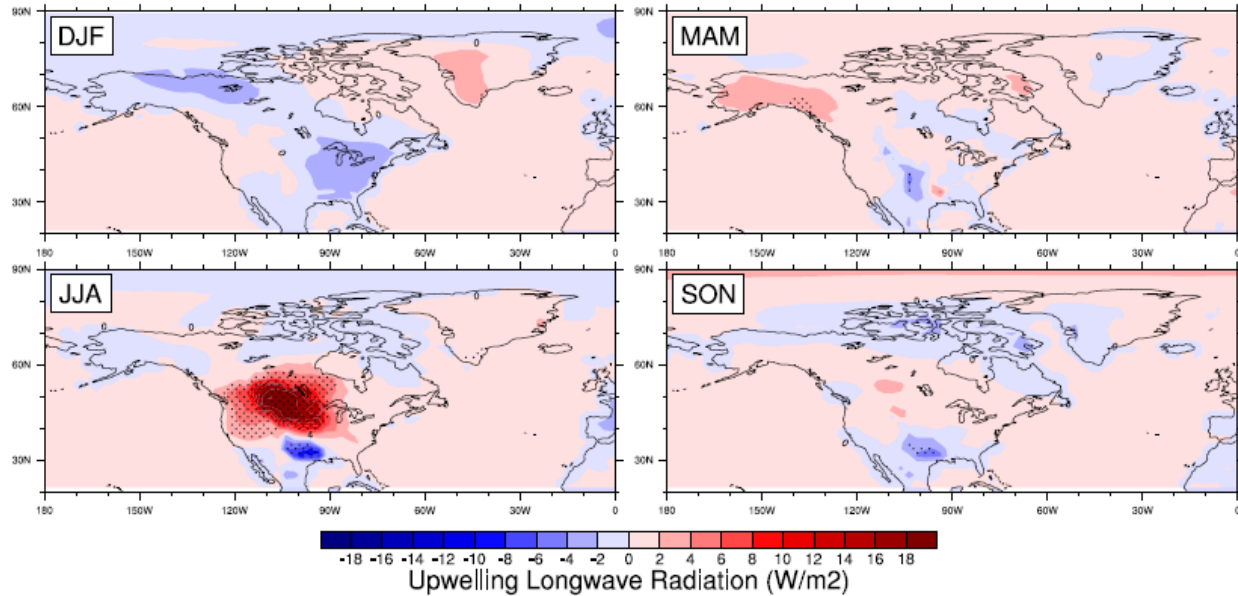


Figure 4.6: Map of response upwelling longwave radiation results in  $W/m^2$  represented as described in Figure 4.3.

All of the changes discussed so far indicate that there will be significant changes in the energy balance. The net radiation is the total amount of energy available to do work and it is divided into three components. They are: latent heat, sensible heat, and ground heat (Oke, 1987). By significantly altering the balance of short and longwave radiation being sent up to the atmosphere, the balance of latent and sensible heat should be impacted as well. Under the GRASS land cover case, the ground heat component accounts for a very small portion of the overall net radiation (Figure 4.7a). The residual plot (Figure 4.7b) shows that the AGRIC land cover does not have a large or significant impact either. The ground heat flux is not output by the land model. Instead, it was calculated as a residual from the energy balance equation:

$$Q_G = 0 - (Q_{LE} + Q_H + Q^*) \quad (4.1),$$

where  $Q_{LE}$  is the latent heat component,  $Q_H$  is the sensible heat, and  $Q^*$  is the net radiation.

In the GRASS case, net radiation increases until June. This is being driven by the increasing latent and sensible heat at the beginning of the year. When temperature begins to decrease after June, latent heat follows. Sensible heat continues to increase until August (Figure

4.7a). Under the AGRIC simulation, sensible heat increases significantly between May and August while the latent heat component decreases significantly between June and August (Figure 4.7b). However, the response plot shows that the net radiation demonstrates very little change; with the exception of March, when the slight increase was statistically significant. The changes to sensible and latent heat are therefore occurring because the available energy is being rebalanced, not because of a change to the overall available energy within the environment. This is why there is no significant change to net radiation during the summer. The alterations to the albedo, temperature, and the energy balance carry implications onto the water balance, which is particularly important in the prairies which is such a water sensitive environment. The next section will discuss the changes that were found in the water balance. In addition to changes caused by the energy balance response, these changes were impacted by a shift in the prescribed variables: depth of the root network, the areal density of the root network, and the roughness length of the vegetation.

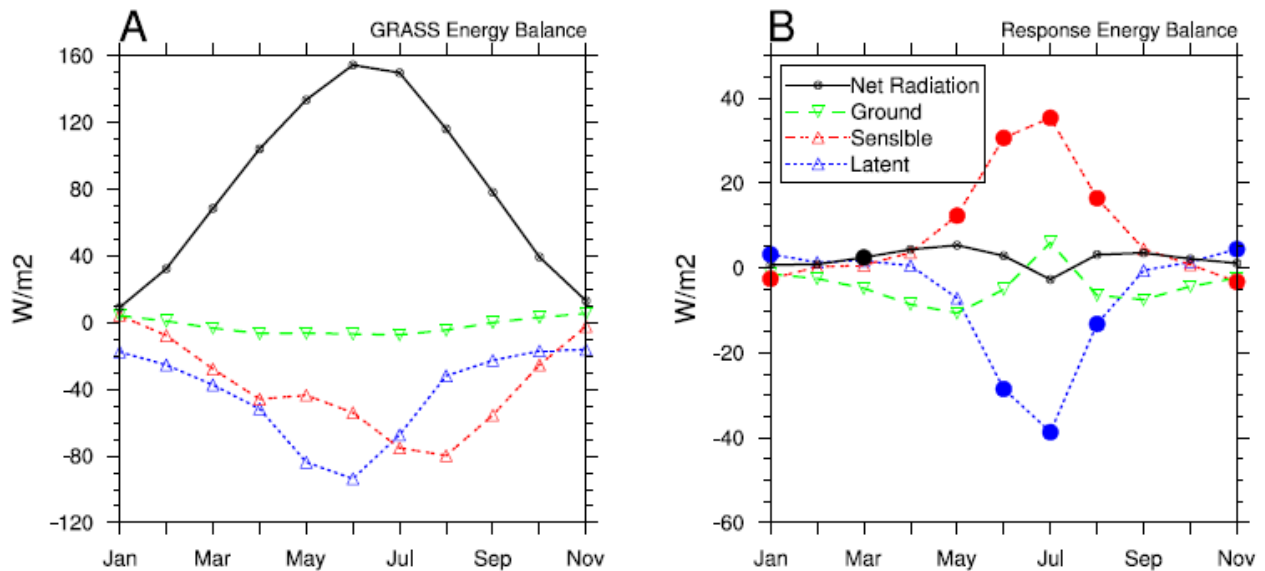


Figure 4.7a/b: (A) GRASS energy balance and (B) response energy balance in  $W/m^2$  represented as described in Figure 4.2.

#### 4.1.2 Water Balance

As described in section 2.2.2, the hydrologic cycle of the AM2-LM2 model is represented by a condensed set of pathways and reservoirs. The entire series of pathways for water, once it enters the LM2 component, is outlined in Figure 2.1. The mean monthly plots (Figure 4.8a-d) demonstrate the GRASS scenario results as well as the response created by the difference in conditions for the AGRIC scenario. This discussion will separate precipitation and evaporation from surface (root zone) and groundwater reservoirs because there are separate processes which influence each set of reservoirs.

Precipitation, in the GRASS scenario, increases monthly from January and continues to exceed evaporation until May, creating an atmospheric moisture surplus in the first half of the year (Figure 4.8a). Evaporation however, continues to increase in June. This change is reflected in the latent energy response which also reaches its annual maximum in June (Figure 4.7a). This creates a moisture deficit (Response in Figure 4.7a), which lasts until October. This is expected because of the albedo GRASS plot in Figure 4.1a. As discussed in that section (4.1), the model uses two prescribed albedo variables, one for snow covered and one for snow free conditions. Under snow free conditions, the grasslands land cover type is prescribed a value of 0.18 so when in October, albedo begins to increase, it is because of snowfall which is contributing to the overall volume of precipitation.

The moisture deficit is greatest in June and July before evaporation rates quickly begin to decrease until October. As precipitation decreases, the available water for evaporation also decreases, driving down the latent heat component. This change was also forecast in the previous discussions because temperature continues to increase until July, forcing sensible heat to become the dominant component of the energy balance after the June peak in latent heat (Figures 4.2a &

4.7a). This is what creates the summer time hot and dry conditions that characterize the prairies (Peel, Finlayson, & McMahon, 2007).

The second half of the water balance encompasses the pathways that control water once it reaches the surface. In the LaD, those are the root zone and groundwater reservoirs (Figure 4.8c). The root zone reservoir closely follows the monthly trends in the precipitation and snowfall model outputs. It reaches its annual maximum in May and decreases until October when both precipitation and snowfall increase again. The volume of water in the groundwater reservoir is completely controlled by the field capacity of the root zone reservoir and a 30 day residence time (section 2.2.2). Without recharge from the root zone, this reservoir will slowly empty. The peak groundwater volume occurs one month after the peak root zone volume, and it decreases steadily until the end of the year. Once evaporation exceeds precipitation, the root zone reservoir is depleted too quickly to discharge to the groundwater reservoir. The increased water inputs from precipitation and snowfall at the end of the year are not large enough to exceed the root zone field capacity.

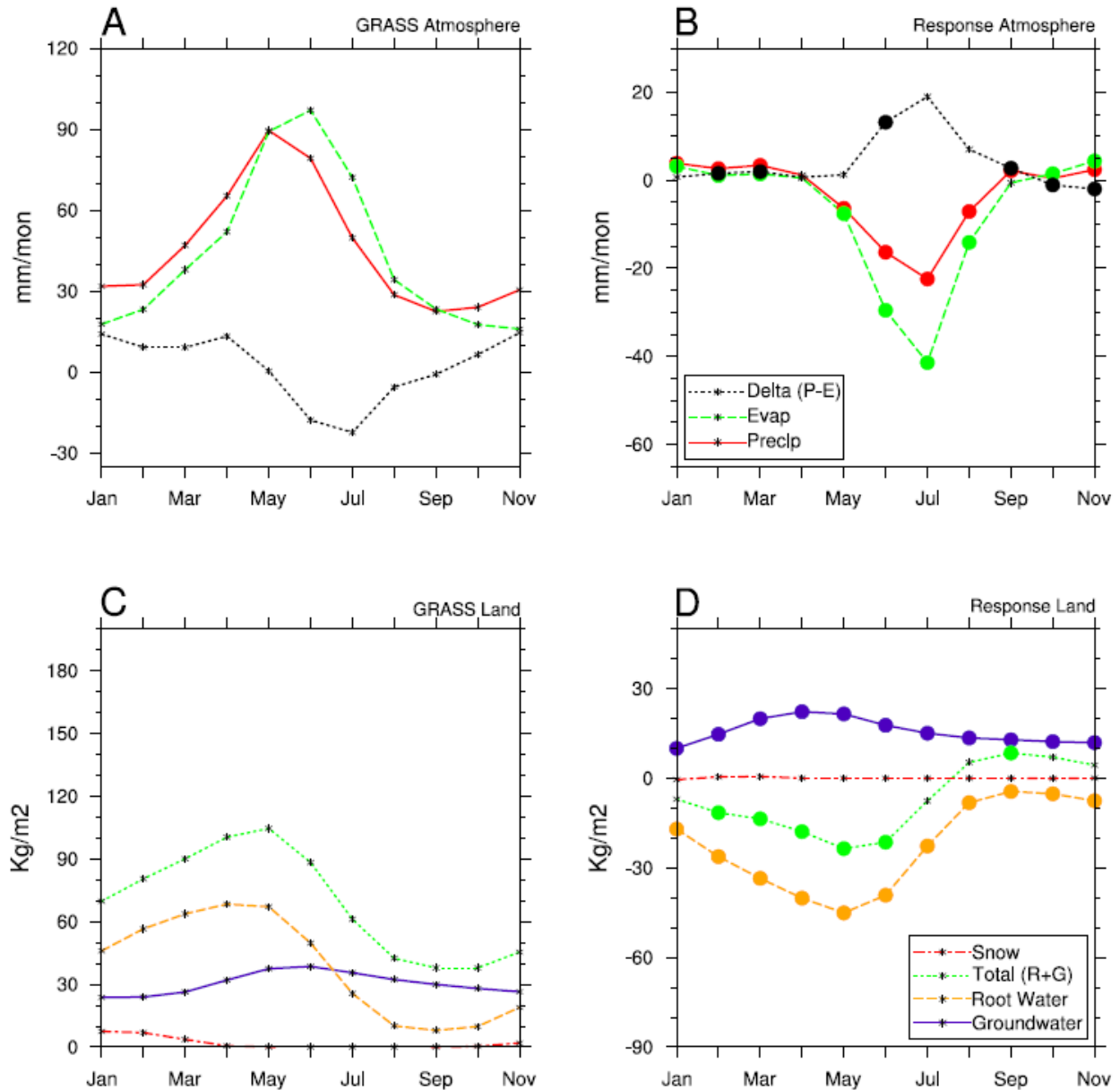


Figure 4.8a-d: (A) GRASS atmospheric water balance and (B) response atmospheric water balance in mm/month. (C) GRASS land water balance and (D) response land water balance for the entire prairies. Statistical significance is represented as described in Figure 4.2. In A and B, Delta (P-E) is the net moisture left on the ground (effective precipitation). In C and D, Total (R+G) is the total water available on the ground. Root zone and groundwater contribute to this total.

The GRASS scenario demonstrates that precipitation and evaporation (and snow to a much lesser extent) control the entire water balance of the LaD model. When the AGRIC scenario was run, there were significant changes to these two variables across almost the entire

year (Figure 4.8b), which have a cascading influence on the entire hydrologic cycle. The largest changes occurred between May and August when both variables were reduced. The greater decrease in summertime evaporation reduces the moisture deficit. The effects of these changes are visible in the energy balance response plots (Figure 4.7b) in the decrease in latent energy, the result of less moisture available for evaporation. The result of these changes is a drier environment. The root zone reservoir therefore is also reduced. Groundwater however, is increased significantly at the beginning of the year. This change appears to be the result of an increase in snowfall during the winter.

The reduction in both precipitation and evaporation is caused by two of the prescribed land cover variables: root depth ( $Z_R$ ) and roughness length ( $z_0$ ), and linked to the change in root zone water availability, and subsequently groundwater observed in Figure 4.8d. Root depth is based on the calculation of the root network density at depth. Using a generalised rate of decreasing root density, known as an extinction depth scale, the model calculates the depth at which the roots will reach a critically diminished value. Milly & Shmakin (2002a), assign this value a global constant of  $0.5 \text{ Kg/m}^3$  in the LaD model. In the AM2-LM2, the global constant was reduced to  $0.125 \text{ Kg/m}^3$  (Anderson, et al., 2004). Each land cover type has a different root biomass density at the surface which determines the root extinction depth (Milly & Shmakin, 2002a). These values were drawn from Jackson, et al. (1996), where it was found that temperate grasslands have a substantially greater surface root biomass, meaning that in the LM2 component of the model, the grassland land cover type has a greater overall  $Z_R$  (i.e.  $0.26 \text{ m} = \text{GRASS}$ ;  $0.25 \text{ m} = \text{AGRIC}$ ). However, the difference is extremely small (1 cm). Additionally, the authors acknowledge a possible source of error in this methodology when a constant rate of biomass decay is applied to both natural and agricultural vegetation types (Milly & Shmakin, 2002a). No

solution or correction was recommended since, as noted previously, the original version of the model does not include the agricultural land cover definition.

This change is seen in Figure 4.8d when root zone water storage is reduced by root depth, particularly during the spring and early summer months. The shallower root zone reaches field capacity sooner, draining water to the groundwater reservoir at a faster rate when field capacity is exceeded. This is seen in the significant increase in groundwater volume during this same time period. Shallower roots also limit evaporation. The model is designed to avoid water stress on the vegetation. It does not reduce water storage to below 75% of field capacity (equation 2.6). The remaining 25% of root zone water volume is smaller under the AGRIC scenario, reducing evaporation. This has a recursive effect on precipitation as less moisture is available in the atmosphere for convection and cloud formation. Nevertheless, a slightly shallower root zone is probably not able to initiate such a large response in the hydrologic cycle alone. The drier conditions and lesser evaporation and precipitation are also being driven by the higher summer temperatures and decreasing latent energy availability (Figures 4.2b & 4.7b).

The second prescribed variable, roughness length, has an impact that is slightly more difficult to quantify in the response plots. Roughness length is related to the drag imposed on the vertical wind profile by the height of the vegetation. It represents the point at which the vertical wind profile represents a wind speed of zero (Oke, 1987; Rohli & Vega, 2008). In the model, grasslands are assigned a  $z_0$  of 0.07m and agriculture has a  $z_0$  of 0.4 m (Milly & Shmakin, 2002a). This is reflected in the observed data which show that in general, prairie crops tend to be taller than the preceding vegetation (Cho, et al., 2012). In this case, the taller vegetation will alter the aerodynamic resistance which has implications in the model on the calculation of sensible heat as well as having an additional influence on evaporation over a vegetation surface (equation

2.6) (Milly & Shmakin, 2002a). Given an unlimited supply of water, evaporation would likely increase. That scenario is in agreement with the current literature which shows that under non-irrigated conditions, the prairies dried very quickly, causing extended periods of drought (Rosenberg, et al., 1999; Cook, et al., 2007). But, under irrigated conditions, where water limitations are removed, greater convective activity and a greater proportion of convective storms have been observed (Raddatz & Hanesiak, 2008), indicating more evaporation.

All of the changes, which have been noted above, including the significant decrease in precipitation, demonstrate that there is overall less water available in the entire prairie ecosystem. Following the chain of changes which occurred when the AGRIC scenario was imposed can be summarized by the following processes. First, height and root zone depth of the vegetation in the AGRIC scenario has lead to an increase in sensible heat and potential evaporation over vegetated surfaces. Second, the faster rate of drainage to the groundwater reservoir and the smaller field capacity constrains the available water for evaporation. Third, available atmospheric water decreases, reducing precipitation and putting more stress on the root zone, eventually slowing groundwater drainage. If the model had been run for a multi-year period instead of only 12 months, it is probable that this trend would have continued, eventually creating a desert environment over the prairies.

## **4.2 Subdividing the Prairies**

Since the area under examination is so geographically large, and crosses several climatic zones, it is also useful to look at changes in climate at a smaller scale. Doing so makes it easier to account for the differences in inter-seasonal variability and snow accumulation at different latitudes. The prairies were divided into a northern and southern portion along the 45° latitude line. The division was made at this latitude in order to emphasize the contribution of the snow

mass to the water balance. Snow melt is one of the contributing sources to root zone water storage (equation 2.5). Figure 4.8c demonstrates that there is a small amount of snowfall between January and March, which does contribute to the root zone, and eventually groundwater reservoirs. The importance of snow mass becomes apparent in Figure 4.9. The majority of the response in groundwater storage is occurring north of 45° latitude. Figure 4.10 demonstrates that under the GRASS scenario, the majority of prairie snow mass also occurred largely above 45° north. The response in snow mass is not very large or statistically significant (Figure 4.8d) but there is a change which is occurring during the winter months and the majority of that change is occurring above 45° north.

This change has indicated that there is a stronger connection between the volume of snowfall and the AGRIC land cover type than the original control GRASS type which may have been masked by evaluating the full extent of the prairies. In the examination of the prairies as a whole, water scarcity under the AGRIC scenario appears as a significant change to the environment. The separation of the northern and southern prairies helps to establish the importance of snow for maintaining soil water levels.

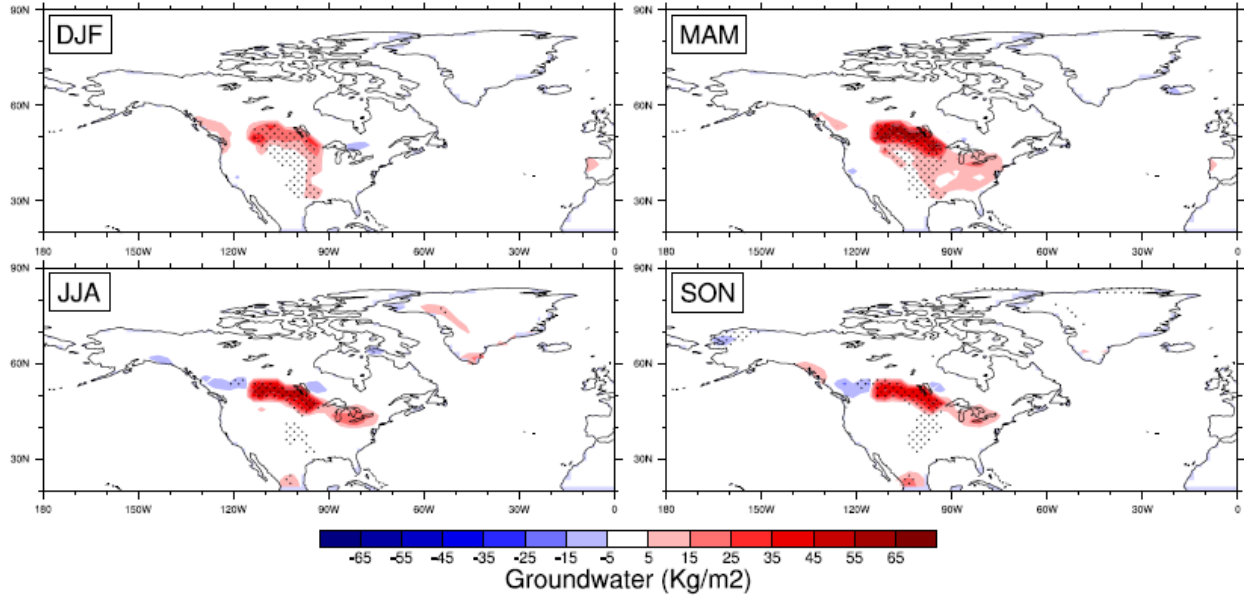


Figure 4.9: Map of response groundwater storage in  $\text{Kg/m}^2$  represented as described in Figure 4.3.

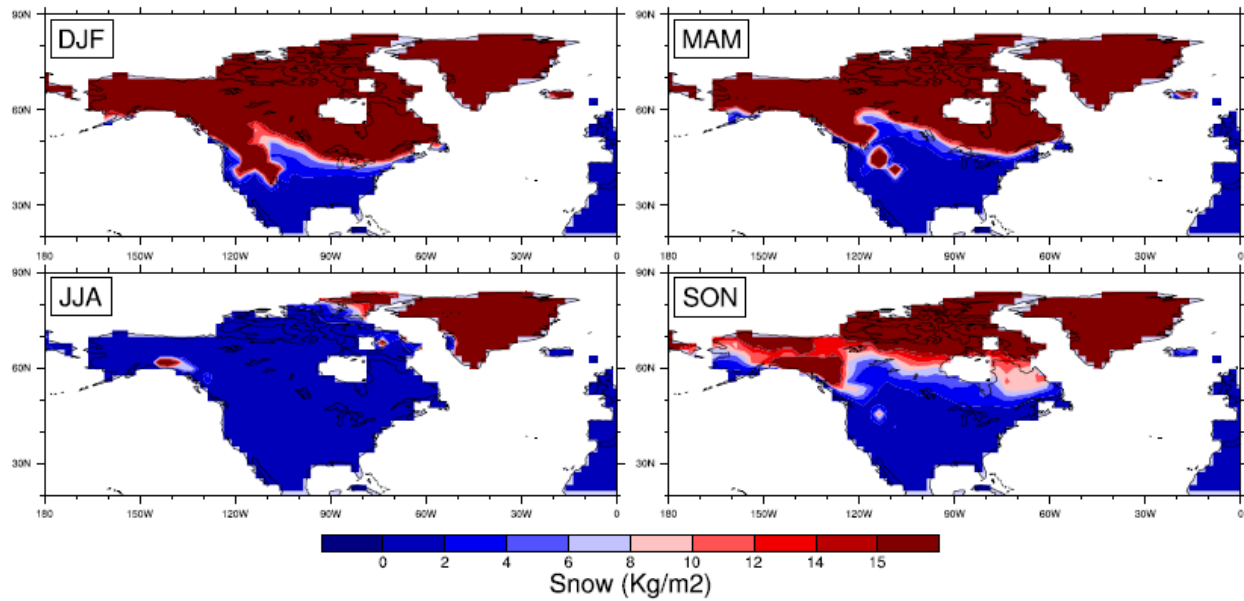


Figure 4.10: Map of GRASS snow mass in  $\text{Kg/m}^2$  represented as described in Figure 4.3.

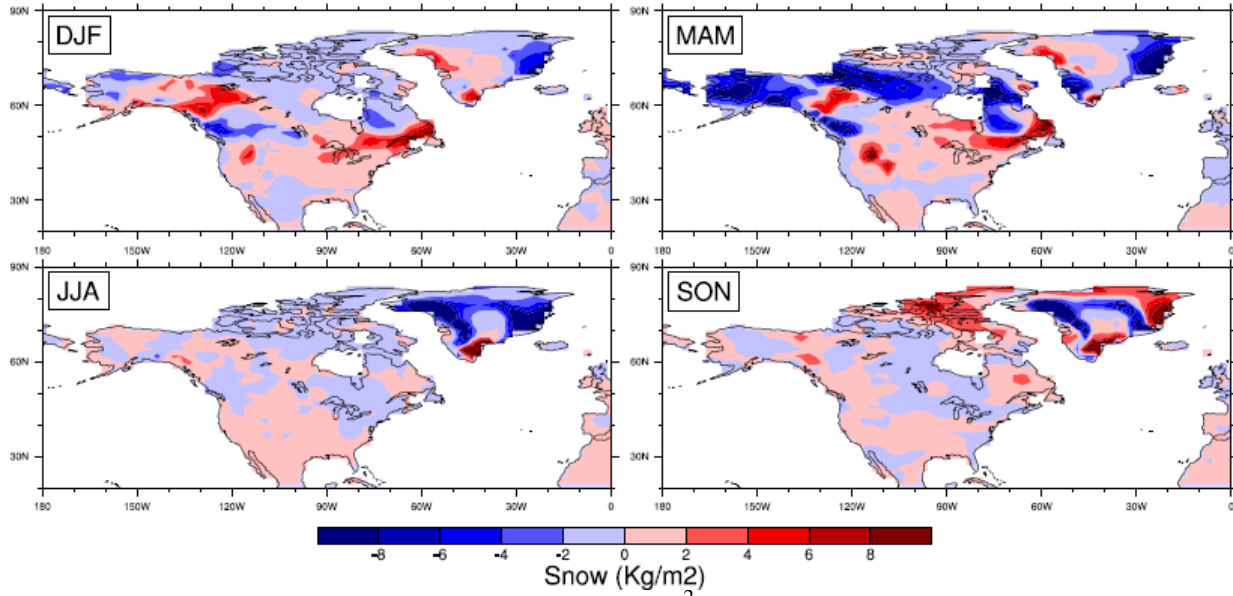


Figure 4.11: Map of response snow mass in  $\text{Kg/m}^2$  represented as described in Figure 4.3.

#### 4.2.1 Northern Prairie

When the prairie is divided into two regions, the difference in the radiation and hydrologic balances is more visible in the AGRIC case. The fourfold increase in snow mass in the northern prairie over the volume in the south, is the only variable that is substantially different between the two regions. Therefore, the rate of snow fall, in addition to the increased rate of precipitation, which is likely the result of cooler temperatures, is the fundamental difference in the north. The radiation balance shows that the increased water availability within the root zone is contributing to a greater latent heat component later in the year (Figure 4.12c). The change is because of evaporation, which is only limited by the field capacity of the root zone. The increase in overall precipitation (i.e. snow and rain) is allowing evaporation to continue without limitation (Figure 4.13a). These two changes to precipitation are visible in the root zone water storage which is draining at a faster rate to the groundwater reservoir, particularly in spring time as snow mass drops (Figure 4.13c).

In the response plots, the radiation balance shows that the peak in outgoing longwave radiation is substantially greater, leading to a larger increase in sensible heat and decrease in

latent heat during the summer months (Figure 4.12d). The response temperature plot (Figure 4.2b) shows this change with the greatest increase in temperature occurring in the north. These changes are a clear indication that the shorter rooting depth of the agricultural land cover type is allowing more of the incoming water to be evaporated or drained even faster. This is made clear in the water balance response plot where the springtime increase in groundwater is greater than the entire prairie case and that simultaneously, the total root zone water availability is much lower (Figure 4.13d). There is more water under greater demand. Subsequently, the decreases in measured precipitation and evaporation seen in Figure 4.13b, shows that the change in land cover type is increasing early year evaporation and subsequently, by the summer, all of the additional water has been either sent to the groundwater or evaporated away. All of these trends indicate that while the exact same changes are occurring, the presence of fourfold the amount of snow found in the northern prairies is impacting the water balance.

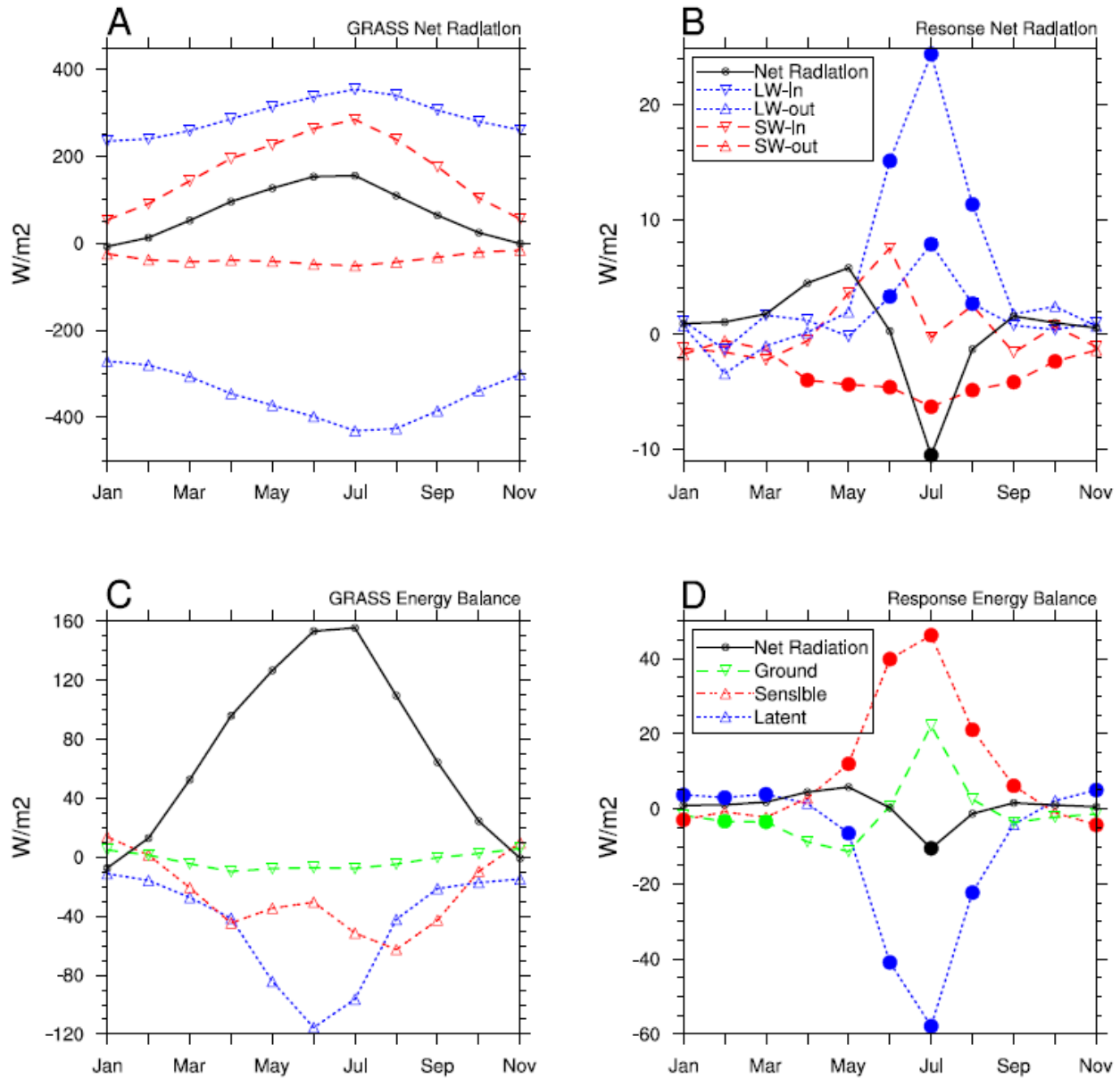


Figure 4.12a-d: Northern Prairie: (A) GRASS net radiation and (B) response net radiation in  $W/m^2$ . (C) GRASS energy balance and (D) response energy balance in  $W/m^2$ . Statistical significance is represented as described in Figure 4.2.

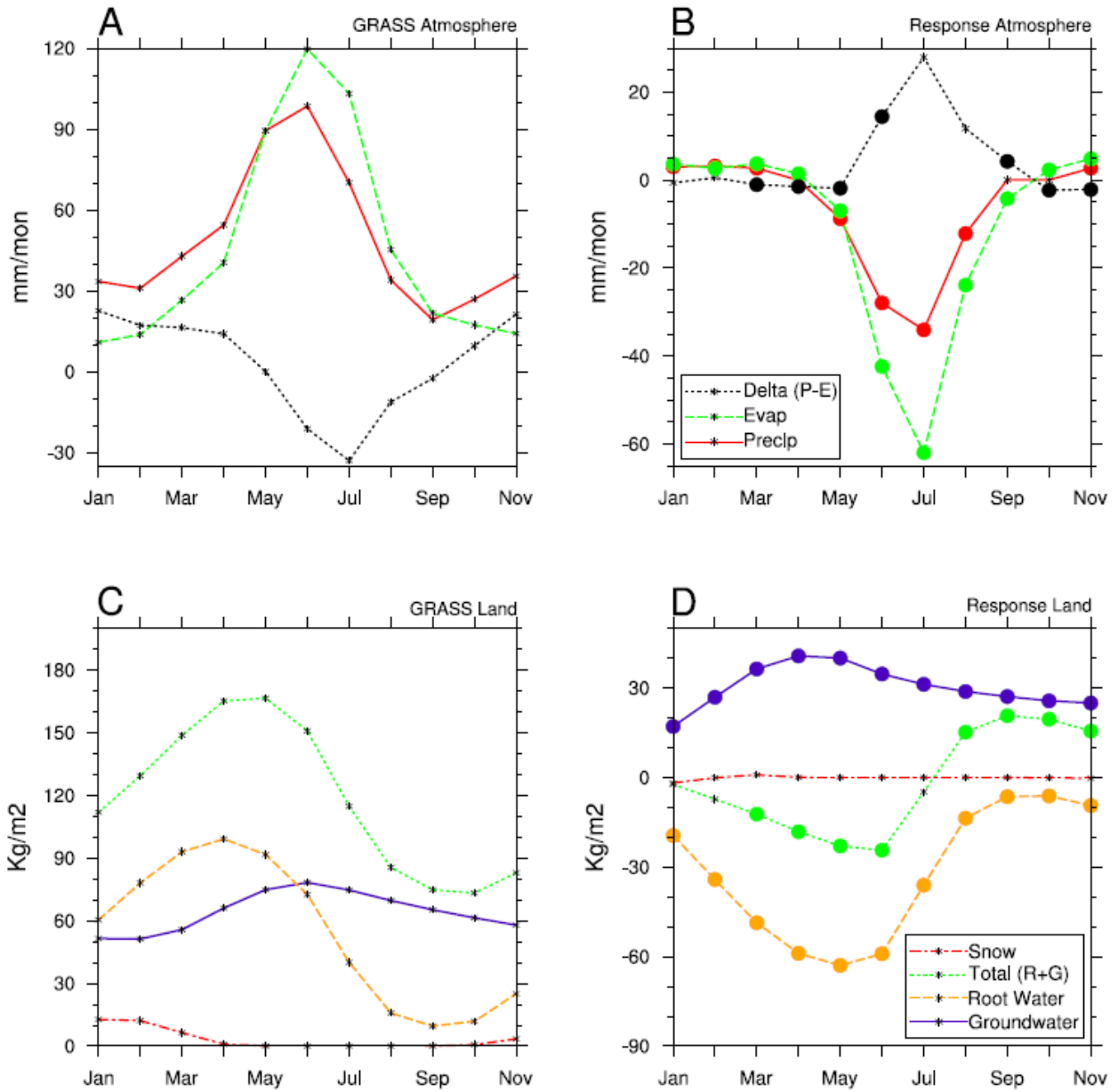


Figure 4.13a-d: Northern Prairie: Atmospheric and land water balance as described in Figure 4.8.

#### 4.2.2 Southern Prairie

Where the patterns were exaggerated in the northern prairies because of the additional snowfall, the decrease in average monthly total snow in the southern prairies has had the opposite effect on the hydrologic and radiation balances in the south. Less water availability in the spring in the control case is shown by a drop in the latent heat component after May (two months earlier than in the north) (Figure 4.14c). The control case water balance shows that there

is substantially less root zone water available throughout the year. This has repercussions on the rate of drainage and evaporation which more closely follows the rate of precipitation (Figure 4.15a). This indicates that the root zone is under so much pressure that any new water is evaporated almost immediately, reducing the total volume that can be drained downwards. As precipitation drops off after mid-summer, total water availability is highly limited. In the response plots, the same patterns presented in both the whole prairie and northern prairie areas is still found, however, all of the changes are minimized. The change in temperature is very small and the difference in snow covered albedo is the smallest of the three regions (Figures 4.1b & 4.2b). Any change that the taller crop species would have had on the fractional area covered by snow is minimal as there is less snow to begin with. These differences lead to the diminished (but still significant) increase in outgoing longwave radiation during July; and explain why the increase in sensible heat and decrease in latent heat are much smaller under the perturbation (Figure 4.14b). The drying effect that shifting vegetation will therefore have less of an impact in the south, not because the change is less powerful in the south but because there is less water available there (Figure 4.15b, c, and d).

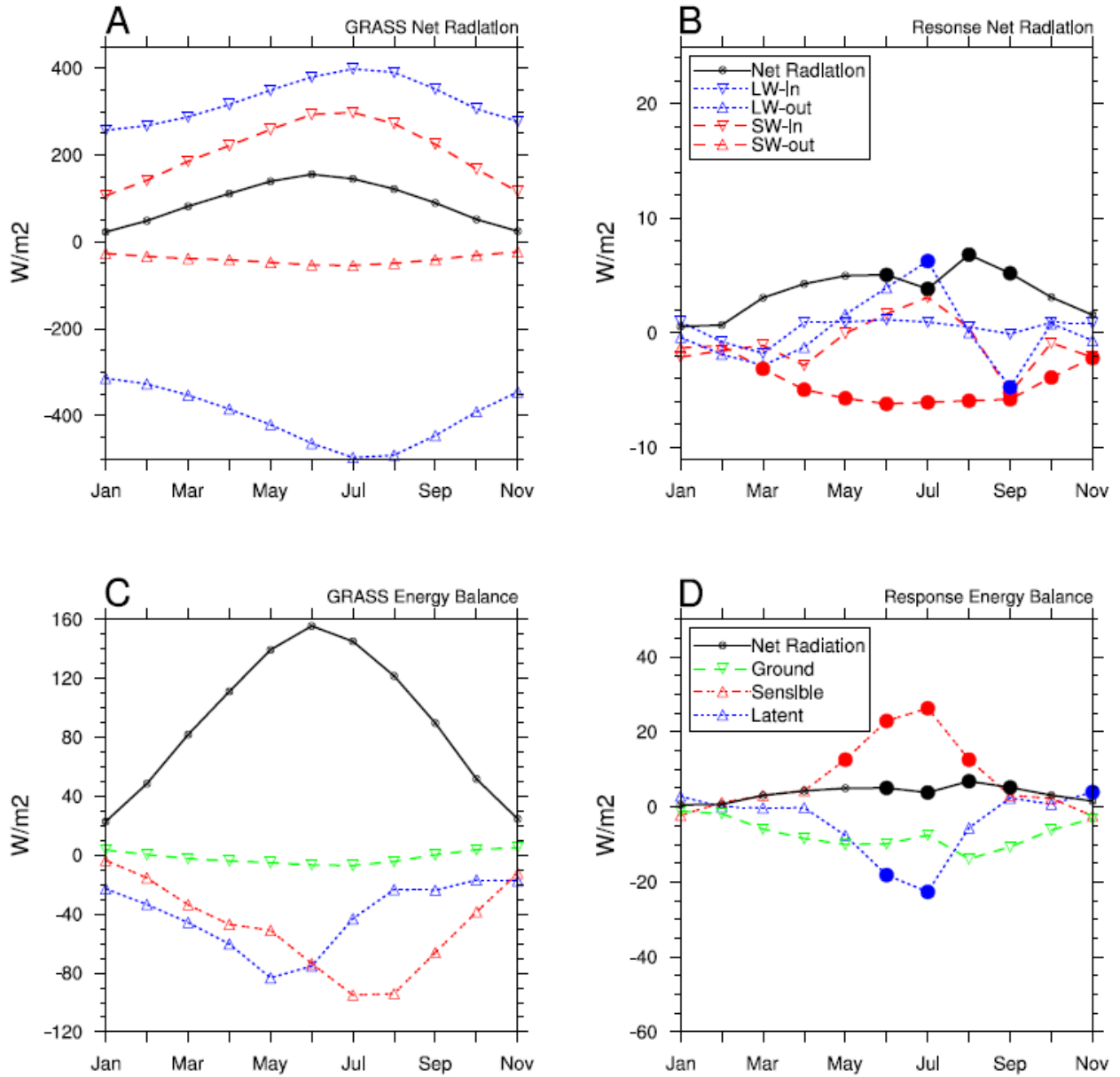


Figure 4.14a-d: Southern Prairie: Net radiation and energy balance as described in Figure 4.8.

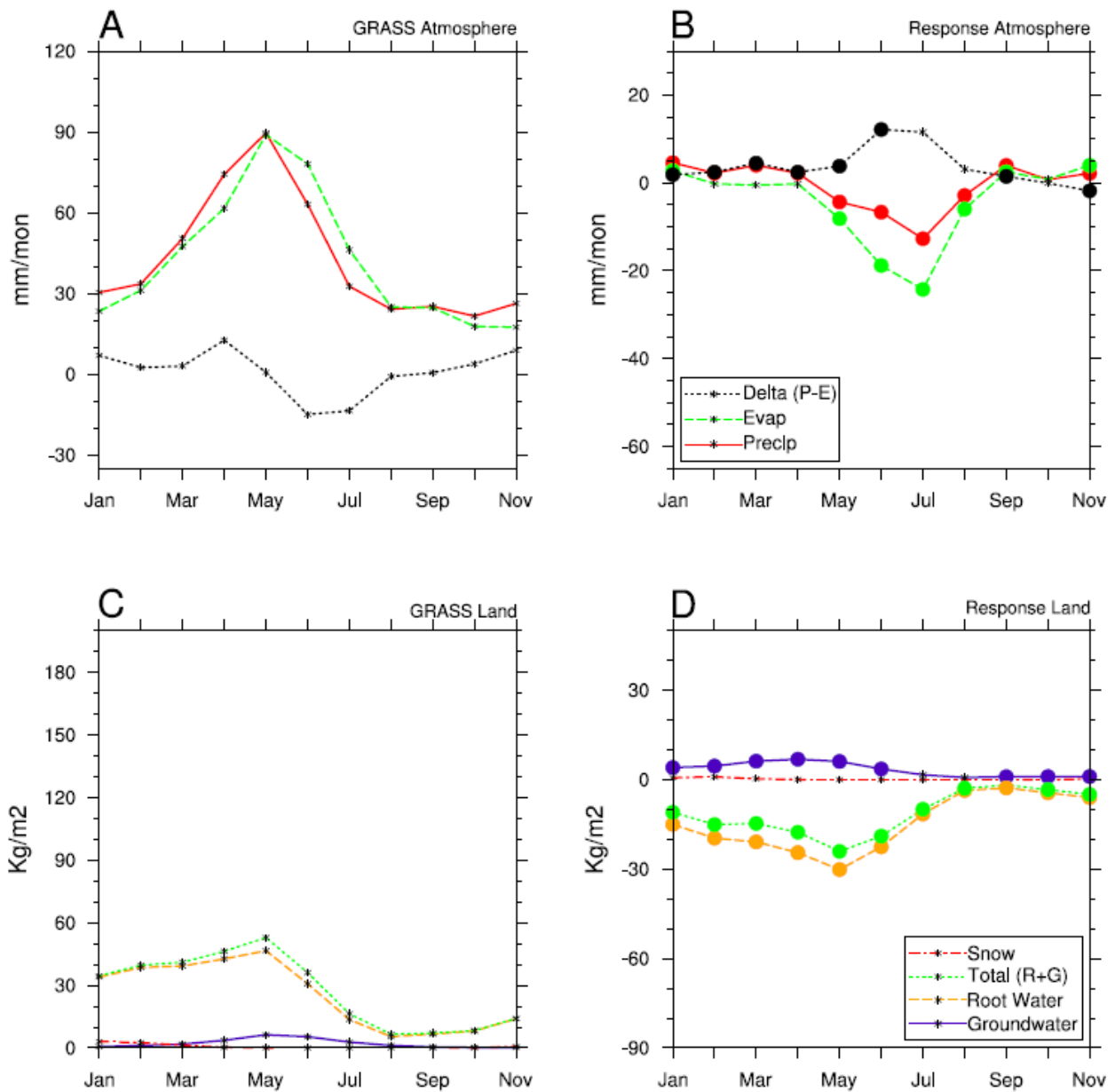


Figure 4.15a-d: Southern Prairie: Atmospheric and land water balance as described in Figure 4.8.

### 4.3 Limitations and Summary

This type of experiment provides a very good design for evaluating the influence of the change in land cover on the prairies in the simplest possible terms. It is able to evaluate the change over a specific ecosystem within a global model. Additionally, the minimized list of vegetation types and the strict definitions of each type based on a small set of prescribed

variables means that the results of the response can be more easily evaluated. However, these very advantages become limitations when trying to apply the results of this study to the real world situation. The oversimplification of the vegetation types means that both the grasslands and agricultural land cover definitions are representative of the average characteristics of these environments from around the world. In the case of grasslands, this is less of a limitation, as grasslands are biologically very similar no matter where they are found. A generalized agricultural definition however, is more complicated as agriculture includes a wide variety of plant classes. The land cover definitions used in this model are based on Matthews (1983). This study defined areas of agriculture, or cultivated lands, based on the percentage of permanently disturbed area for each of the other land cover types. In section 2.5, it was stated that the agricultural type does closely resemble a wheat variety, which is from the Dorman & Sellers (1989) classification scheme. This paper assigned the prescribed values to the different types outlined in Matthews (1983). That study does include an agriculture type which is called 'Broadleaf-deciduous trees with winter wheat'. This type is also shown to be primarily located over the North American Prairie area with some smaller areas in Eastern Europe and India. Because the amalgam of vegetation types used to define agriculture includes winter wheat (Dorman & Sellers, 1989), the relationship between the two types is still similar enough to the real world for the results of this study to be meaningful. Winter wheat is a major prairie crop and accounts for three quarters of all wheat grown in the United States (McPherson, Stensrud, & Crawford, 2004).

In a similar vein, this methodology does not reflect the full extent of changes which have actually occurred on the prairies because of agriculture. The biggest difference is the lack of irrigation. As discussed in Chapter 1, irrigation is heavily relied upon to sustain prairie

agriculture, and the vast majority of water used for this purpose is drawn from groundwater reservoirs in the American prairies, the largest portion of this ecosystem (Scanlon, et al., 2007). The methodology used to calculate the water balance in the LaD model disregards water once it enters the groundwater reservoir. While under natural grasslands, this mechanism simulates actual conditions. The groundwater aquifers are too deep influence surface conditions. Under an irrigated system however, this limitation would be overcome. Nevertheless, by not including irrigation in this model experiment, the results can be used to explain how quickly prairie agriculture would become unsustainable without irrigation. It would also demonstrate how agricultural disasters such as the Dust Bowl of the 1930s occurred when natural droughts were exacerbated by non-irrigated agriculture, as discussed in the literature review.

A final limitation to this study is its short time scale. The model was only run for one year. This provides a good evaluation of the immediate impacts of changing land cover types, however the longitudinal influences are not shown by the response plots. In recognition of these study limitations, there are many possible future directions for research into land cover change in the prairies. The first would be an extension of the current model run. By comparing the residual in the energy balance and water balance over a number of years, it may be possible to establish whether the changes observed in this chapter would continue or if the environment would eventually reach a new equilibrium. Future research directions will be discussed in more depth in the next chapter.

## **Chapter 5: Future Research Possibilities and Conclusions**

### **5.1 Research Summary**

Anthropogenic modification of the surface of the planet has been going on for centuries. However, not until the mid-19<sup>th</sup> century, in the centre of North America, was land cover change carried out so extensively and rapidly with little consideration to environmental maintenance (Ramankutty & Foley, 1999). The change to prairie land cover has impacted the land-atmosphere fluxes of energy and water and has put the region at greater risk of more intense, sustained drought periods. This has occurred due to differences between the original grasslands and the replacing agricultural crops at a biological, field, and ecosystem scale. Agricultural development in the North American prairies has introduced a completely new ecosystem on a continental scale.

This thesis was conducted to try and answer the question: does agriculture have a recognizable influence on prairie climate which can be separated from all other climate forcings, and can this influence be observed at the continental scale. The research was undertaken in two sections. The first was a strictly observation-based examination of change to climate over the 20<sup>th</sup> century, the period of greatest land cover change. This was carried out in two phases. First, by comparing changes from the beginning of the century to the end of the century, and the inter-annual variations in temperature, atmospheric water vapour content (WVC), and convective available potential energy (CAPE) using the 20<sup>th</sup> Century Reanalysis Product (20CR), it was observed that temperatures cooled slightly while WVC increased. Additionally, it was found that there was more WVC over cropped areas and that these places were cooler when compared to areas that had remained largely natural. Second, after it was observed that the results from the 20CR product were biased towards changes occurring in the troposphere, the Observation Minus Reanalysis (OMR) method was applied. By subtracting the 20CR from in-situ station

temperature data, the experiment was focused on temperature changes from within the boundary layer. From both observation datasets, temperature was still found to be cooler over agricultural areas, but increasing over time. Both components of this section provided some evidence that agricultural development was creating some modifications to the expected prairie climate. However, producing any specific analysis from this experiment is problematic because of the numerous sources of error in long term observation datasets. Additionally, both the reanalysis and the OMR methodologies are unable to definitively isolate the land cover signal from the larger climate change noise. A much more efficient way to directly evaluate the influence of land use and land cover change (LULCC) is through a modelling study where the problems of in-situ network density and climate change can be overcome.

The second section of this thesis used the AM2-LM2 atmosphere-land model to directly compare climate when the prairie region was completely overtaken by agriculture (AGRIC) against a totally natural environment (GRASS). It found that there is a statistically significant change in albedo, temperature, and in the fluxes of energy and water, particularly during the spring and summer months. Under the AGRIC simulation, the prescribed reduction in albedo forced a change to the net radiation, reducing outgoing shortwave radiation and causing surface temperatures to increase. The reduced field capacity (shallower root zone) meant that PET was reached more quickly, and the excess energy was transformed into sensible heat, which then further contributed to increasing surface temperatures. Both of these changes combined to reduce water available for precipitation, creating a deficit within the root zone, which was simultaneously drying faster and receiving less precipitation input. Overall, this section demonstrated that the major difference between a natural and a cropped prairie is a hotter and drier climate under agriculture.

Due to the limitations in the two observation studies, it is also evident that LULCC carries a very small signal in the larger climate variability found in North America, which includes sources of both forced (e.g. greenhouse gases) and natural (ENSO and PDO) climate variability. Nevertheless, by controlling for these other processes in the modelling experiment, it becomes apparent that land cover change does have an influence on prairie climate. All of the changes found in that study were the result of the change to the land cover, the only variable that was changed in the AGRIC scenario. The results of this study have therefore achieved the purpose of this thesis, which was to determine if the influence of LULCC on prairie climate could be recognized. While the results are not strong enough to conclusively state the strength of this connection outside of a modelled environment, the 20CR and OMR studies suggested that there was a connection, despite the difficulties in separating the LULCC signal from the 20<sup>th</sup> century trends, which was largely supported by the significant and more robust response found using the AM2-LM2 model. This also offers support to the hypothesis stated in section 1.4. While the results of these experiments cannot be used to conclusively quantify the exact forcing of LULCC on climate, they have demonstrated that a relationship exists at the continental scale. The most important result of this thesis was that it opened up a series of possible future research directions to be explored. Additionally, it helps to emphasize the argument made by Pielke, Sr., et al. (2005), that the study of LULCC and its role in anthropogenic climate change remains underdeveloped.

## **5.2 Future Directions**

These results open several possible future research directions. A first route would be to further refine the modelling experiment of Chapter 4. The changes in the water balance are explained as the result of the combined change in the root depth ( $Z_R$ ) and roughness length ( $z_0$ ).

In order to understand the separate influence of each of these prescribed variables would require the creation of two new land cover types in the land model. Each would be identical to the AGRIC scenario but one of  $Z_R$  and  $z_0$  would be reset to match the GRASS value. Then the water balance results from both of these new scenarios would be compared with the AGRIC scenario from the original experiment. Because it was noted that the influence of a greater roughness length is difficult to directly attribute onto changes to the hydrologic cycle, this experiment would help to isolate that influence. Additionally, it would clarify exactly how significant the influence of the 1 cm decrease in  $Z_R$  is, which initially appeared to be a very small change.

As extensions of the original modelling experiment, there are three different research directions that could be carried out using the same AM2-LM2 coupled model. The first would be to expand the scope of the model study. This could be done in several ways. The first would be to run the GRASS and AGRIC scenarios for multiple years in order to evaluate the long term changes which would appear in the response plots. Without such an analysis, it cannot be stated definitively if the presented results are representative of the beginning of a long term trend or if they are a one year anomaly, which would re-equilibrate after a short period of time. A second way would be to use more than one model as part of an ensemble. Because the LaD component of the AM2-LM2 model is so simplistic, using a series of more complex models could paint a more realistic picture of the true influences of agriculture on prairie climate. This would also provide a stronger result for changes to the hydrologic cycle, including how evaporation from surface water bodies occurs when it is not immediately taken up by the vegetation layer or is drained to the groundwater. These are simple changes which could easily be integrated into a next steps project. The second and third directions are more involved proposals.

The second future research direction would be to force the agricultural definition in the LaD model to better represent the variety of crop types found on the prairies. Currently, the agriculture land cover type is completely static and is represented by a generalized winter wheat definition. Additionally, there is no allowance for irrigation or timed growing season within the model structure. To create a more accurate representation of the prairies would entail the creation of a completely new map of the prairies under an agricultural regime where the land cover type is determined for each cell based on the majority crop type grown therein. Monfreda, Ramankutty, & Foley (2008) identify each major crop type group (corn, barley, etc.) and their map series, which show the percentage of each 5 min resolution cell dominated by each group, could be used as a mask to identify these areas. This map would also have to include a period of bare soil both before germination and after harvest time. This would require controlling the land cover type on a monthly basis as the model is running. Irrigation can be introduced by either increasing the residence time within the root zone or by artificially increasing the rate of precipitation. To achieve the former, either the rooting depth of the crop land cover types could be extended or the field capacity could be increased, delaying drainage to the groundwater reservoir. Because water is completely separated from the vegetation and surface layers once it reaches the groundwater reservoir, and discharge to the riverine systems is controlled almost uniformly around the world by a constant 30 day residence time, reducing the overall volume of water in the groundwater will not have an impact on the results produced by the model. The later method, altering precipitation, would require a thin layer of water to be added directly to the root zone reservoir. This would be 'new' water in the hydrologic cycle. Alternatively, the LM2 model could be run in 'offline' mode with prescribed meteorology (Milly & Shmakin, 2002a). The recognized difference (Chapter 1) between the rate and patterns of growth between crops and

grassland species, as well as the differences in albedo as each plant type develops makes this a potentially interesting future research direction.

The third and final primary research direction is the utilization of field research. This would shrink the geographic scope of the research to a field scale but it would allow for a more complete image of water and energy fluxes under different vegetative environments. This approach would also produce a more accurate image of the timing of crop growth and the influence of irrigation. Irrigated and non-irrigated fields could be compared under different crop types. Overall, a combination of the above three future directions would be a good next step for this type of research. Integrating field observations with a more complex model system could be better used to evaluate how agriculture has impacted the prairies. Additionally, such a research project could be used to address a noted gap in the literature. Many sources discount the influence that land use and land cover change can have on climate because its signal in climate records is easily masked by other, larger variables like climate change, particularly in the 20<sup>th</sup> century (Kalnay, et al., 2006). While the results presented here can be used alone to demonstrate a link between prairie LULCC and climate, it is apparent that there are still many other avenues of research that could be used to more accurately describe this relationship. However, in order to properly design and carry out such future research projects, the foundational connection had to be first established. That requirement has been largely met by this thesis, the results of which can now be carried forward in any of the future research directions outlined in this chapter.

## References

- Adegoke, J. O., Pielke, Sr., R., Carleton, A. M. (2005). Observational and modeling studies of the impacts of agriculture-related land use change on planetary boundary layer processes in the central U.S. *Agricultural and Forest Meteorology*, 142, 203-215.
- Aguado, E., & Burt, J. E. (2012). *Understanding weather and climate*. Boston: Pearson.
- Anderson, J. L., Balaji, V., Broccoli, A. J., Cooke, W. F., Delworth, T. L. Dixon, K. W., ... Wyman, B. L. (2004). The new GFDL Global Atmosphere and Land Model AM2-LM2: Evaluation with prescribed SST simulations. *Journal of Climate*, 17, 4261-4673.
- Anderson, R. C. (2006). Evolution and origin of the Central Grassland of North America: Climate, fire and mammalian grazers. *The Journal of the Torrey Botanical Society*, 133(4), 626-647.
- Annamalai, H., Okajima, H., & Watanabe, M. (2007). Possible impact of the Indian Ocean SST on the northern hemisphere circulation during El Nino. *Journal of Climate*, 20, 3164-3189.
- Axelrod, D. I. (1985). Rise of the grassland biome, Central North America. *The Botanical Review*, 51(2), 163-201.
- Brown, R. D., Brasnett, B., & Robinson, D. (2010). Gridded North American monthly snow depth and snow water equivalent for GCM evaluation. *Atmosphere-Ocean*, 41(1), 1-14.
- Buyanovsky, G. A., & Wagner, G. H. (1986). Post-harvest residue input to cropland. *Plant and Soil*, 93, 57-65.
- Canadell, J., Jackson, R. B., Ehleringer, J. R., Mooney, H. A., Sala, O. E., & Schulze, E. -D. (1996). Maximum rooting depth of vegetation types at the global scale. *Oecologia*, 108, 583-595.
- Cho, J., Miyazaki, S., Yeh, P. J.-F., Kim, W., Kanae, S., Oki, T. (2012). Testing the hypothesis on the relationship between aerodynamic roughness length and albedo using vegetation structure parameters. *International Journal of Biometeorology*, 56, 411-418.
- Compo, G. P., Whitaker, J. S., Sardeshmukh, P. D., Matsui, N., Allan, R. J., Yin, X., ... Worley, S. J. (2011). The Twentieth Century Reanalysis Project. *Quarterly Journal of the Royal Meteorological Society*, 137, 1-28.
- Cook, E. R., Woodhouse, C. A., Eakin, C. M., Meko, D. M., Stahle, D. W. (2004). Long-term aridity changes in the Western United States. *Science*, 306, 1015-1018.

- Cook, E. R., Seager, R., Cane, M. A., & Stahle, D. W. (2007). North American drought: Reconstructions, causes and consequences. *Earth-Science Reviews*, *81*, 93-134.
- Dirmeyer, P. A., Jin, Y., Singh, B., & Yan, X. (2013). Evolving land-atmosphere interactions over North America from CMIP5 simulations. *Journal of Climate*, *26*, 7313-7327.
- Dodds, W. K., Gido, K., Whiles, M. R., Fritz, K. M., & Matthews, W. J. (2004). Life on the edge: The ecology of great plains prairie streams. *BioScience*, *54*(3), 205-216.
- Dorman, J. L., & Sellers, P. J. (1989). A global climatology of albedo, roughness length and stomatal resistance for atmospheric general circulation models as represented by the Simple Biosphere Model (SiB). *Journal of Applied Meteorology*, *28*, 833-855.
- Ehleringer, J. R., Cerling, T. E., & Helliker, B. R. (1997). C<sub>4</sub> photosynthesis, atmospheric CO<sub>2</sub>, and climate. *Oecologia*. *112*, 285-299.
- Eronen, J. T., Fortelius, M., Micheels, A., Portmann, F. T., Puolamaki, K., & Janis, C. M. (2012). Neogene aridification of the Northern Hemisphere. *Geology*, *40*(9), 823-826.
- Fall, S., Niyogi, D., Gluhovsky, A., Pielke, Sr., R. A., Kalnay, E., & Rochon, G. (2010). Impacts of land use land cover on temperature trends over the continental United States: Assessment using the North American Regional Reanalysis. *International Journal of Climatology*, *30*, 1980-1993.
- Fang, X., Pomeroy, J. W., Westbrook, C. J., Guo, X., Minke, A. G., & Brown, T. (2010). Prediction of snowmelt derived streamflow in a wetland dominated by prairie basin. *Hydrology and Earth System Sciences Discussions*, *7*, 1103-1141.
- Ferguson, C. R., & Villarini, G. (2012). Detecting inhomogeneities in the Twentieth Century Reanalysis over the central United States. *Journal of Geophysical Research*, *117*, 1-11.
- Findell, K. L., Pitman, A. J., England, M. H., & Pегion, P. J. (2009). Regional and global impacts of land cover change and sea surface temperature anomalies. *Journal of Climate* *22*, 3248-3269.
- Fletcher, C. G., & Kushner, P. J. (2010). The role of linear interference in the annual mode response to tropical SST forcing. *Journal of Climate*, *24*, 778-794.
- Foley, J. A., Ramankutty, N., Brauman, K. A., Cassidy, E. S., Gerber, J. S., Johnston, M., ... Zaks, D. P. M. (2011). Solutions for a cultivated planet. *Nature*, *478*, 337-342.
- Fye, F. K., Stahle, D. W., & Cook, E. R. (2003). Paleoclimatic analogs to twentieth-century moisture regimes across the United States. *Bulletin of the American Meteorological Society*, *84*(7), 901-909.
- Gan, T. Y. (2000). Reducing vulnerability of water resources of Canadian Prairies to potential droughts and possible climatic warming. *Water Resources Management*, *14*, 111-135.

- Gutentag, E. D., Heimes, F. J., Krothe, N. C., Luckey, R. R., & Weeks, J. B. (1984). *Geohydrology of the High Plains Aquifer in parts of Colorado, Kansas, Nebraska, New Mexico, Oklahoma, South Dakota, Texas, and Wyoming* (U.S. Geological Survey Professional Paper 1400-B). Alexandria, VA: U.S. Geological Survey.
- Haxeltine, A., & Prentice, C. (1996). BIOME3: An equilibrium terrestrial biosphere model based on ecophysiological constraints, resource availability, and competition among plant functional types. *Global Biogeochemical Cycles*, *10*(4), 693-709.
- Heim, Jr., R. R. (2002). A review of twentieth-century drought indices used in the United States. *Bulletin of the American Meteorological Society*, *83*, 1149-1165.
- Hu, Z. -Z., & Huang, B. (2009). Interferential impact of ENSO and PDO on dry and wet conditions in the U.S. Great Plains. *American Meteorological Society*, *22*, 6047-6065.
- Intergovernmental Panel on Climate Change [IPCC]. (2007). *Fourth Assessment Report: Climate Change 2007: Working Group I: The Physical Science Basis* (4<sup>th</sup> ed.). Geneva, Switzerland: IPCC.
- Jones, P. D., Lister, D. H., Osborn, T. J., Harpham, C. , Salmon, M., & Morice, C. P. (2012). Hemispheric and large-scale land-surface air temperature variation: An extensive revision and an update to 2010. *Journal of Geophysical Research*, *117*, 1-29.
- Kalnay, E., Cai, M., Li, H., & Tonin, J. (2006). Estimation of the impact of land-surface forcings on temperature trends in eastern United States. *Journal of Geophysical Research*, *111*, 1-13.
- Kebart, K. K., & Anderson, R. C. (1987). Phenological and climatic patterns in three tallgrass prairies. *The Southwestern Naturalist*, *32*(1), 29-37.
- Keeley, J. E., & Rundel, P. W. (2005). Fire and the Miocene expansion of C<sub>4</sub> grasslands. *Ecology Letters*, *8*, 683-690.
- Kunkel, K. E., Palecki, M. A., Ensor, L., Easterling, D., Hubbard, K. G., Robinson, D., & Redmond, K. (2009). Trends in twentieth-century U.S. extreme snowfall seasons. *Journal of Climate*, *22*, 6204-6216.
- Leff, B., Ramankutty, N., & Foley, J. A. (2004). Geographic distribution of major crops across the world. *Global Biogeochemical Cycles*, *18*, 1-33.
- Luaenroth, W. K., Burke, I. C., & Gutmann, M. P. (1999). The structure and function of ecosystems in the Central North American Grassland Region. *Great Plains Research*, *9*, 223-259.
- Lyle, M., Barron, J., Bralower, T. J., Huber, M., Lyle, A. O., Ravelo, A. C., ... Wilson, P. A. (2008). Pacific ocean and cenozoic evolution of climate. *Review of Geophysics*, *46*, 1-47.

- Mahmood, R., Leeper, R., & Quintanar, A. I. (2011). Sensitivity of planetary boundary layer atmosphere to historical and future changes of land use/land cover, vegetation fraction, and soil moisture in Western Kentucky, USA. *Global Planetary Change*, 78, 36-53.
- Matsuura, K., & Willmott, C. J. (2009). Terrestrial air temperature: 1900-2008 gridded monthly time series. Retrieved from [http://climate.geog.udel.edu/~climate/html\\_pages/Global2\\_Ts\\_2009/README.global\\_ts\\_2009.html](http://climate.geog.udel.edu/~climate/html_pages/Global2_Ts_2009/README.global_ts_2009.html)
- Matthews, H. D., Weaver, A. J., Eby, M., & Meissner, K. J. (2003). Radiative forcing of climate by historical land cover change. *Geophysical Research Letters*, 30(2), 1-4.
- McGee, D., Boon, S., & van Meerveld, H. J. (2012). Impacts of rural water diversions on prairie streamflow. *Canadian Water Resources Journal*, 37(4), 415-424.
- McCabe, G. J., Betancourt, J. L., Gray, S T., Palecki, M. A., & Hidalgo, H. G. (2008). Associations of multi-decadal sea-surface temperature variability with US drought. *Quaternary International*, 188, 31-40.
- McPherson, R. A., Stensrud, D. J., & Crawford, K. C. (2004). The impact of Oklahoma's winter wheat belt on the mesoscale environment. *Monthly Weather Review*, 132, 405-421.
- Milly, P. C. D. (1992). Potential evaporation and soil moisture in general circulation models. *Journal of Climate*, 5, 209-226.
- Milly, P. C. D., & Dunne, K. A. (2002). Macroscale water fluxes 1. Quantifying errors in the estimation of basin mean precipitation. *Water Resources Research*, 38(10), 1-14.
- Milly, P. C. D., & Shmakin, A. B. (2002a). Global modeling of land water and energy balances. Part I: The Land Dynamics (LaD) Model. *Journal of Hydrometeorology*, 3, 283-299.
- Milly, P. C. D., & Shmakin, A. B. (2002b). Global modeling of land water and energy balances: Part II: Land-characteristics contributions to spatial variability. *Journal of Hydrometeorology*, 3, 301-310.
- Milly, P. C. D., & Wetherald, R. T. (2002). Macroscale water fluxes 3. Effects of land processes on variability of monthly river discharge. *Water Resources Research*, 38(11), 1-12.
- Mishra, A. K., & Singh, V. P. (2010). A review of drought concepts. *Journal of Hydrology*, 391, 202-216.
- Mo, K. C., & Schemm, J. E. (2007). Droughts and persistent wet spells over the United States and Mexico. *Journal of Climate*, 21, 980-994.

- Monfreda, C., Ramankutty, N., & Foley, J. A. (2008). Farming the planet: 2. Geographic distribution of crop areas, yields, physiological types, and net primary production in the year 2000. *Global Biogeochemical Cycles*, *22*, 1-19.
- Morgan, J. A., LeCain, D. R., Pendall, E., Blumenthal, D. M., Kimball, B. A., Carrillo, Y., ... West, M. (2011). C4 grasses prosper as carbon dioxide eliminates desiccation in warmed semi-arid grassland. *Nature*, *476*, 202-206.
- O'Connell, J. L., Johnson, L. A., Smith, L. M., McMurry, S. T., & Haukos, D. A. (2012). Influence of land-use and conservation programs on wetland plant communities of the semiarid United States Great Plains. *Biological Conservation*, *146*, 108-115.
- Oke, T. R. (1987). *Boundary Layer Climatology* (2 ed.). New York, NY: Methuen & Co. Ltd.
- Pearcy, R. W., Tumosa, N., & Williams, K. (1981). Relationships between growth, photosynthesis and competitive interactions for a C3 and a C4 plant. *Oecologia*, *48*, 371-376.
- Peel, M. C., Finlayson, B. L., & McMahon, T. A. (2007). Updated world map of the Köppen-Geiger climate classification. *Hydrology and Earth System Sciences*, *11*, 1633-1644.
- Pielke, Sr., R. A. (1998). Interactions between the atmosphere and terrestrial ecosystems: Influence on weather and climate. *Global Change Biology*, *4*, 461-475.
- Pielke, Sr., R. A. (2001). Influence of the spatial distribution of vegetation and soils on the prediction of cumulus convective rainfall. *Reviews of Geophysics*, *39*(2), 151-177.
- Pielke, Sr., R. A. (2005). Land use and climate change. *Science*, *310*, 1625-1626.
- Pielke, Sr., R. A., Adegoke, J. O., Chase, T. N., Marshall, C. H., Matsui, T., & Niyogi, D. (2006). A new paradigm for assessing the role of agriculture in the climate system and in climate change. *Agricultural and Forest Meteorology*, *142*, 234-254.
- Pielke, Sr., R. A., Adegoke, J., Beltran-Przekurat, A., Hiemstra, C. A., Lin, J., Nair, U. S., ... Nobis, T. E. (2007). An overview of regional land-use and land-cover impacts on rainfall. *Tellus B*, *59*(3), 587-601.
- Pielke, Sr., R. A., Pitman, A., Niyogi, D., Majmood, R., McAlpine, C., Hossain, F., ... de Noblet, N. (2011). Land use/land cover changes and climate: Modeling analysis and observational evidence. *WIREs Climate Change*, *2*, 828-850.
- Polley, H. W., Briske, D. D., Morgan, J. A., Wolter, K., Bailey, D. W., & Brown, J. R. (2013). Climate change and North American rangelands: Trends, projections, and implications. *Rangeland Ecological Management*, *66*, 493-511.

- Raddatz, R. L. (2005). Moisture recycling on the Canadian Prairies for summer droughts and pluvial from 1997 to 2003. *Agricultural and Forest Meteorology*, *131*, 13-26.
- Raddatz, R. L., & Hanesiak, J. M. (2008). Significant summer rainfall in the Canadian Prairie Provinces: modes and mechanisms 2000-2004. *International Journal of Climatology*, *28*, 1607-1613.
- Ramankutty, N., & Foley, J. A. (1998). Characterizing patterns of global land use: An analysis of global cropland data. *Global Biogeochemical Cycles*, *12*(4), 667-685.
- Ramankutty, N., & Foley, J. A. (1999). Estimating historical changes in global and cover: Croplands from 1700 to 1992. *Global Biogeochemical Cycles*, *13*(4), 997-1027.
- Riemann-Campe, K., Fraedrich, K., & Lunkeit, F. (2009). Global climatology of convective available potential energy (CAPE) and convective inhibition (CIN) in ERA-40 reanalysis. *Atmospheric Research*, *93*, 534-545.
- Rodell, M., & Famiglietti, J. S. (2002). The potential for satellite-based monitoring of groundwater storage changes using GRACE: The High Plains aquifer, Central US. *Journal of Hydrology*, *263*, 245-256.
- Rohli, R. V., & Vega, A. J. (2008). *Climatology*. Sudbury, MA: Jones and Bartlett Publishers.
- Rosenberg, N. J., Epstein, D. J., Wang, D., Vail, L., Srinivasan, R., & Arnold, J. G. (1999). Possible impacts of global warming on the hydrology of the Ogallala Aquifer region. *Climate Change*, *42*, 677-692.
- Rubel, F., & Kotteck, M. (2010). Observed and projected climate shifts 1901-2100 depicted by world maps of the Köppen-Geiger climate classification. *Meteorologische Zeitschrift*, *19*(2), 135-141.
- Samson, F., & Knopf, F. (1994). Prairie conservation in North America. *BioScience*, *44*(6), 418-421.
- Samson, F. B., Knopf, F. L., & Ostlie, W. R. (2004). Great Plains ecosystems: Past, present and future. *Wildlife Society Bulletin*, *32*(1), 6-15.
- Scanlon, B. R., Jolly, I., Sophocleous, M., & Zhang, L. (2007). Global impacts of conversions from natural to agricultural ecosystems on water resources: Quantity versus quality. *Water Resources Research*, *43*, 1-18.
- Schafer, M., & Holland, K. J. (2009). In the Beginnig, 1828-1900. In K. EuDaly, M. Schafer, J. Boyd, S. Jessup, A. McBride, & S. Glischinski, *The Complete Book of North American Railroading* (14-41). Minneapolis, MN: Voyageur Press.

- Schenk, H. J., & Jackson, R. B. (2002a). Rooting depth, lateral root spreads, and below-ground/above-ground allometries of plants in water-limited ecosystems. *Journal of Ecology*, *90*, 480-494.
- Schenk, H. J., & Jackson, R. B. (2002b). The global biogeography of roots. *Ecological Monographs*, *72*(3), 311-328.
- Sieg, C. H., & Flather, C. H. (1999). Recent biodiversity patterns in the Great Plains: Implications for restoration and management. *Great Plains Research*, *9*, 277-313.
- Song, J. (1999). Phenological influences on the albedo of prairie grassland and crop fields. *International Journal of Biometeorology*, *42*, 153-157.
- Sterl, A. (2004). On the (in)homogeneity of reanalysis products. *Journal of Climate*, *17*, 3866-3873.
- Steyaert, L. T., & Knox, R. G. (2008). Reconstructed historical land cover and biophysical parameters for studies of land-atmosphere interactions within the eastern United States. *Journal of Geophysical Research*, *113*, 1-27.
- Still, C. J., Berry, J. A., Collatz, G. J., & DeFries, R. S. (2003). Global distribution of C<sub>3</sub> and C<sub>4</sub> vegetation: Carbon cycle implications. *Global Biogeochemical Cycles*, *17*(1), 1-14.
- Strassberg, G., Scanlon, B. R., & Chambers, D. (2009). Evaluation of groundwater storage monitoring with the GRACE satellite: Case study of the High Plains aquifer, central United States. *Water Resources Research*, *45*, 1-10.
- Teeri, J. A., & Stowe, L. G. (1976). Climate patterns and the distribution of C<sub>4</sub> grasses in North America. *Oecological (Berl.)*, *23*, 1-12.
- Weaver, J. E. (1954). *North American Prairie*. Lincoln, NE: Johnsen Publishing Company.
- Wilkes, G. (2004). Corn, strange and marvelous: But is a definitive origin known?. In Smith, C. W., Betran, J., & Runge, E. C. A. (Eds.), *Corn: Origin, history, technology, and production* (3-64). Hoboken, NJ: John Wiley & Sons, Inc.
- Wittrock, V., & Ripley, E. A. (1999). The predictability of autumn soil moisture levels on the Canadian prairies. *International Journal of Climatology*, *19*, 271-289.
- Wood, W. W., & Sanford, W. E. (1995). Chemical and isotopic methods for quantifying groundwater recharge in a regional, semiarid environment. *Groundwater*, *33*(3), 458-468.
- Zhang, X. C. (2012). Cropping and tillage systems effects on soil erosion under climate change in Oklahoma. *Soil Science Society of America Journal*, *76*, 1789-1797.

Zhang, Y., Wang, X., Pan, Y., & Hu, R. (2013). Diurnal and seasonal variations of surface albedo in a spring wheat field of arid lands of Northwestern China. *International Journal of Biometeorology*, 57, 67-73.